Journal of
Materials Chemistry C

Materials for optical, magnetic and electronic devices

Accepted Manuscript

This article can be cited before page numbers have been issued, to do this please use: Q. Xiao-Ni, L. Dang, W. Qu, Y. Zhang, H. Yao, Q. Lin and T. Wei, *J. Mater. Chem. C*, 2020, DOI: 10.1039/D0TC01401J.

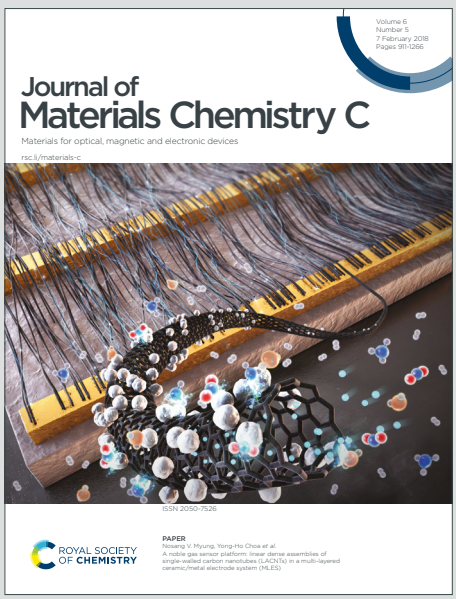

ROYAL SOCIETY OF CHEMISTRY

rsc.li/materials-c

View Article Online
DOI: 10.1039/D0TC01401J

Based on the phenazine derivatives for optical sensing: a review

Xiao-Ni Qi, Li-Rong Dang, Wen-Jun Qu, You-Ming Zhang, Hong Yao, Qi Lin* and Tai-Bao Wei*

Key Laboratory of Eco-Environment-Related Polymer Materials, Ministry of Education of China, Key Laboratory of Polymer Materials of Gansu Province, College of Chemistry and Chemical Engineering, Northwest Normal University, Lanzhou, Gansu, PR China

Abstract: Phenazine, featuring the electron-deficient skeleton, lone pair electrons on nitrogen atoms, and other properties (such as tunable structures, excellent optical performance and proper binding abilities), can effectively sense target ions or molecules by non-covalent interactions, involving hydrogen bond, anion–π interactions, metal coordinated and other weak forces. These distinctive characteristics enable phenazine derivatives to be available in a variety of sensors, and that have already been confirmed to exhibit enormous successes in the field of sensing. More importantly, phenazine derivatives can be adequately applied in the biosensors. Therefore, the latest progress related to the application of phenazine derivatives in optical sensing is summarized. It is expected that the phenazine derivatives will receive a bright future in fabricating sensors and bio applications.

1. Introduction

In the past decades, phenazine derivatives have attracted much attention in the supramolecular chemistry due to their fascinating properties[1-3]. The phenazine-containing compounds discovered and reported by researchers have exceeded 6000 species[4-7]. Since then, a plenteous of phenazine derivatives have been identified and[1]investigated based on their attractive performance. The original natural phenazine was produced by the soil habitants as well as microorganisms[8,9], which served as antibiotic drugs to cure the related diseases in the clinical medicine. After that, the phenazine derivatives gradually come into sights of researchers and have taken place great changes. As reported by relevant reports[10-13], the phenazine structure generally contains three linear fused aromatic rings[14-19]. This structural motif is also named as 9,10-*N*, *N*-anthracene phenazine ($C_{12}H_8N_2$

*Corresponding author
Tel: +086 9317973191; E-mail address: weitaibao@126.com; linqi2004@126.com.

in Table 1) by international union of pure and applied chemistry nomenclatures (IUPAC)[20] and with high melting point of 175–176 °C[21]. The history of the chemical synthesis of the phenazine compounds could be dated back to almost 100 years ago[22-24]. This interesting nitrogen−containing compounds with condensed ring was firstly synthesized by P Karrer et al. in 1917, by combining 1,4-benzoquinone or 2,5-dihydroxy-1,4-benzoquinone to achieve the phenazine compound[25-27], which was the initial artificial synthetic phenazine substance though chemical technology[28-30]. Eventually, various synthetic methodology sprung following the first reported methods[31-33], which provided broad space for extensive application of the phenazine compounds in following optical sensing field[34-37].

Phenazine derivatives research have made very considerable efforts in the aspect of exploring their sensing properties at the limited wavelength[38-41], which may be the starting point to design effective sensing materials for target detection. Generally, phenazine derivatives possess special backbone structure[42-46], including π system containing electron deficiency, the lone pair of electrons on nitrogen center, three fused aromatic rings, and excellent optical properties (high fluorescence quantum yield, narrow emission band, cross-interaction of π-π electrons, large stokes displacement, and maximum absorption and emission wavelength in the visible region). The special structure makes them efficiently sense target molecules or ions by supramolecular interactions, such as anion-π interaction, coordinate bindings and other forces[47]. Moreover, the backbone structure shows high flexibility, which is easily modified with functional ligands and special groups, or coordinated with metals for tuning the sensing properties and enhancing sensitivity and selectivity[48]. Due to those outstanding strengths, a plentiful of phenazine derivatives have been applied as active sensing elements, appealing to attentions in the field of materials science[49-54].

It was well documented that the functional groups or ligands tuning of phenazine derivatives have close relationship with their opto-electronic properties, which significantly influence their sensing response[55-59]. In general, the functional group have been introduced into the phenazine backbone as the binding sites, which could enhance charge transfer properties involving the photoinduced electron transfer (PET), intermolecular electric charge transfer (ICT), excited-state intramolecular proton transfer (IPT), fluorescence resonance energy transfer (FRET), and other interaction modes. For example, after fusing thiophene or benzene rings, an obvious variation in

band gap and strengthening of ICT character could be noticed. Furthermore, due to protonation of different pyridine type by introducing into the phenazine skeleton, an enhancement in electron withdrawing ability and stabilization of LUMO were observed, which could further cause an evident red-shift in absorption[60-62]. Hence, proper chemical modifications of phenazine backbone could lead to enhancement of their optical or electrochemical properties by adjusting the location of heteroatom or introducing alternative π-conjugated cores. Besides, many potential molecular structures as the chemical sensors could be obtained by the artificial technology on the basis of the phenazine derivatives, of which the introduction of functional groups not only tune the sensing properties but also enrich the diversity of phenazine derivatives. Importantly, it can enlarge the range of application of novel sensors in supramolecular sensing field, as well as hold great potential in biosensing.

Keep this in minds, photometric characteristics of many chemical sensors based on phenazine derivatives have been continuously explored, and enormous achievements have been gained. Although, there have been a number of longitudinal studies involving phenazine derivatives that have been published[63-65], it is true that few of newest summary were made about the applications of the phenazine derivatives in the optical sensing field. In view of this and our group's long-standing interest on sensing supramolecular materials, we attempt to discuss and summarize the recent progress of the phenazine derivatives in optical sensing and bioimaging. The interrelated molecule structure of phenazine derivatives have been listed in Table 1.

View Article Online
DOI: 10.1039/D0TC01401J

Table 1 The molecule formula of phenazine for metal ions sensing

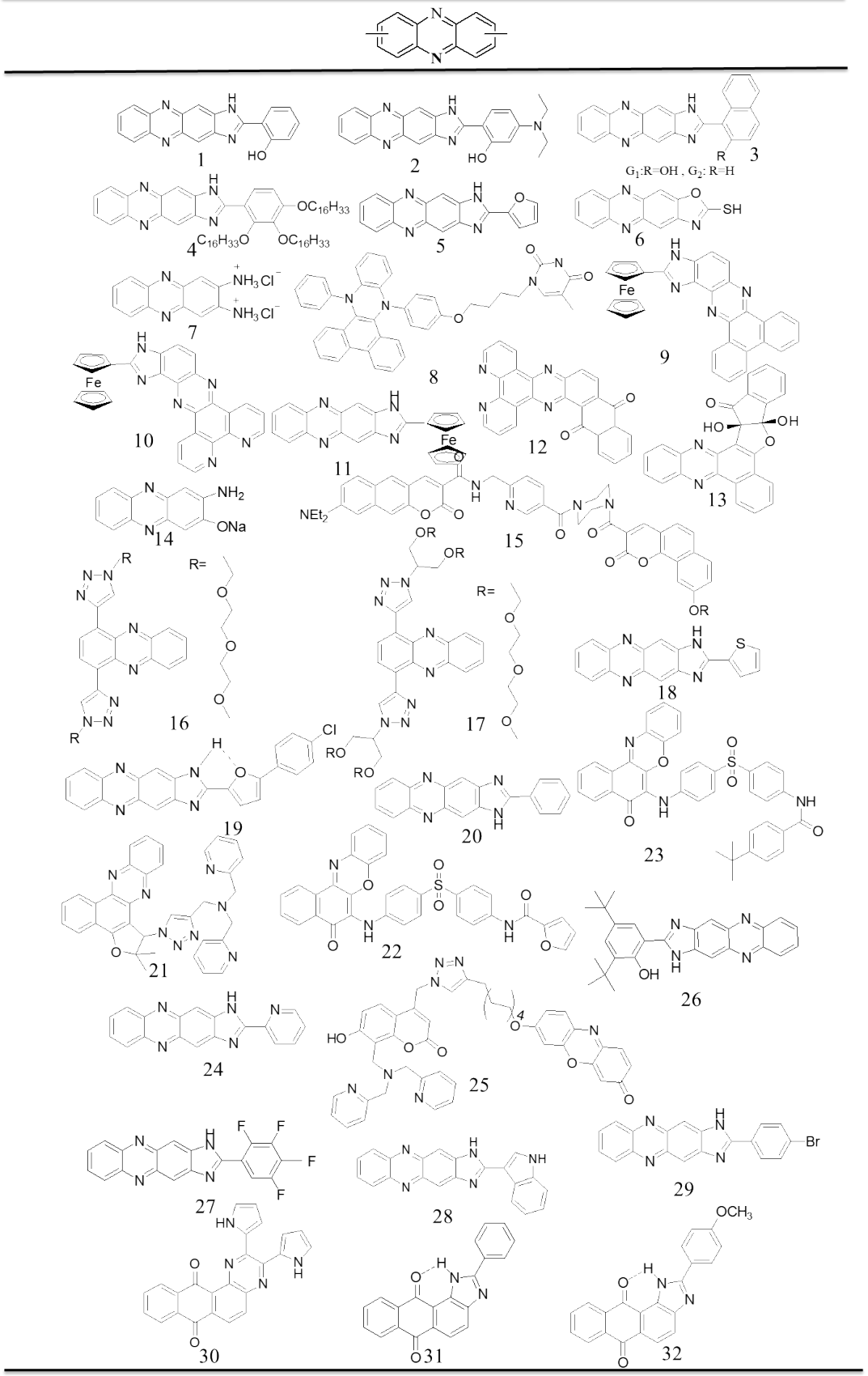

View Article Online
DOI: 10.1039/D0TC01401J

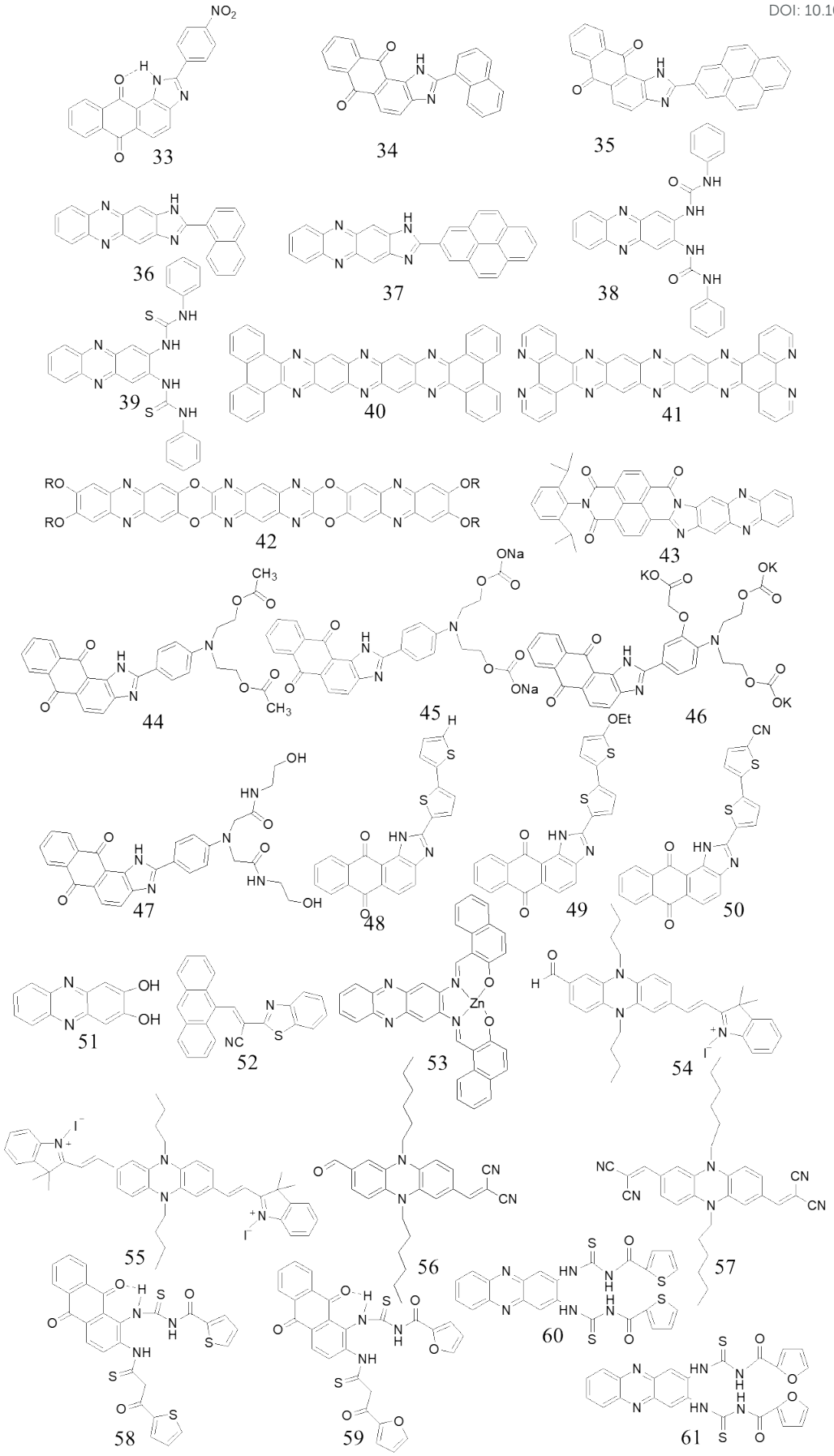

View Article Online
DOI: 10.1039/D0TC01401J

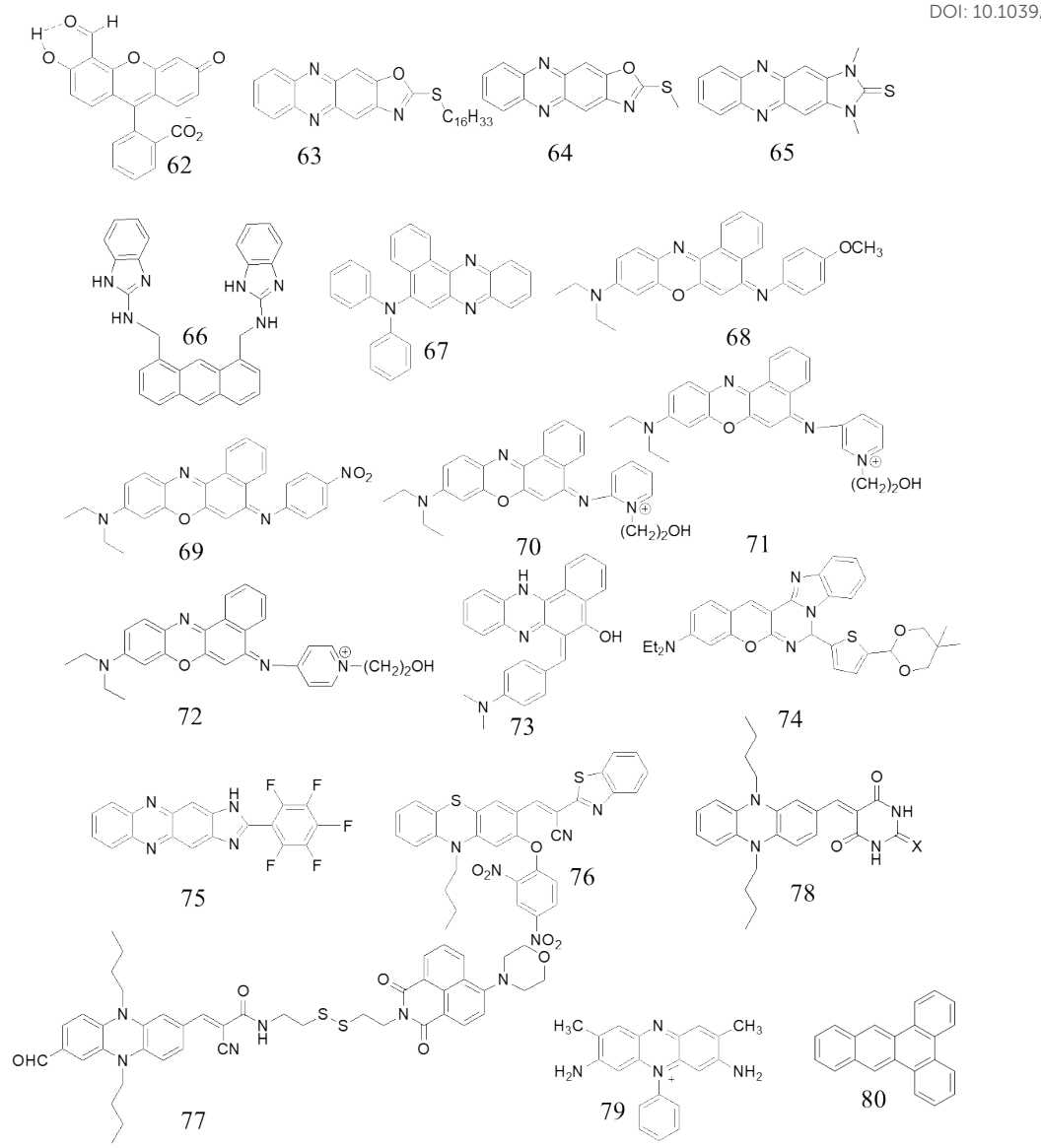

2.0 Sensing metal ions

Phenazine backbone can be modified and adjusted with different functional groups or special ligands, which could flexibly tune charge distribution of the fused aromatic ring, leading to enhancement of optical sensing performance[66]. The outstanding strengths of phenazine backbone enable the phenazine compounds properly propitious candidates as optical sensors. Meanwhile, the colorimetric sensors are more desirable for practical application owning to distinct color-changeable response to the target anions or molecules, which can be identified by naked-eyes[67]. Eventually, the supramolecular forces are garnering many research interests in both theoretical and experimental investigations[68-70]. It is generally known that most of the heavy metal ions play a positive role in various fields, such as metallurgical industry, dyeing industry, and electroplating industry. However,

View Article Online
DOI: 10.1039/D0TC01401J

those common heavy metal ions are the most threatening species in surroundings, which could cause severe damage to human being such as prenatal brain damage, cognitive and motion disorders, and even death. Development of a facile and highly selective method for detecting the toxic metal ions has attracted great concern in the supramolecular field. Delightfully, a good deal of sensors for detecting metal ions with excellent optical properties have been reported.

Among all kinds of metal cations, identifying iron ion has gained increasing interests in supramolecular domain by exploiting the sensing probes with high sensitivity and low detection limits. For example, a novel fluorescence probe 1 was successfully synthesized and explored based on the phenazine derivatives by our group. The synthetic process can be achieved by two steps as given in scheme 1. This probe exhibited preferable fluorescent selectivity and excellent sensitivity to Fe^{3+} over various cations in DMSO solution and excited at 408 nm together with a dramatic fluorescent quenching[71]. After adding 20 equiv. Fe^{3+}, an obvious color change from yellow to dark (fluorescence quenching) was observed, and that can be differentiated by naked-eyes under ultraviolet-visible light (UV-vis). The recognition mechanism of the probe toward iron (Ⅲ)could be considered as metal coordination interaction between functional group of the probe and Fe^{3+}. The phenol O-H turned into the "keto" form, and the functional group with electron donating effect and the phenazine backbone with strong electron-withdrawing effect formed a binding pocket for Fe^{3+} ions. According to the MS spectrum, the corresponding MS signals peaks of the probe-Fe^{3+} complex were found and sensing mechanism was described in scheme 2. The binding constant Ka of the complex was measured as 3.91×10^5 M^{-1} and the lowest limits was determined to be 4.8×10^{-6} M. Afterwards, the prepared test paper was proved to act as available tool for detecting and identifying Fe^{3+} in the environment sample.

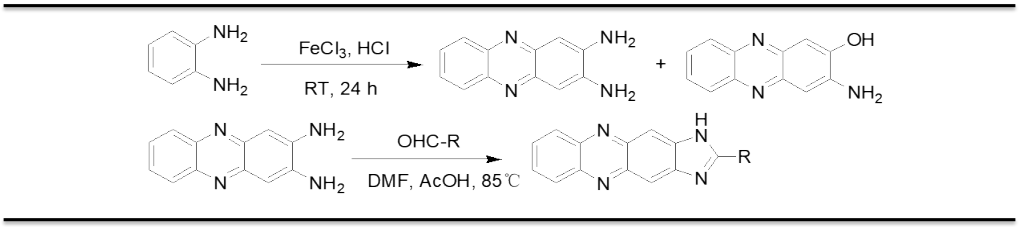

scheme 1 The synthesis of the probe with the imidazole group

View Article Online
DOI: 10.1039/D0TC01401J

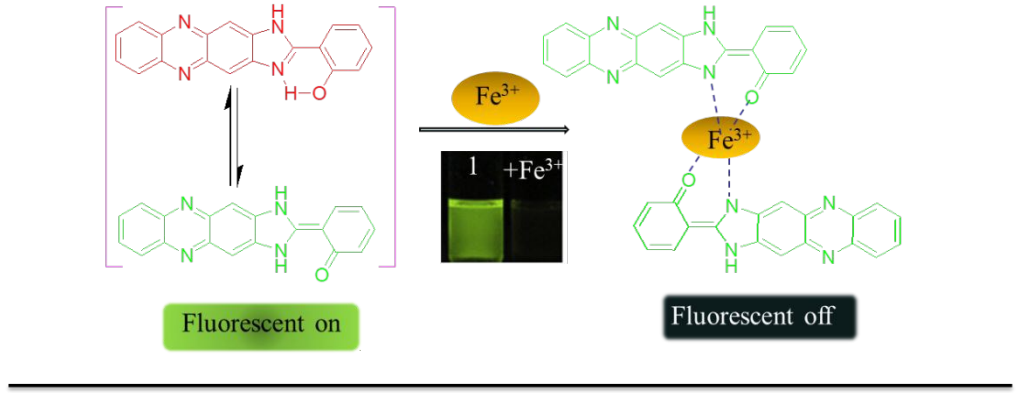

Scheme 2 The sensing mechanism of the probe 1 for detecting Fe^{3+}.Reproduced with permission from reference 71 (Copyright©2013 Elsevier B.V. All rights reserved).

Another probe 2 was designed and synthesized by our group in 2014 through introducing the diethylamino with electron-donating group into the phenazine skeleton. The synthetic routes are described in scheme 1. The probe 2 can selectively detect Fe^{3+} and $H_2PO_4^-$ in dimethyl sulfoxide (DMSO) solution via fluorescence responses[72]. In addition, the probe 2 existed two kinds of tautomeric forms including "enol" form and "keto" form in the presence of Fe^{3+} ion, and its "enol" with no fluorescence emission was principal existing form due to intramolecularly hydrogen bond interaction (OH group and -C=N) in the DMSO solution(as shown in scheme 3). Afterwards, the fluorescent response (FL) of showed that the emission intensity of the probe−Fe^{3+} complex was steadily enhanced with increasement of $H_2PO_4^-$. However, the fluorescence response of the probe 2 could been quenched again after gradually adding the Fe^{3+} ions and this "off-on-off" type response can be repeated for seven times with little energy loss. According to the sensitive experiment, the lowest detection limits of the probe for $H_2PO_4^-$ and Fe^{3+} were determined to be 1.69×10^{-8} mol/L and 4.99×10^{-10} mol/L, respectively. The mechanism was believed to metal coordination interaction and excited state intramolecular proton transfer (ESIPT) process. The recognition procedure of this probe was speculated that the metal-complex was firstly formed among the nitrogen (C=N), oxygen(O−H) and Fe^{3+} ion, then Fe^{3+} was captured by the $H_2PO_4^-$ and coordination compound ($Fe(H_2PO_4)^{2+}$) was obtained. This coordination could release the free probe molecule and recover the fluorescence. To sum up, the sensing mechanism of the probe 2 was very similar to the probe 1. The detailed sensing diagram is shown in scheme 3.

View Article Online
DOI: 10.1039/D0TC01401J

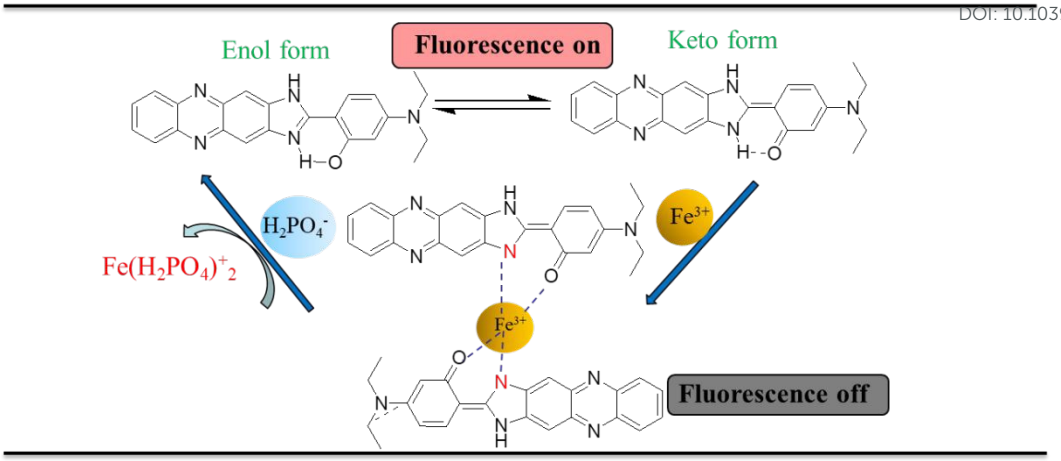

Scheme 3 The sensing mechanism of the probe 2 for detecting Fe^{3+} and $H_2PO_4^-$

When the functional group of diethylamino in probe 2 was replaced by the naphthol ring, another new sensor for recognizing Fe^{3+} and $H_2PO_4^-$ was obtained by our group as the probe 3. Similar to the probe 2, it also has two different existing forms[73]. Certainly, the "Enol" form was much more stable than another one, mainly existing in the solution (as shown in scheme 4). Besides, the probe could exhibit "ON−OFF−ON" fluorescence response for Fe^{3+} and $H_2PO_4^-$ with excellent selectivity and sensitivity in DMSO solution. The detection limit of the probe to Fe^{3+} and $H_2PO_4^-$ were measured to be 2.860×10^{-7} M and 1.866×10^{-7} M, respectively. Interestingly, this probe also can be served as recyclable fluorescence sensing materials. Although, the sensing properties of probe 3 was similar to the probe 2, the low limitation for the Fe^{3+} and $H_2PO_4^-$ was inferior to the former, which illustrated that the electron transition ability or ICT effect of the naphthol group was weaken than the diethyl aminophenol group. The proposed sensing process is shown in scheme 4.

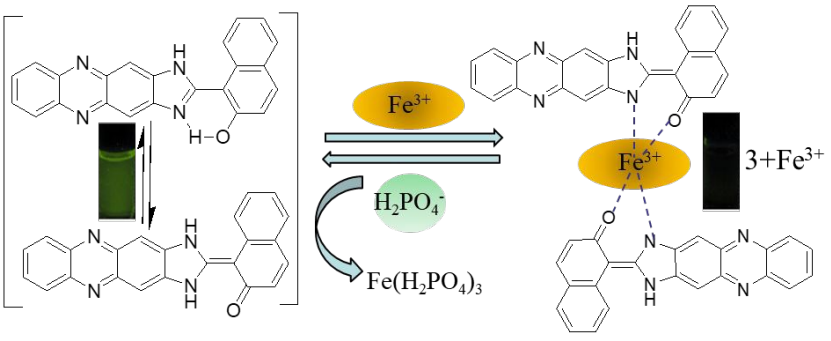

Scheme 4 The sensing mechanism of the probe 3 for detecting Fe^{3+} and $H_2PO_4^-$. Reproduced with permission from reference 73 (Copyright©2015 Elsevier B.V. All rights reserved).

In 2017, the Lin et al.[74] in our research group, designed and developed a new probe 4, namely

imidazole phenazine based on supramolecular metallogel (Gel), which could sever as the $H_2PO_4^-$ acceptor and a recyclable fluorescent intelligent material with high selectivity and excellent sensitivity. To our knowledge, the imidazole phenazine group fixed on this probe worked as binding site, π–π stacking site, and fluorophore. After gradual addition of Fe^{3+} into the organogel, the aggregation induced emission (AIE) of the probe was quenched and a stable metallogel (FeG) was formed with no fluorescence. Interestingly, the fluorescence of the metallogel (FeG) can be recovered by continuously adding $H_2PO_4^-$ anion along with forceful aggregation induced emission (AIE) and an obvious color change from the dark to yellow. The detection limit of this probe for $H_2PO_4^-$ was measured to be 1.0×10^{-6}M. The sensing mechanism was proved the competitive coordination interaction among gelator, $Fe^{3+}$and $H_2PO_4^-$. The authors proposed that the metallogel (FeG) could act as reversible $H_2PO_4^-$sensor and convenient $H_2PO_4^-$ test kits. In addition, the FeG film also could serve as a rewritable fluorescent display material. The detailed sensing process is shown in scheme 5.

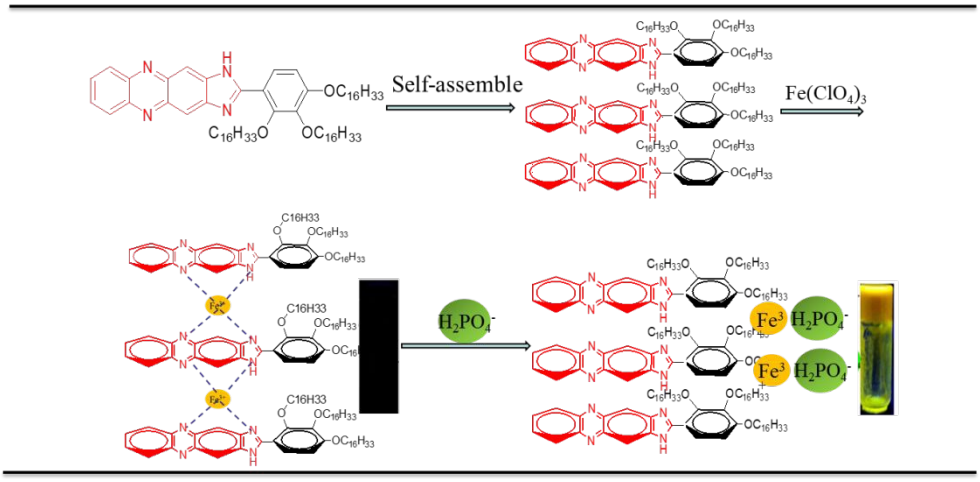

Scheme 5 The sensing mechanism of the probe 4 for detecting Fe^{3+} and $H_2PO_4^-$. Reproduced with permission from reference 74 (Copyright©2017 Elsevier B.V. All rights reserved).

Mercury is one of the extreme toxicity cations, which could bind the thiol groups connected to proteins or enzymes and directly result in the cell apoptosis as well as various clinical manifestation. Nevertheless, the traditional detection methods of the Hg^{2+} mainly depended on the sensors involved with a sulfur group, which leaded to a combination of the Hg^{2+} with sulfur group to obtain the HgS products[75].Also synthetic procedure of the most of the sensors are difficult and costly. To address this issue, our group have designed and developed a new probe based on the phenazine derivative. A furan group with electron-rich group was introduced into phenazine backbone to obtain the probe

5, which showed excellent selectivity and high sensitivity for Hg^{2+} in aqueous solution, exhibiting a clear color change from yellow to jacinth[76]. The detection limit of the probe towards Hg^{2+} was calculated as 1.6×10^{-7} M, and other ions, including Fe^{3+}, Ca^{2+}, Cu^{2+}, Co^{2+}, Ni^{2+}, Cd^{2+}, Pb^{2+}, Zn^{2+}, Cr^{3+}, and Mg^{2+} had nearly no interference on the sensing behavior. Therefore, this probe could act as recyclable components in optical sensing materials after adding the I^- ions. The test strip of probe 5 was prepared, which could be taken as a convenient and efficient Hg^{2+} test kits. The visualized sensing mechanism is depicted in scheme 6.

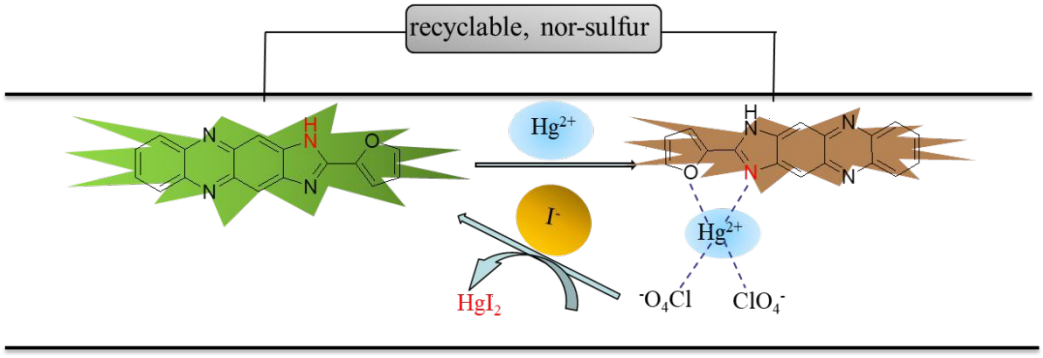

Scheme 6 The sensing mechanism of the probe 5 for detecting Hg^{2+} and I^-.

According to the reaction shown in scheme 1, the functionalized oxazole group was introduced into the phenazine framework as a class of the new sensors for Hg^{2+} ions detection. Generally, the probe was framed with phenazine backbone as a luminophore and a sulfhydryl group acting as recognition sites, and that can be easily synthesized under the mild conditions[77]. The probe presented a distinct blue shift in absorption after adding the Hg^{2+} appearing an obvious color variation from yellow to blue. Furthermore, it also could detect mercury (II) ions in pH range of 2 to 8, which demonstrated that the detection procedure can be conducted in aqueous solution with a wide pH range. The naked−eye detection for the Hg^{2+} revealed that the color of test paper gradually changed from the blue to yellow after continuous addition of Hg^{2+} as presented in scheme 7. The sensing mechanism was considered as metal ligand complex formed between the probe and Hg^{2+}. The detailed sensing procedure is described in scheme 7.

View Article Online
DOI: 10.1039/D0TC01401J

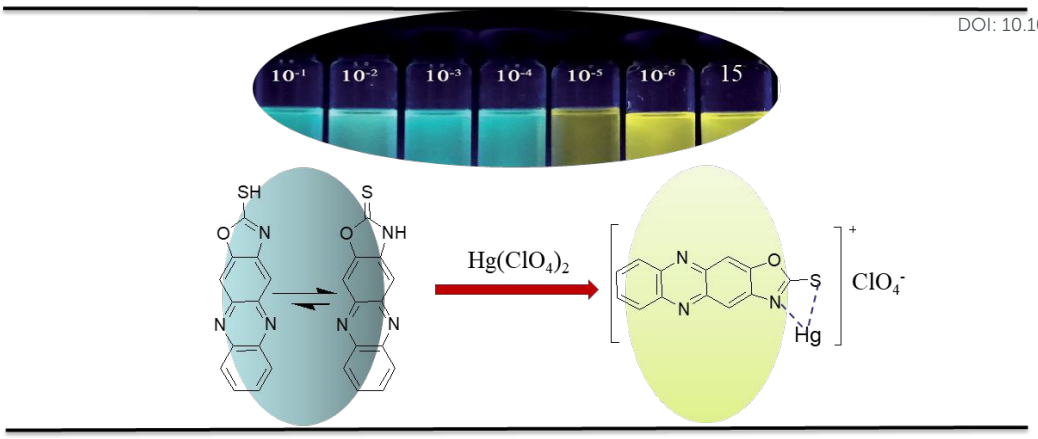

Scheme 7 The sensing mechanism of the probe 6 for detecting Hg^{2+}. Reproduced with permission from reference 77 (Copyright©2017 Royal Society of Chemistry).

Mercury sensing has attracted considerable attention in the ions sensing areas. Recently, our group newly designed and synthesized a probe based on the water-soluble phenazine derivatives. The phenazine hydrochloride (DAPH) was exploited as the probe 7 for detecting and removing Hg^{2+} by dual channel response in natural water resource with excellent selectivity and preferable sensitivity[78]. The colorimetric (Col) sensing response indicated that maximum absorbance band at 260 nm enhanced obviously in the UV–vis spectroscopy after adding the Hg^{2+}. Nevertheless, successively adding the Hg^{2+}, the absorption peaks can approach saturation at 348 nm and the curve descended rapidly accompanied with a significant increasing band centering at 419 nm. Moreover, a remarkable decrease was observed when the concentration of Hg^{2+} reached up to 20 equiv. The color change from dark red to transparent can be captured by the UV lamp at 365 nm. Finally, the low detection limits of the probe for Hg^{2+} was computed to be 1.4 uM and 70 μM via the fluorescent and UV-vis titration, respectively. The detection limits in buffer solution (pH=7.0) we evaluated and the results were close to the above value. The adsorption rate established by the ICP analysis almost reached up to 96.75% in the pure water. The sensing process is described in scheme 8.

Tian et al.[79] exploited a sensing probe 8 based on the phenazine derivatives in light of the superiority of vibration-induced emission (VIE) mechanism. The probe was named as *N*, *N*′-diphenyl dihydrodibenzo [*a*, *c*] phenazine, which could be applied as a scaffold for fabricating sensors. And it was feasible to combine the phenazine backbone with sufficiently designed layout as a scaffold to recognize Hg^{2+} owning to the specific coordination site with certain metal ions by

using the vibration-induced emission (VIE) mechanism. The fluorescence titration experiment was carried out in THF/H_2O solution to explore the sensing performance of the probe for Hg^{2+}(as shown in scheme 9). When the concentration of the Hg^{2+} was up to 2.20 equiv., the dual emission appeared an obvious change. With continuous addition of Hg^{2+}, the absorption band at 470 nm was boosted vastly along with a gradual decrease of intensity in orange-red emission (601 nm) region. These observations demonstrated a perfect application of VIE mechanism for recognizing Hg^{2+}. The sensing process is described as scheme 9.

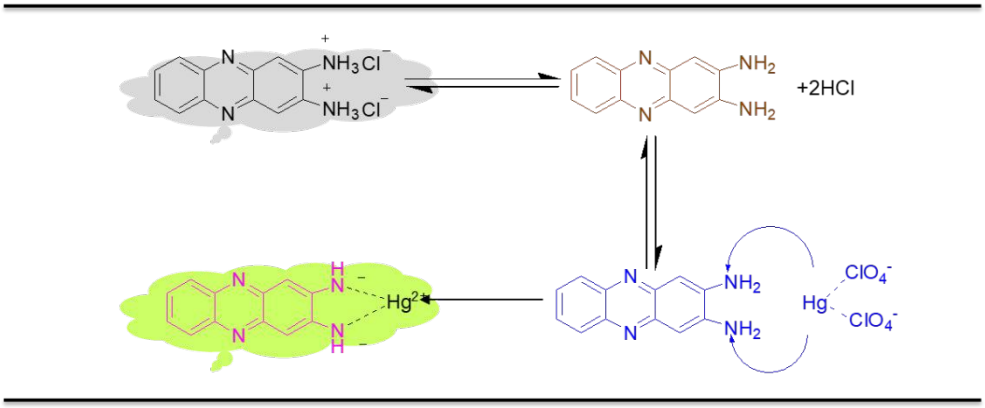

Scheme 8 The sensing mechanism of the probe 7 for detecting Hg^{2+}.

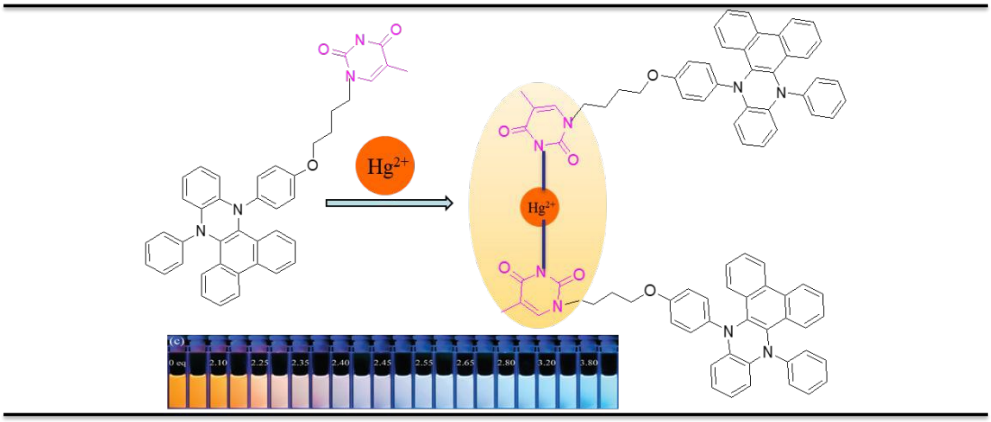

Scheme 9 The sensing mechanism of the probe 8 for detecting $Hg^{2+}$and the fluorescence photographs of adding various equivalent Hg^{2+}. Reproduced with permission from reference 79 (Copyright© 2016 Wiley-VCH Verlag GmbH & Co. KGaA, Weinheim).

Different from the above sensing mechanism of Hg^{2+}, the electrochemistry combined with optical sensing also displayed special superiority for detecting and recognizing Hg^{2+} and others metal ions. For example, the probe 9 and 10 were successfully synthesized and explored by the Pedro Molina et al.[80] based on the ferrocene imidazole phenazine dyads. Those probes delivered an

excellent selectivity and sensitivity for recognizing Pb^{2+} and Hg^{2+} in aqueous solution. The emission band (λ=317 nm) exhibited a distinct fluorescence enhancement (CHEF=47) after adding Pb^{2+}, appearing a new absorption band at 502 nm together with a signal peak of oxidation redox according to the shift ($\Delta E_{1/2}$=230 mV). The linear sweep voltammetry (LSV) studies showed a remarkable shift of the electrochemical response signals after addition of Hg^{2+} in the CH_3CN solution. Those results illustrated that the probe 10 bearing with two fused pyridine rings exhibited preferable selectivity for sensing Hg^{2+} by different channel (such as electrochemical sensing and fluorescent response). The proposed mechanism is depicted in scheme 10.

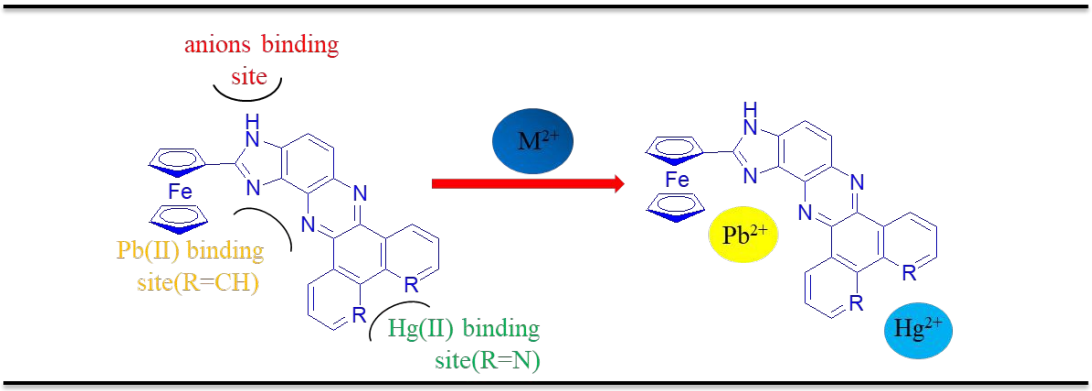

Scheme 10 The sensing mechanism of the probe 9 and 10 for detecting Pb^{2+} and Hg^{2+}.

It is well known that the lead deemed as hazardous ions widely distributes in different fields such as batteries, gasoline and pigments industry. Many researchers agreed that the detection and adsorption of lead ions has become an urgent task. In 2009, a novel ferrocenyl−containing imidazopyridine was introduced into the phenazine structure to obtain the probe 11 for detecting Pb^{2+} which exhibited preferable affinity for Pb (II) ions over other metal ions, and the Pb (II) ions can be monitored by different channels[81]. For example, the probe could be regarded as an excellently selective redox, chromogenic, or fluorescent sensor for sensing metal Pb^{2+}. In the absorption spectrum, the probe 11 was viewed to show an obvious color change from colorless to orange after gradually adding the Pb^{2+}, which provided the potential convenience for "naked eye" detection. Meanwhile, the fluorescence emission spectrum appeared an evident fluorescence enhancement (CHEF) effect and obtained an unprecedented limitation for Pb^{2+} as 2.7 μg L^{-1}. The authors favored the sensing mechanism can be explained as hydrogen bonding interaction between the probe and the ligands (e.g. the solvent and perchlorate anions). The pyridine H−5 and the ferrocene Cp1−H and Cp2−H atoms related to the coordination sphere involved this course of hydrogen bonding. The

detailed diagram of sensing mechanism and calculated structure for complexes is described as scheme 11.

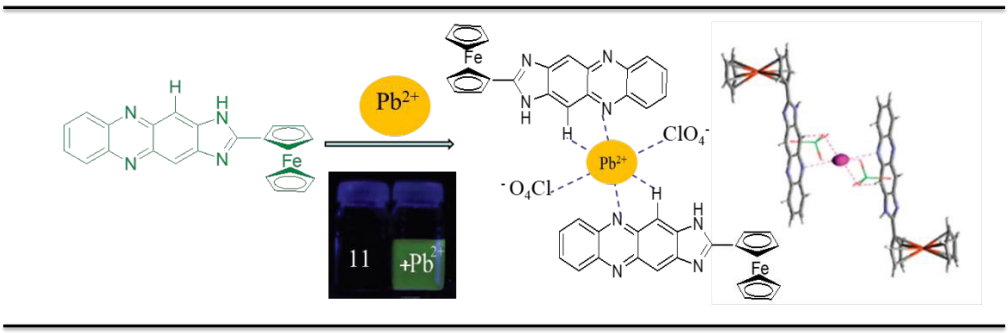

Scheme 11 The sensing mechanism of the probe 11 for detecting Pb^{2+}. Reproduced with permission from reference 81 (Copyright©2009 American Chemical Society).

In 2016, the derivative of 1,10-phenanthroline was firstly constructed by the Atashbar et al.[82] on basis of fused benzene rings and treated as an electrode sensitive layer for detecting the heavy metal Pb^{2+}. This compound can be applied as the probe 12 fixed on electrodes (Ele) to sense the Pb^{2+}, which achieved a nice electrode performance to quantificationally determine the concentration of lead ions by controlling the electrochemical parameter such as working counter and reference electrode. The cyclic voltammetry signals of the probe were noticed in reduction peaks at 0.2 eV, and the average peak currents altered 87%. The maximum concentration of Pb^{2+} ions was determined to be 50 μM in this system. The results illustrated that it might be advantageous for selectively identifying the poisonous heavy metal ions by combining the traditional electrochemical technology with synthesized chemicals. The sensing mechanism is pictured in scheme 12.

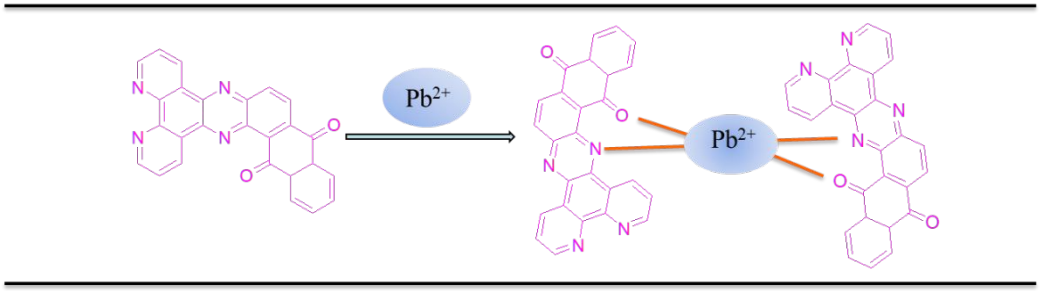

Scheme 12 The sensing mechanism of the probe 12 for detecting Pb^{2+}

In recent, Khurana et al.[83] have synthesized a sensor as a novel probe 13 by connecting the phenazine with indenofuran moieties for detecting metal ions Pb^{2+} and Cu^{2+}. This probe displayed a good selectivity for Cu^{2+} and Pb^{2+} in presence of other interference ions with occurrence of two different absorption band centering at 250 to 300 nm and 404 nm, respectively. After addition of

metal ions, a distinct color variation was viewed from the pale yellow to light yellow under the UV-vis light (as shown in scheme 13). The fluorescence quenching was found after gradual increment of Cu^{2+} and Pb^{2+} (0–1.0equiv.), which was attributed to the coordination effect of probe and metal ions. Interestingly, the fluorescence response could be recovered by adding the EDTA salts to form the EDTA-M complex and released the free probe 13. The low detection limits of the probe for Cu^{2+} and Pb^{2+} was measured to be 3.98 μM and 1.32 μM, respectively. The detection diagram is shown in scheme 13.

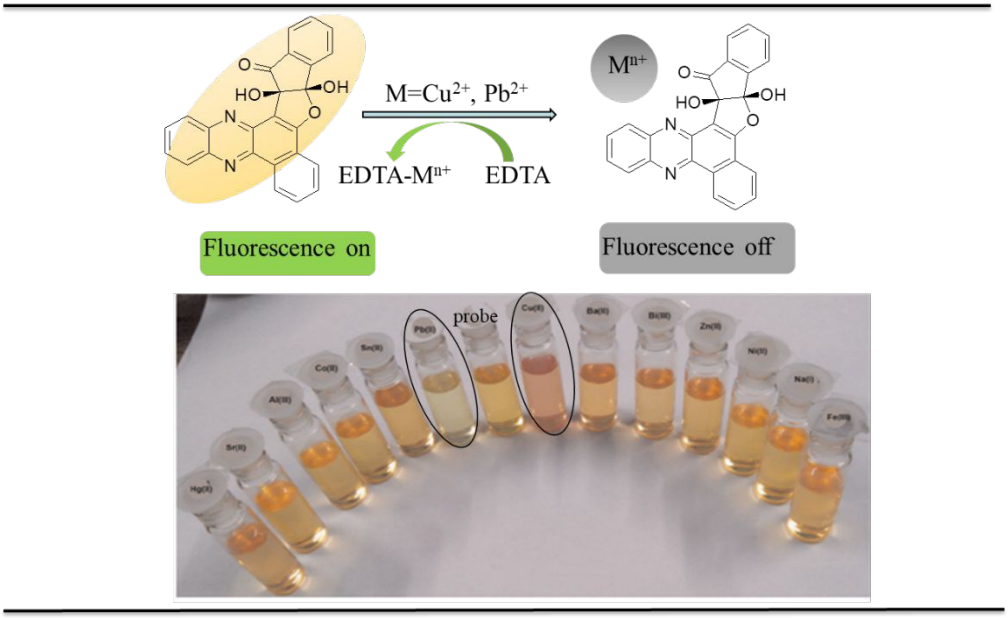

Scheme 13 The sensing mechanism of the probe 13 for detecting Pb^{2+} and Cu^{2+}. Reproduced with permission from reference 83 (Copyright©2015 Elsevier B.V. All rights reserved).

The phenazine compound with high water solubility was explored as the novel probe 14 for recognizing Cu^{2+} ions because most of the toxic ion or molecule existed in the aqueous solution. The probe 14 exhibited excellent selectivity and preferable sensitivity for detecting and removing Cu^{2+} in natural water through the double channel (colorimetric/fluorogenic detection) with a rapid, low cost and high effective sensing performance[84]. The lowest detection limits for Cu^{2+} was measured to be 7.6×10^{-6} M and 2.2×10^{-7} M by using the UV–vis and fluorescence titration. What's more, the eliminating efficiency of Cu^{2+}could almost reach up to 76%. The available test papers were fabricated, which illustrated that the probe was possible to detect and remove Cu^{2+}. The interaction mechanism of probe for Cu^{2+} may be attributed to the metal coordination broking the hydrogen bonds as well as weaken the NH–π and π–π stacking interactions. The interaction process is shown in scheme 14.

View Article Online
DOI: 10.1039/D0TC01401J

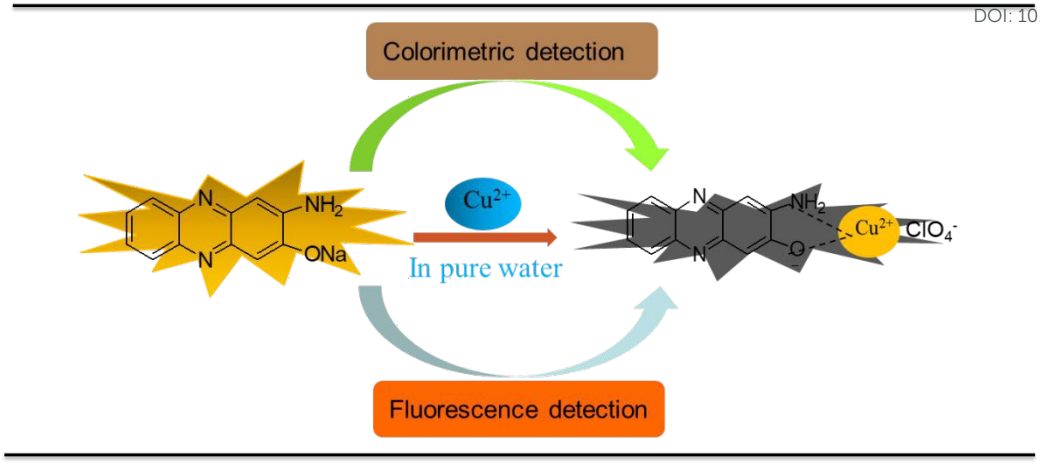

Scheme 14 The sensing mechanism of the probe 14 for detecting Cu^{2+}.

The probe 15 was fabricated by Cho et al.[85] based on the coumarin with phenazine derivative framework, which presented a good selectivity and sensitivity for sensing Cu^{2+} in vitro and in living organisms. The probe appeared an obvious yellow fluorescence enhancement centering at 555 nm as a result of an effective FRET process, which could activate the charge transform from the coumarin to the sulfonyl benzoxadiazine. In addition, the probe featured a ratiometric fluorescence response for sensing Cu^{2+} in company with decreasing of the original fluorescence emission. And a new band centering at 460 nm was viewed after interacting with Cu^{2+}. Likewise, the probe appeared two distinct fluorescence emission bands containing phenazine backbone with the π-extended effect located at blue emission section and red emission scope. As a result, this probe was applied to detect Cu^{2+} in the real colon tissues. The observations demonstrated that the probe could be effective for tracking the Cu^{2+} in the living tissues. The images of sensing Cu^{2+} are shown in Fig 1.

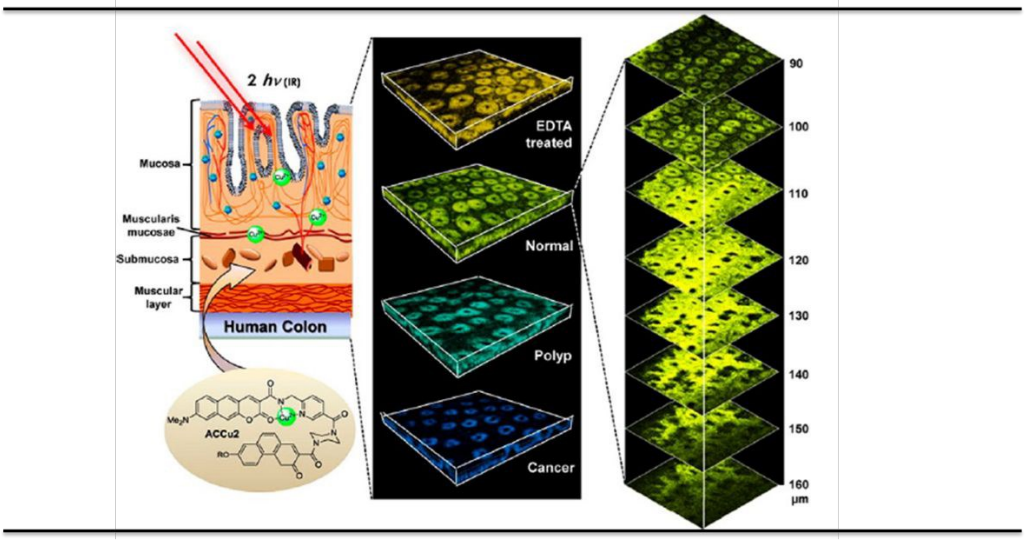

Fig 1. (left) 3-Dimensional ratiometric TPM images of EDTA treated normal, normal, polyp, and

colon cancer tissues labeled with probe 15 (20 μM) at a depth of 90−160 μm with magnification at 20×. This depth corresponds to the mucosal and submucosal layers of clinical importance. (right) Ratiometric TPM images of normal colon tissue at different depth. The images shown are representative images out of 50 sectional images obtained a depth of 90−160 μm. Reproduced with permission from ref 85 (Copyright ©2014 American Chemical Society).

The redox performance of phenazine derivatives have attracted a great deal of interests in developing potential sensors. Some sensors for silver ion identification was reported a few on basis of fluorescence response properties in early time. In 2012, Bunz et al.[86] have designed and synthesized various water-soluble phenazines derivatives based on ethoxylated and bis-triazolyl cycloadducts acting as the probe 16 and 17 with fluorescence response. These probes could be used for detecting Ag^+ ions, which presented a preferable binding ability with Ag^+ by coupling with nitrogen atom of the phenazine ring (as shown in scheme 15). The authors considered the hydrophilic arms of the two probes offered excellent water solubility, and the triazole group could construct a charming binding pocket for Ag^+ by using the N atoms of the thiadiazole. Meanwhile, the hyperchromic effect of the triazole units enhanced the luminescence properties of the probe 16 and 17. Upon the addition of the Ag^+ ions, a prominent color variation was observed from the blue/green region to the yellow range (as shown in scheme 15). The sensing mechanism can be attributed to the participation of the triazole ring resulting in the binding affinity enhancement. The binding constant K of probe 16 and 17 for Ag(I) was measured to be log K = 3.75 ± 0.09 and log K = 2.84 ± 0.02, respectively. Eventually, the controlled experiment was used to verify the significance of triazole as the binding elements and interaction sites. Although bonding constant of the controlled probe was similar to the probe 16, the sensing performance of the alkylated phenazine was inferior to the probe 16 and 17.

View Article Online
DOI: 10.1039/D0TC01401J

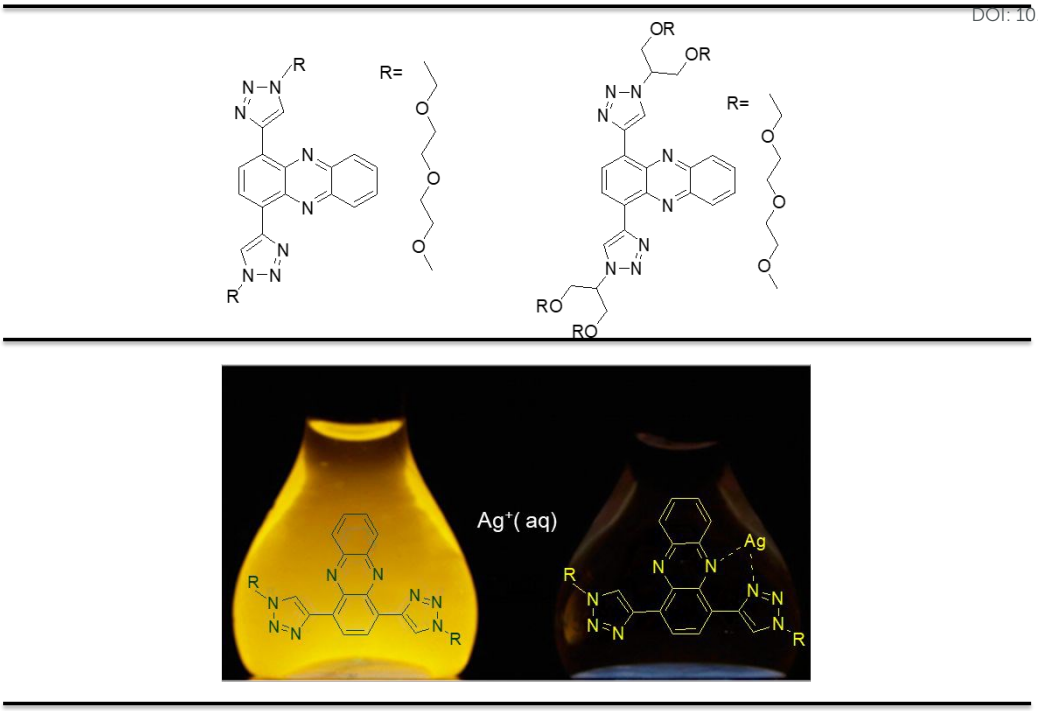

Scheme 15 The sensing mechanism of the probe16 and 17 for detecting Ag^+. Reproduced with permission from reference 86 (Copyright©2015 American Chemical Society).

In 2016[87] and 2017[88], our group successively developed and synthesized various novel sensors for identifying Ag^+. The thiophene−functionalized as well as the furan functionalized introduced into the phenazine structure obtained the target probe 18 and 19. The sensing mechanism of probe 18 for Ag^+ involved in metal ligand complex and competition interaction among the self−assembly of the probe molecules (as shown in scheme 16). This novel interaction mechanism enabled the probe 18 exhibit excellent sensitivity and high selectivity for Ag^+. The detection limit of probe 18 for Ag^+ was determined to be 8.75×10^{-7} M and 8.18×10^{-9} M by the UV-vis and fluorescence spectrum, respectively. However, the probe 19 laid out the rapid color response from the yellow to shallow orange distinguished by the naked−eye after adding the equivalent Ag^+. The sensing process was regarded as a sequence dependent molecular keypad lock by using I^- as the key, which was different from the probe 18. The lowest detection limit of the probe 19 was measured as 4.07×10^{-7} M and 3.84×10^{-7} M according to the UV-vis and fluorescence titration. It was not as good as the former (probe 18) by comparing the detection performance. Furthermore, the recyclable recognition performance of probe 19 was needed to improve in the coming years. Finally, the authors provided a simple sensing mechanism for probe 19, indicated that the complex of probe-Ag^+ played a key

role in the continuous identification as a "ON−OFF−ON" fluorescence switch. The sensing process is pictured in scheme 17.

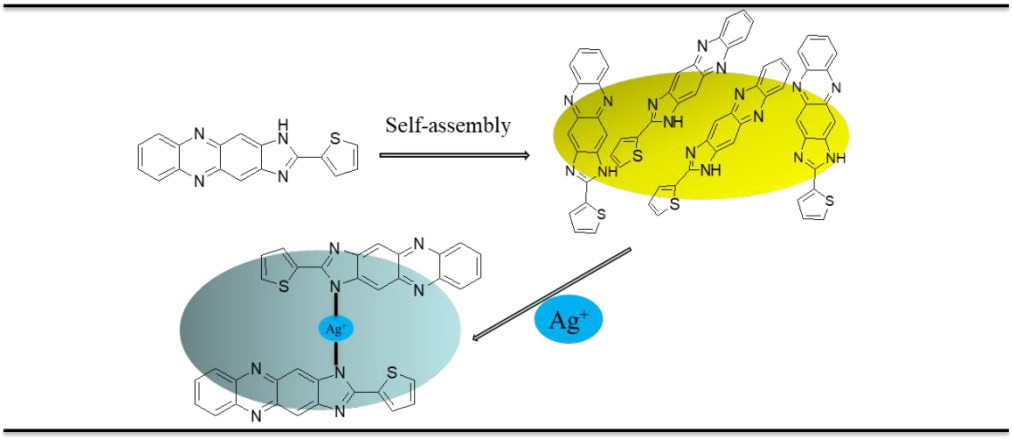

Scheme 16 The sensing mechanism of the probe 18 for detecting Ag^+

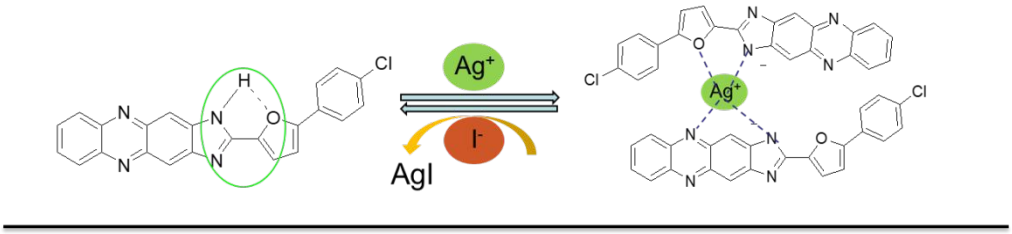

Scheme 17 The sensing mechanism of the probe 19 for sensing Ag^+ and I^-

Most of the fluorescent sensor molecules were modified with a fluorophore and binding sites for anions detection or cations identification. For instance, our group recently synthesized and explored a novel phenazine derivative by connecting the 2,3-diamino-phenazine and benzaldehyde to achieve the target probe 20[89-90]. The general synthetic scheme of the probe 20 is shown in scheme 1 by using the DMF solvent and acetic acid as catalyst. The phenyl group introduced into the imidazole ring could not only enhance fluorescence emission, but also display multiple responses properties to CN^-, Ag^+ and I^- with high sensitivity and selectivity over a lot of cations and anions in DMSO aqueous solution. After addition of CN^-, a visible color change was found from pale yellow to pink in absorption spectra. And fluorescence change was also observed from yellow to dark blue at the excitation (λ=428 nm). The sensing mechanism (as shown in scheme 18) was considered as the self−assembly of π−π stacking of phenazine cores and intermolecular hydrogen bonds interaction by the deprotonating process. However, gradually adding the Ag^+, evident color change was captured by the naked-eyes (e.g. from the light blue to yellow in the UV−vis responses and the green to blue under the fluorescent emission). Those observations demonstrated that the probe 20

was different from the above others sensor and can be used to detect simultaneously the multiple ions in various solutions. Finally, the interaction modes of probe with Ag^+ was speculated the π−π stacking was broken after adding Ag^+. The diagram is described in scheme 18.

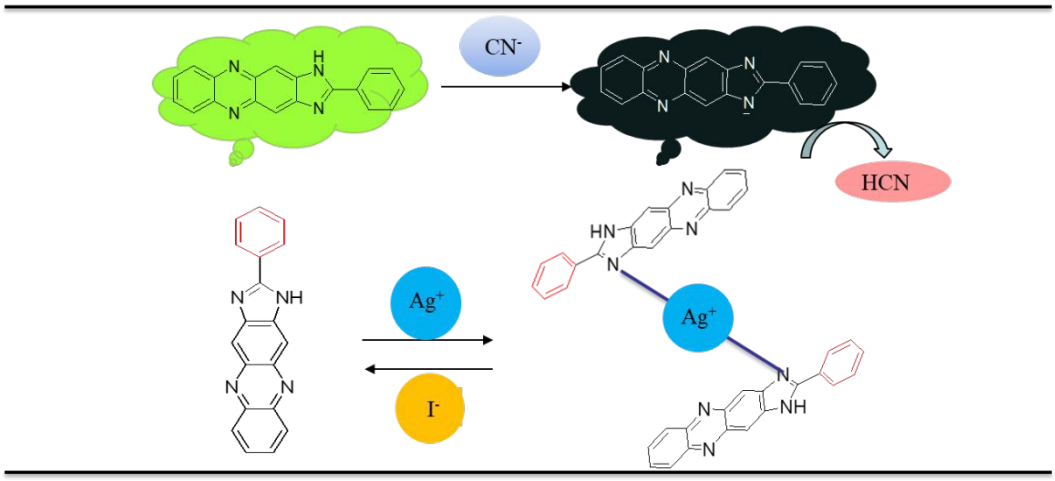

Scheme 18 The sensing mechanism of the probe 20 for detecting Ag^+ and CN^-

Among all kinds of metal ions, cadmium (Cd) was well known for a poisonous metal ion in the environment. In 2014, a 1,2,3−triazole luminescent probe 21 was developed and synthesized by the Júnior et al.[91] based on the natural product lapachol. The fluorescence properties of the probe 21 have been investigated in the presence of a series of metal ions (Cd^{2+}, Ca^{2+}, Co^{2+}, Cu^{2+}, Fe^{3+}, Hg^{2+}, Mg^{2+}, Na^+, Ni^{2+}, Ag^+, Pb^{2+}, Zr^{2+}, and Zn^{2+}). The results proved that the probe could merely recognize the Cd^{2+} in the H_2O/CH_3CN (8.5:1.5 v/v) medium. Meanwhile, an obvious color change was noticed from the blue to green under the ultraviolet excitation (as shown in scheme 19), which illustrated that it can be acted as a sensor for Cd^{2+} identification by the naked eyes observation. Furthermore, the emission spectrum exhibited a redshift from 454 nm to 515 nm and presented a prominent hyperchromic effect. The interaction mechanism was believed to undergo metal coordination interaction rather than a fluorescence quenching of photoinduced electron transfer (PET). The proposed interaction mode is described in scheme 19.

View Article Online
DOI: 10.1039/D0TC01401J

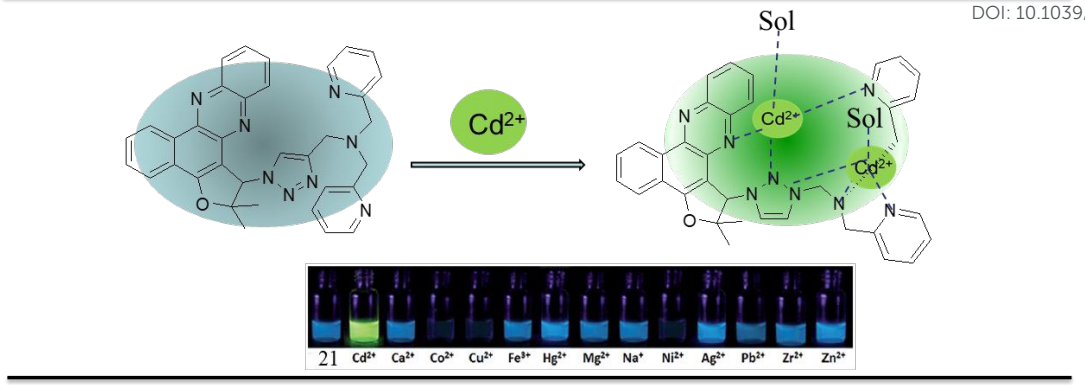

Scheme 19 The sensing mechanism of the probe 21 for detecting Cd^{2+}. Reproduced with permission from reference 91 (Copyright©2014 Wiley-VCH Verlag GmbH & Co. KGaA, Weinheim).

In 2020, Yoo et al.[92,93] reported the novel synthesis based on the *N*-(4-((4-((5-oxo-5*H*-benzo[*a*]phenoxazin-6-yl)amino)phenyl)sulfonyl)phenyl)furan-2-carboxamide and [(4-(tert-butyl)-*N*-(4-((4-((5-oxo-5*H*-benzo[*a*]-phenoxazin-6-yl)amino)phenyl)sulfonyl)phenyl)benzamide)], which could be applied as a good fluorescence probe 22 and 23 for selective detection of Cd^{2+}, CN^{-} and Ba^{2+} ions in CH_3CN/H_2O (99:1 v/v) system. As far as we known, the probe 22 was the first fluorescence probe for detecting Cd^{2+} and CN^{-} ions based on "turn-on" and "turn-off" type fluorescence response generated by the metal ions. After adding Cd^{2+}, 130-fold fluorescence enhancement was noticed, which can be ascribed to the charge transfer (ICT)effect between the lone electron pair and amide groups (–NH) of the phenoxazine moiety. The reversibility of the probe displayed commutative increasing and decreasing of fluorescence intensity by continuously adding Cd^{2+} and CN^{-}. Since the lone pair electrons was available in nitrogen and oxygen atoms, which made the metal coordination interaction easily formed between the probe and ions. The sensing mechanism of probe 22 for Cd^{2+} was agreed to ICT effect (inducing the formation of the metal complex and inhibiting the fluorescence enhancement). The rigorous sensing mechanism was shown in scheme 20. Moreover, the authors evaluated its toxicity to cancer cells (MCF−7) by performing MTT test and further used to track the Cd^{2+} in zebrafish to investigate practical application of the probe in the living. The photographs of confocal images of sensing Cd^{2+} are shown in Fig 2.

View Article Online
DOI: 10.1039/D0TC01401J

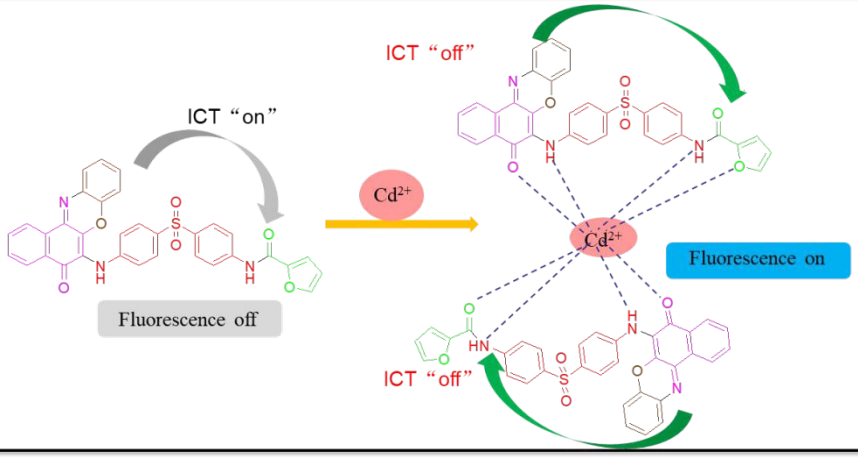

Scheme 20 The sensing mechanism of the probe 22 for detecting Cd^{2+}

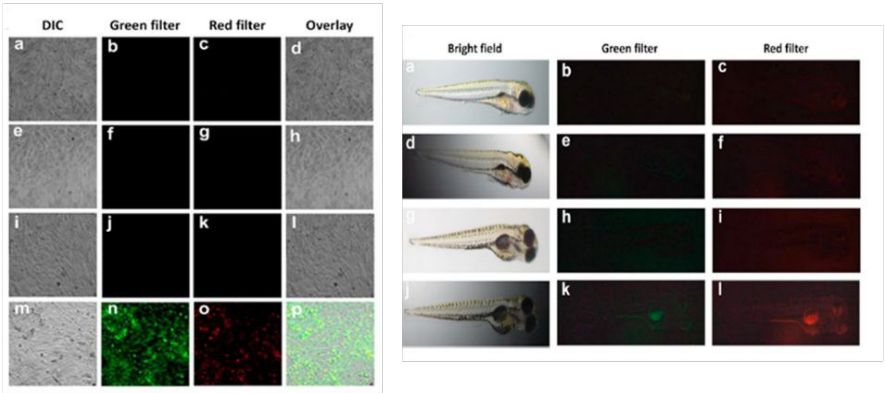

Fig 2. (a) Fluorescence confocal images of sensing of Cd^{2+} and probe 22 in MCF−7 cells. The images a–d belongs to the control cells of MCF−7. The images e–h goes to the cells incubated with Cd^{2+} salt solution (6.25 μM). Images of i–l respect to the cells incubated with the probe (12.5 μM). At last, the images m–p goes to the cells incubated with Cd^{2+} salt solution (6.25 μM) and the probe 60 (12.5 μM). (Excitation wavelength: 470 nm for green channel, 550 for red channel; Emission wavelength: 480–530 nm for green channel;560–610 nm for red channel); (b) Confocal images of detection of probe and Cd^{2+} in zebrafish larvae. The images are arranged into four rows and three columns. The images a–c belongs to the control zebrafish. The images d–f goes to the zebrafish incubated with the ligand NPC (12.5 μM). Images of g–i represent the zebrafish incubated with Cd^{2+} (6.25 μM). Images j–l goes to the zebrafish incubated with the probe (12.5 μM) and Cd^{2+} salt solution (6.25 μM). (Excitation wavelength: 550 nm for green channel; 630 nm for red channel; Emission wavelength: 580 nm for green channel; 660 nm for red channel). (For the understanding of the references to color in this figure legend, the reader is referred to the web version of this article). Reproduced with permission from reference 92 (Copyright © 2019 Elsevier B.V. All rights reserved).

Different from the probe 22, the probe 23 exhibited outstanding sensing selectivity for detecting Ba^{2+} in the presence of various metal ions. The ^1H NMR titration experiment suggested that the probe 23 have an excellent binding attraction to Ba^{2+}. The 1:1 binding stoichiometry also

could be achieved by UV/vis spectra according to the Benesi−Hildebrand curve. The lowest limitation of the probe to Ba^{2+} was measured to be 0.282 μM by using the linear fitting equation according to the fluorescence titration assay. Moreover, the probe 23 could obtain a good linear relationship at 535 nm fluorescence emission. And, a possible sensing mechanism of forming the probe 23−Ba^{2+} complex was proposed to ICT process, producing a weak fluorescence emission in the free probe 23 as shown in scheme 21 (After gradually adding Ba^{2+}, −NH and −C=O attacked Ba^{2+} by using the metal coordination interaction and produced an intensive ICT effect and fluorescence enhancement response). Bioimaging in living cell (MCF−7 cells) verified the cell permeability of the probe was good. Meanwhile, the sensing Ba^{2+} in the MCF-7 cell illustrated its practical application was feasible in the living. The fluorescence photographs are collected in Fig 3.

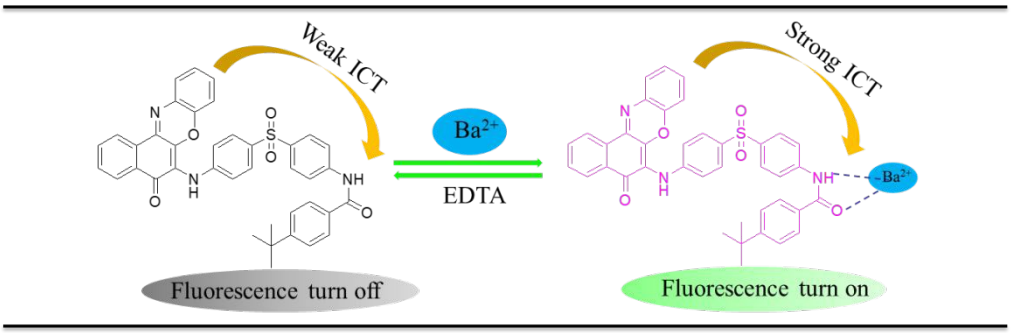

Scheme 21 The sensing mechanism of the probe 23 for detecting Ba^{2+}

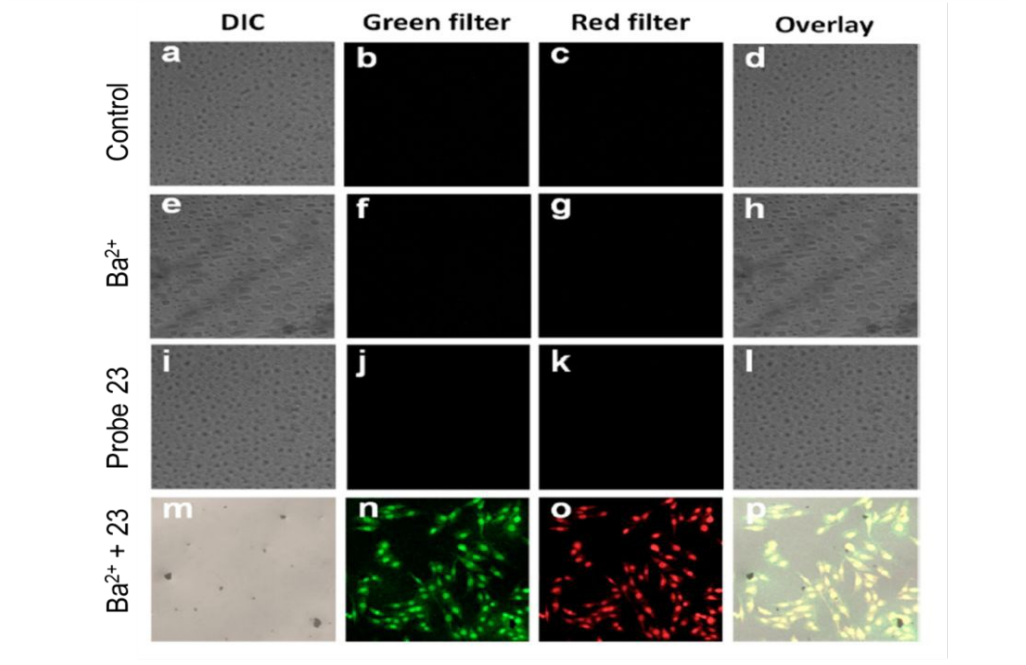

Fig 3. Confocal fluorescence images of detection of probe 23 and Ba^{2+} in MCF−7 cells. The figures are divided into four rows; four columns. The images lie in a separate column goes to a particular

filter written on the top of the column. The images a−d respect to the control cells, images e−h belongs to the cells treated with Ba^{2+} (0.781 μM). The images of i−l belong to the cells treated with probe 61 (0.781 μM) finally, images m−p are of the cells treated with Ba^{2+} (0.781 μM) and probe (0.781 μM). (Excitation: 480 nm for green filter, 560 for red filter; Emission collected: 490−540 nm for green filter; 570−620 nm for red filter). Reproduced with permission from reference 93 (Copyright ©2019 American Chemical Society).

As we all known, the pyridine group is one family member of aromatic compound which has strong electron−withdrawing effect. Recently, our group reported a novel probe 24 bearing with 2−Pyridine−1*H*−imidazo[4,5−*b*] phenazine[94], which exhibited nice fluorescent response to Zn^{2+} and $H_2PO_4^-$. The sensing profiles of probe 24 (15 equiv.) towards various ions were mainly investigated by the double channel (colorimetric and fluorescent response). The absorption spectrum of this probe showed two absorption peaks at 418 nm and 509 nm, respectively. After adding 40 equiv. of $H_2PO_4^-$, a dramatic color change was noticed from red to yellow. And continuous addition the $H_2PO_4^-$ to the probe 24−Zn system, the complex was disintegrated leading to the pyridine and phenazine units almost coplanarity via the conformational transition. Thus, the $H_2PO_4^-$ could prohibit the electron transfer of ICT due to the interactions between $H_2PO_4^-$ and Zn^{2+}. The proposed sensing mechanism is advertised in scheme 22.

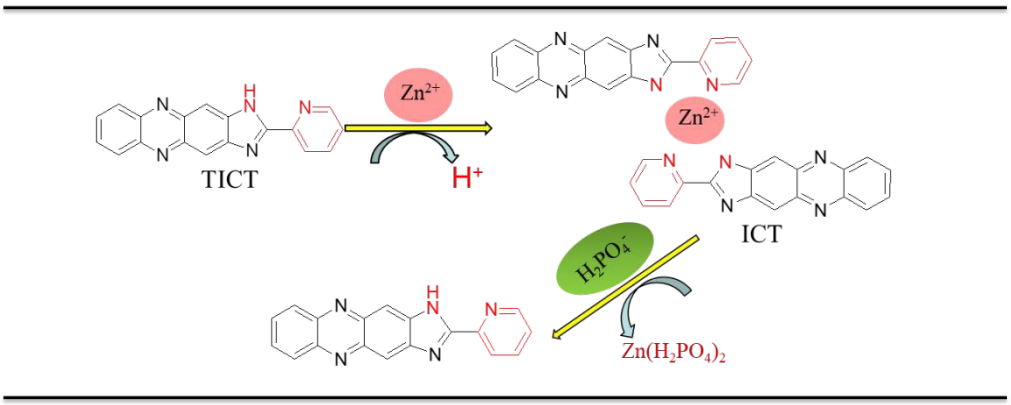

Scheme 22 The sensing mechanism of the probe 24 for detecting Zn^{2+} and $H_2PO_4^-$

In 2012, Nam et al.[95] developed a special phenazine compound serving as probe 25, and this probe was constructed by connecting blue fluorescent umbelliferone with an energy-accepting chromophore. The probe 25 could be acted as a fine sensor for detecting Zn^{2+} in DMSO aqueous solution. After binding zinc ion, the fluorescence "turn on" response of the umbelliferone emission was enhanced through meal-complex by suppressing the PET process[96] (intramolecular photoinduced electron transfer) and facilitating resonance energy transfer to the energy acceptors.

As the authors speculated, the changes did not cause a distinct sensitization fluorescence. The fluorescence emission spectra illustrated that probe 25 endowed high selectivity and special sensitivity for detecting Zn^{2+} ions. The sensing mechanism of probe 25 was explained to intramolecular electron transfer as well as energy transfer by exploring the photophysical perfoemance, such as the steady-state and transient photoluminescence spectrum. The detailed sensing process is depicted in scheme 23. Finally, the probe was confirmed to be available in biosensing by detecting Zn^{2+} in intracellular of the live HeLa cells. The corresponding photographs are laid out in Fig 4.

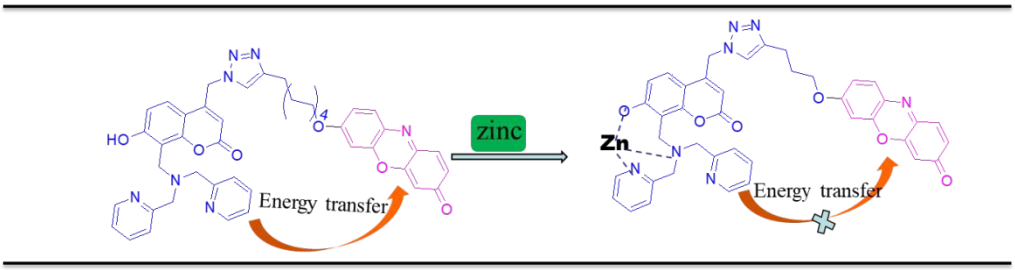

Scheme 23 The sensing mechanism of the probe 25 for detecting Zn^{2+}

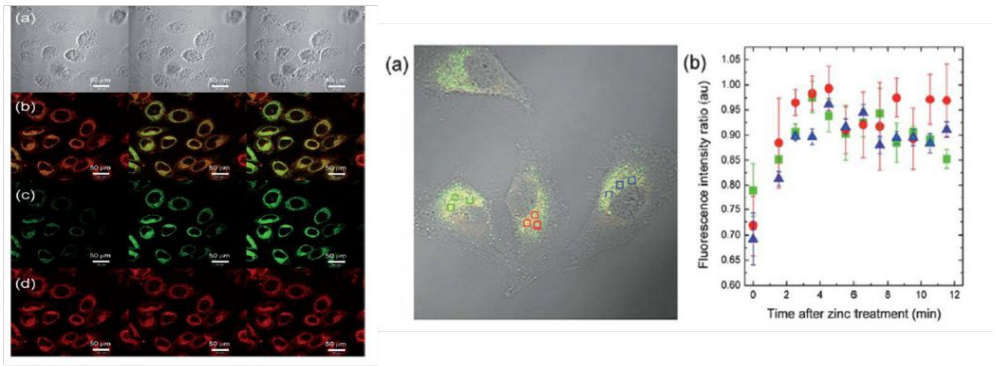

Fig 4. Fluorescence microscopy imaging of live HeLa cells incubated with probe 25 at left: left column, before treatment with Zn PT; middle column, 5 min after treatment with Zn PT; right column, 15 min after treatment with Zn PT. (a) DIC images. (b) Merged images. (c)Fluorescence images obtained through the green channel (430–522 nm). (d) Fluorescence images obtained through the red channel (603–656 nm). scale bar=50 mm. (a) An overlay of the DIC and fluorescence micrographs of live HeLa cells obtained 12 min after zinc treatment. (b) Time-dependent changes in the fluorescence intensity. Reproduced with permission from reference 95 (Copyright @ The Royal Society of Chemistry 2012).

Wu et al.[97] designed a new compound based on the AIE effect by connecting the imidazole moiety bearing with substituted salicylaldehyde with 2,3-diaminophenazine. This compound could act as the novel probe 26 with a ‘‘turn-on’’ fluorescein response for sensing Al^{3+}. The studies of absorption spectrum of the probe 26 presented an obvious fluorescence enhancement after gradually

adding Al^{3+}at the maximum exciting band 430 nm. And also, others cations did not show strong fluorescence response. The fluorescence emission intensity of probe increasingly enhanced upon the addition of Al^{3+} (0.2-4.0 equiv.) saturated at 4.0 equiv. Those results suggested that the probe can selectively detect Al^{3+} with no interference. Interestingly, the reusability of the probe was investigated with EDTA titration. After gradual addition of EDTA to the solution of probe 26-Al^{3+} complex, a fluorescence quenching was observed. And this recycling can be repeated by continuous addition of Al^{3+} ions and EDTA, which appeared "on-off-on" type fluorescence response. The sensing mechanisms were believed to aggregation effect of Al^{3+} ions with probe molecules and van der Waals forces. The detailed interaction process is described in scheme 24. Finally, the authors applied the probe 26 to detect Al^{3+} in the live cell with RAW264.7. The images are collected in scheme 24.

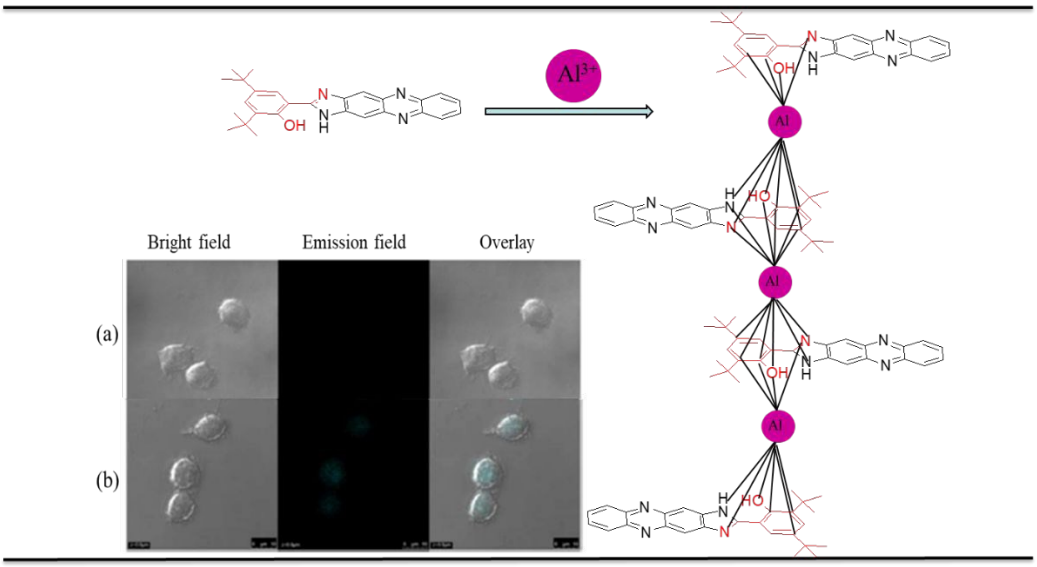

Scheme 24 The sensing mechanism of the probe 26 for detecting Al^{3+} and confocal fluorescence images of Raw264.7 cells. (Left) Bright field image;(Middle) Emission field image and (Right) merged image. (a) Control; (b)The cells were incubated with probe (100μM) and Al^{3+} (20μM) for 30 min. Images were taken at λem=510 nm. Reproduced with permission from reference 97 (Copyright© 2017 the Royal Society of Chemistry).

In general, the probes for sensing Fe^{3+}, Hg^{2+}, Ag^{+}, Cu^{2+}, Cd^{2+}, Pb^{2+}, Zn^{2+}, $Ba^{2+}$and Al^{3+} in various solutions are summarized on basis of the structural features, optical properties and bioimaging. The comparison of sensing performance among probe 1-26 have been made as shown in Table 2, which fully explained that the different functional groups connected with phenazine backbone have large effects on the metal binding ability and further influence the sensing properties.

The sensing mechanism of those probes was generalized as metal coordination interaction and intermolecular charge transfer (ICT) effect. It is expected the application of obtained probe in metal ions sensing could offer empirical reference for exploring novel probes in the coming years.

Table 2 Comparison of different the probes for sensing various ions

Number	Ions	limitation(M)	Solvent	Sensing mode	Ref
1	Fe^{3+}	4.8×10^{-6}	DMSO	FL	71
2	Fe^{3+}	4.99×10^{-10}	DMSO	FL	72
3	Fe^{3+}	2.86×10^{-7}	DMSO	FL	73
4	Fe^{3+}	n.d	Gel	FL	74
5	Hg^{2+}	1.67×10^{-7}	DMSO/H_2O	FL	76
6	Hg^{2+}	2.14×10^{-8}	DMSO/H_2O	FL	77
7	Hg^{2+}	1.4×10^{-6}	H_2O	FL/Col	78
8	Hg^{2+}	2.17×10^{-6}	THF/H_2O	Rat	79
9/10	Hg^{2+}/Pb^{2+}	n.d	CH_3CN	FL/UV-vis	80

View Article Online
DOI: 10.1039/D0TC01401J

				Ele,	
11	Pb^{2+}	2.7×10^{-6}	CH_3CN	FL	81
12	Pb^{2+}	n.d	Electrode	Ele	82
13	Pb^{2+} /Cu^{2+}	1.32×10^{-6}/ 3.98×10^{-6}	CH_3OH/H_2O	FL/UV-vis	83
14	Cu^{2+}	7.6×10^{-6} 2.2×10^{-7}	H_2O	UV-vis/FL	84
15	Cu^{2+}	n.d	$EtOH/H_2O$	FL,Rat	85
16/17	Ag^{+}	n.d.	H_2O	FL	86
18	Ag^{+}	8.18×10^{-9} 8.75×10^{-7} 3.84×10^{-7}	$DMSO/H_2O$	FL/UV-vis	87
19	Ag^{+}	4.02×10^{-7} 7.73×10^{-8}	$DMSO/H_2O$	FL/UV-vis	88
20	Ag^{+}	2.92×10^{-7}	DMSO	FL/UV-vis	89,90
21	Cd^{2+}	3.0×10^{-6}	CH_3CN/H_2O	FL	91
22	Cd^{2+}	6.0×10^{-5}	CH_3CN/H_2O	FL	92

View Article Online
DOI: 10.1039/D0TC01401J

23	Ba^{2+}	2.82×10^{-5}	CH_3CN/H_2O	FL	93
24	Zn^{2+}	n.d.	$DMSO/H_2O$	FL/UV-vis	94
25	Zn^{2+}	n.d.	CH_3CN/H_2O	FL/UV-vis	95
26	Al^{3+}	n.d.	$DMSO/H_2O$	FL	97

3.0 Anions sensing

All kinds of anions widely distributed in our surroundings play an important role in the physiology of human beings. Therefore, rapid and efficient detection of various anions in drinking water and environments is very significant to provide guidance for assessing the hazard and pollution management[98-101]. Especially, some of poisonous anions can cause severe damage for animals and human being when it immersed into the drinking water and plants[97]. Therefore, the design and synthesis of anion sensors with a good selectivity and sensitivity has become a desired work in the supramolecular chemistry. In recent years, many of the probes based on the phenazine derivatives have been developed as excellent sensors for various anions detection in environment water source and living body. For example, a plentiful of probes for detecting F^- were obtained by modifying different special functional group in phenazine backbone. Especially, some excellent probes with high-efficiency and multiple responses have attracted increasing attention based on various non-covalent interaction. As stated by reports, the functional group with strong electronegativity can enhance the anions sensing performance through multiple weak forces. For instance, in 2014 Zhang et al.[102] have synthesized a 2-(2,3,4,5-tetrafluorophenyl)-1*H*-imidazo[4,5-*b*] phenazine derivatives as the probe 27 with strength electron-withdrawing group, sensing F^- in the DMSO system. The probe 27 exhibited proper sensitivity and selectivity for F^- by colorimetric and fluorescent responses. Distinctly, the probe displayed no response to Cl^-, Br^-, I^-, NO_3^-, HSO_4^-, ClO_4^-, and BF_4^-. After addition of F^-, the absorption wavelength of the probe laid out red shifted

and the color of the solution change was observed from yellow to red under the viable light. The fluorescent response demonstrated the initial maximum absorbance wavelength gradually decreased centering at 392 nm, and that a new absorbance peak progressively increased in 422 nm with gradual addition of F^-. Meanwhile, the broad peak in the range of 438 nm to 491 nm was weaken and a new peak appeared at 540 nm accompanied with an evident color change from the green to yellow. The lowest detecting limit of the probe for the F^- was determined to be 8.62×10^{-5} M. The sensing mechanism was ascribed to hydrogen bond interactions, deprotonation, and anion-π attractive. The detailed sensing process is depicted in scheme 25.

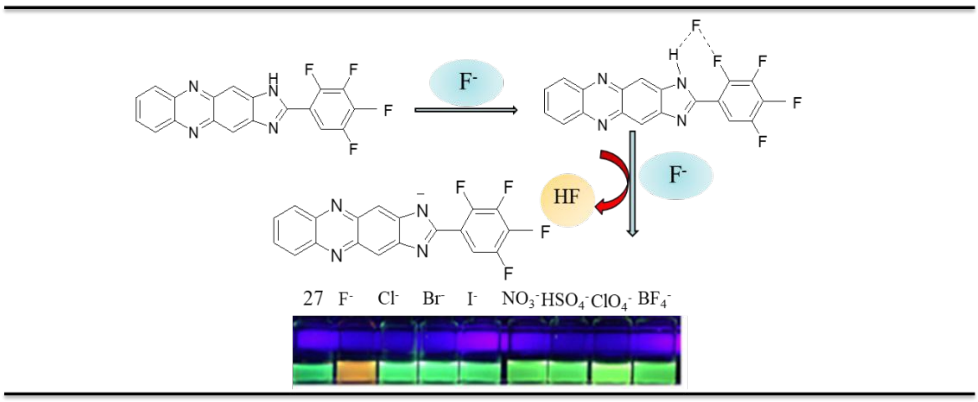

Scheme 25 The sensing mechanism of the probe 27 for detecting F^-. Reproduced with permission from reference 102 (Copyright© 2013 Elsevier Ltd. All rights reserved).

In 2018, Velmathi et al.[103] reported a new compound based on 2-(1*H*-indole-3-yl)-1*H*-imidazo[4,5-*b*] phenazine as the probe 28 for sensing F^- in aqueous dimethyl sulfoxide (30% H_2O+DMSO). The probe 28 could effectively detect the fluoride ion by fluorescence response accompanied with a dramatic color change (from light yellow to brown), noted by the naked eyes. Upon the addition of F^-, a fluorescence quenching about 10-fold was achieved, appearing an obvious color variation from the green to no fluorescence in a matrix containing a series of similar toxic anions. The sensing mechanism was ascertained to the fluoride triggering deprotonation interaction of imidazole(N-H) and indole moiety of probe. The sensing process was pictured in scheme 26. Eventually, the probe 28 was used to detect the F^- in living HeLa cells and zebrafish. As authors expected, the images illustrated that the probe has very preferable permeability and strong fluorescent response in the cell membrane (as shown in Fig 5).

View Article Online
DOI: 10.1039/D0TC01401J

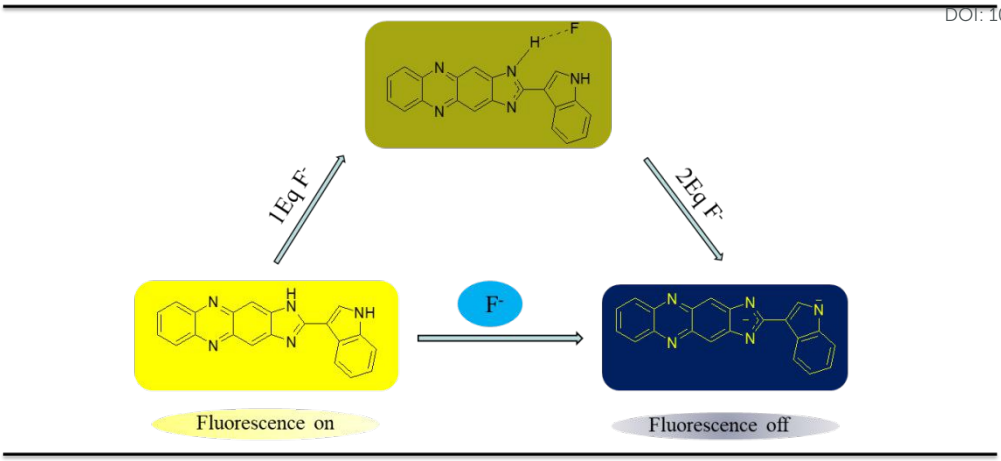

Scheme 26 The sensing mechanism of the probe 28 for detecting F^-

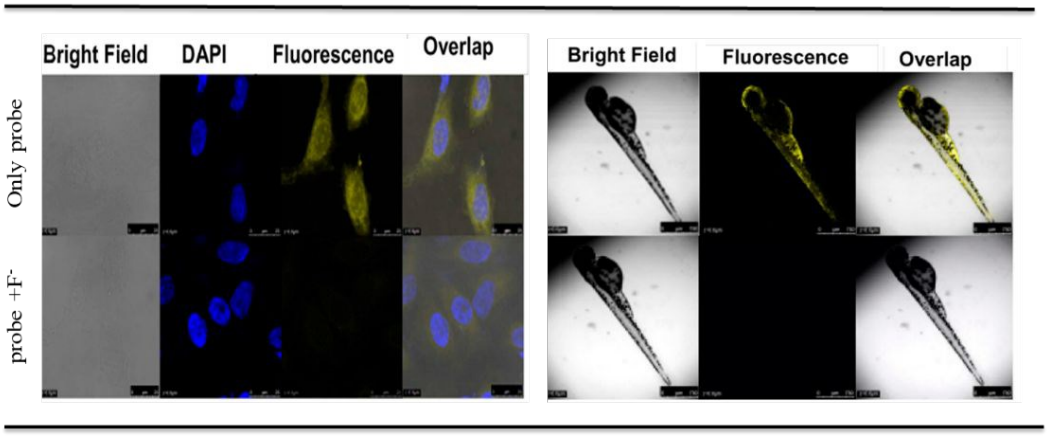

Fig 5. (Left) Fluorescence confocal imaging of HeLa cells for only probe and probe + F^-, (Right) Zebrafish fluorescence imaging experiment of only probe and probe + F^-. Reproduced with permission from reference 103 (Copyright©2019 Wiley-VCH Verlag GmbH & Co. KGaA, Weinheim).

In 2014, our groups developed and synthesized a significative compound as probes 29. The phenyl of bromine substituent was introduced into the imidazole ring of phenazine backbone owning to its moderate electronegativity to improve the selectivity and sensitivity for detecting F^-[104]. The results illustrated that absorption spectra presented notable changes, and shifted from 405 nm to 435 nm after adding F^-, yet no distinct color changes were noticed at presence of the other halogen anions in the visible region. Fluorescence response illustrated that the emission wavelength of probe at 530 nm gradually disappeared and a new emission peak emerged at 650 nm in DMSO solution with increasing addition of fluorine. The lowest limitation of the probe for F^- was determined to be 6.2×10^{-6} M. The results indicated the probe improved the sensitivity and selectivity for detection of F^- after introducing the bromine substituent of moderate electronegativity. The sensing mechanism

of probe 29 was agreed to the intensive intramolecular hydrogen bond interaction (as shown in scheme 27).

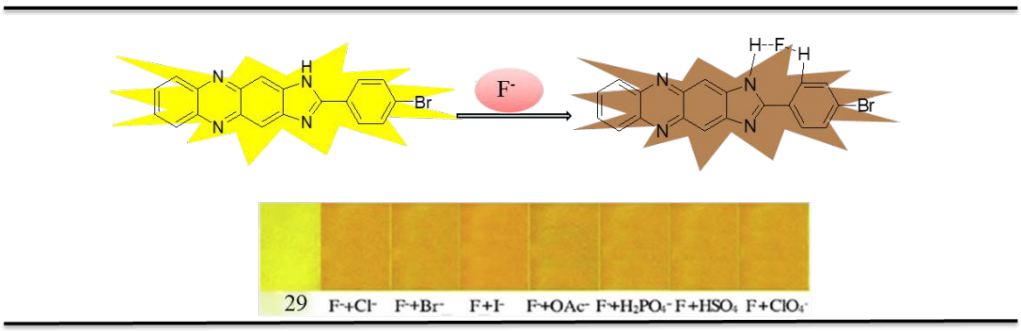

Scheme 27 The sensing mechanism of the probe 29 for detecting F^-. Reproduced with permission from reference 104 (Copyright© 2015 Rui Liu. Published by Elsevier B.V. on behalf of Chinese Chemical Society. All rights reserved).

The probe 30 based on the phenazine derivative with pyrrole subunits has been synthesized by the Maiya et al.[105]. The probe 30 could serve as the sensor for detecting F^- by multiple response (including various optical and electrochemical methods), exhibiting high selectivity and excellent sensitivity for F^- at present in a series of similar anions. After gradually adding F^-anions, a corresponding color change was observed from the red to green under the fluorescence emission in CH_2Cl_2 solution. And continuous addition of various anions, only the F^- and $H_2PO_4^-$ could cause color response from the yellow to red under the UV-vis light. The authors agreed that the binding mode of probe 30 for F^- should be attributed to the rotation of the pyrrole rings, attracting toward the lone pairs of the F^-anion by the NH protons, leading to the formation of intermolecular hydrogen bond. The interaction process is pictured in scheme 28. Finally, the authors confirmed the interaction mechanism between the receptor and anions by calculating the binding energies.

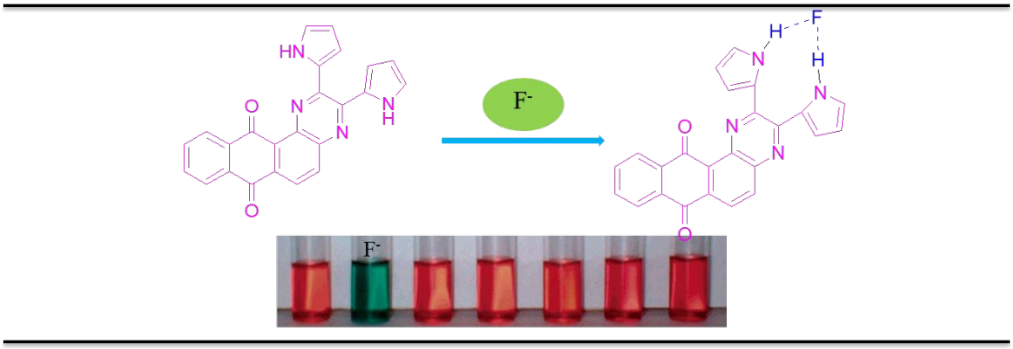

Scheme 28 The sensing mechanism of the probe 30 for detecting F^-. Reproduced with permission from reference 105 (Copyright© 2004 American Chemical Society).

The phenyl-1*H*-anthra[1,2-*d*] imidazole-6,1-dione and its derivatives was explored by the Han

et al.[106] as new colorimetric or ratiometric fluorescent probe 31−33 for detecting F^-. Rigorous fluorescence responses of probe 31−33 to fluoride were investigated in CH_3CN. And the absorption and emission band of those probes emerged an obvious red shift about 100 nm, presenting a very strong ratiometric fluorescent response (R_{max}/R_{min} is 88 for probe 31 and 548 for probe 33) after adding the F^-. The authors deduced that the sensing mechanism was ascribed to a proton−transfer effect according to the absorption properties, fluorescence emission, and ^1H NMR titration spectra (as shown in scheme 29). In ground states, a twostep process was noted in the recognition behaviors, the F^- complex of hydrogen bond was formed firstly and then deprotonation process of the complex was found an ICT effect inducing by fluoride. In excited states, the intermolecular proton−transfer played a key role in deprotonation process, and the sensing performance of probe 31-33 for F^- could be controlled by electron "push−pull" effect of different substituents group, which rooted at in the phenyl para position of the probes. For instance, probe 32 and 33 bearing with electron-donating group and electron-withdrawing group, respectively, exhibited excellent selectivity for the F^-, but the fluorescence emission intensity of the former was inferior to the latter. Those observations illustrated that the electron peculiarity of the substituents group on the para phenyl could tune the fluorescence properties (the stronger electron-withdrawing ability of the substituents, the greater the fluorescence emission enhancement).

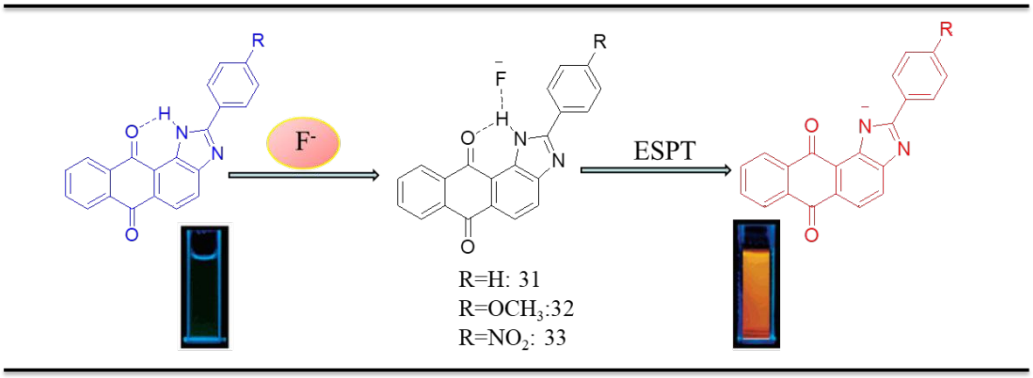

Scheme 29 The sensing mechanism of the probe 31−33 for detecting F^-. Reproduced with permission from reference 106 (Copyright© 2005 American Chemical Society).

The imidazole group normally severs as anion acceptor because it could form an intense intermolecular hydrogen bond thought the N-H proton. Furthermore, the acidity of NH proton could be enhanced by introducing the chromophore element. The four fluorescent acceptor probes 34−37 were successfully synthesized by the Velmathi et al.[107] in 2016, which contained imidazole and two

different signaling units for sensing F^-, CH_3COO^- and CN^- by monitoring the color change with the naked−eyes. The absorption band of fluorescence response of the probe 34 and 35 displayed an evident red shifted from 500 nm to 510 nm in presence of F^-, CH_3COO^- and CN^- ions (as shown in Fig 6). Meanwhile, rapid color response was noted from the green to remarkable orange and the dark to red. Nevertheless, the probe 36 and 37 showed a dramatic fluorescence quenching after adding F^-, CH_3COO^-, and CN^- ions under the UV−vis light emission, appearing a couple of new peaks at 530 nm and 541 nm, respectively. Those observations illustrated a strong molecular charge transfer process (ICT) [108] occurring in the above sensing process. Meanwhile, the probe 35 can be used to detect CN^- and F^- ions in aqueous solution of cassava flour and toothpaste. Yet, the probe 34 was applied to track CN^- ion in RAW 264.7 cells, suggested those probes have a great potential to identify CN^- ion in the living cells or real sample analysis. Photographs of fluorescence response of the probe 34-37 are listed in Fig 6.

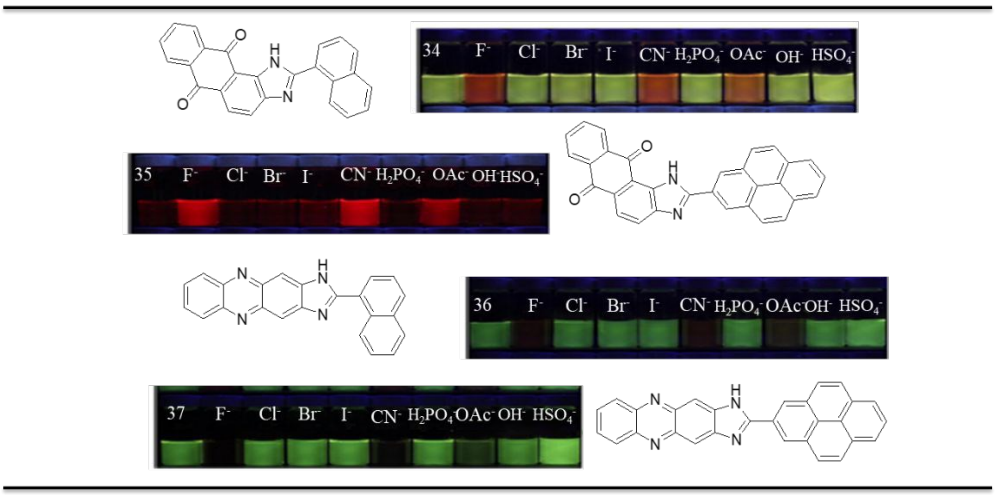

Fig 6. The fluorescent images of the probe 34−37 for detecting F^-, CH_3COO^- and CN^-. Reproduced with permission from reference 107 (Copyright© 2016 Springer Science Business Media New York).

The "naked−eye" recognition of anions without involving any instrumentation methods has been treated as a significant field in the design and building of new receptors for sensing anions[108]. Bhaskar et al.[109] reported two new colorimetric sensing anion acceptors, named as probe 38 and 39 bearing with biuret/thiourea binding sites, exhibited good sensing properties to fluoride, dihydrogen phosphate and acetate anions via the "naked− eye" identification in the presence of other anions. The UV−vis photographs of probe 38 showed a remarkable color change from the colorless to red or orange yellow after adding F^-, $H_2PO_4^-$ and CH_3COO^-. Furthermore, the UV–vis spectral change

of probe 38 detecting $H_2PO_4^-$(10 equiv.) was distinctly different from the F^- and CH_3COO^-, and the maximum absorption gradually shifted from 400 nm to 425 nm. After carefully investigating, the absorption spectral changes of probe 39 was similar to the probe 38 in presence of three ions (dihydrogen phosphate, acetate and fluoride), and the others anions did not cause any spectral changes. The color change is shown in Fig 7.

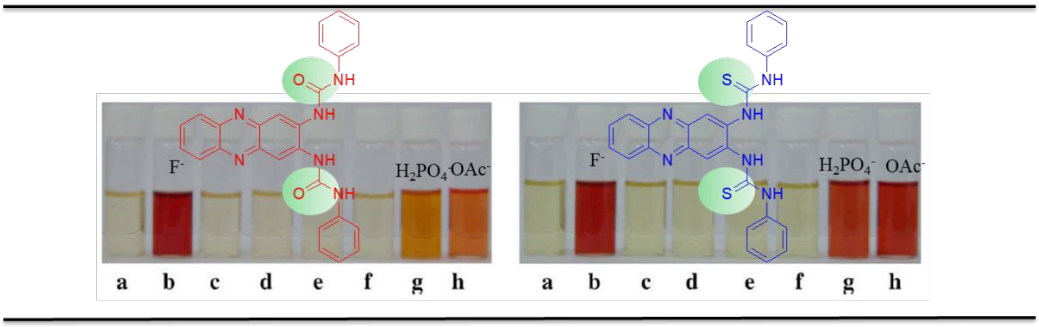

Fig 7. Left side: color changes of probe 38,39 upon the addition of tetrabutylammonium anions (5.0 102 M); (a) = free receptor, (b) = fluoride, (c) = chloride, (d) = bromide, (e) = iodide, (f) = hydrogen sulfate, (g) = dihydrogen phosphate, (h) = acetate; right side: color changes of probe (5.0 10^5 M) in DMSO. Reproduced with permission from reference 109 (Copyright© 2008 Elsevier Ltd. All rights reserved).

The *N*-substituted polycyclic aromatic hydrocarbons (PAHs) with special non-covalent binding sites locating at electron-deficient aromatic rings called anion-π or anion–proton interactions, which have attracted great interests in experimental investigations. Zhang et al.[110,111] has successfully designed and synthesized the innovative larger phenazines as the probe 40,41 and 42, endowing six or ten nitrogen-atoms in the backbones structure for sensing anions. This preferable synthetic strategy offered a promising and easy way to obtain even larger phenazine structure in the future supramolecular chemistry (as shown in Fig 7 and Fig 8). The absorption spectrum of probe 40 displayed a sharp color change from the original pink solution to greenish brown and dark brown at present in F^- and $H_2PO_4^-$, respectively. In addition, the other anions did not cause distinct color change. While probe 41 could selectively detect F^- over a lot of anions (such as F^-, Cl^-, Br^-, I^-, PF_6^-, HSO_4^-, NO_3^-, BF_4^-, CH_3COO^-, and $H_2PO_4^-$). The photographs of absorption spectrum are shown in Fig 8. After adding the F^- to probe 40, a distinct decrease of the absorption band was observed at 525 nm and 575 nm accompanied with the formation of new absorption peaks centering at 455 nm, 675 nm and 750 nm, in line with the greenish brown.

Different from the probe 41, the probe 42 had a special structure with larger stable azaacene (O

and N) as well as eleven linear fused-rings (8N8O), showing preferable optical properties for detecting I^- in presence of various anions based on the "heavy-atom" effect. The absorption spectrum of probe 42 displayed three vital absorption bands at 290 nm, 424nm, and 451 nm, which could be attributed to a localized aromatic π-π* transition. The increasing absorption intensity at 368 nm was observed after gradual addition of iodide. And then, the competition experiments were carried out to illustrated the coexistence anions have no any interference. The corresponding photographs are listed in Fig 9.

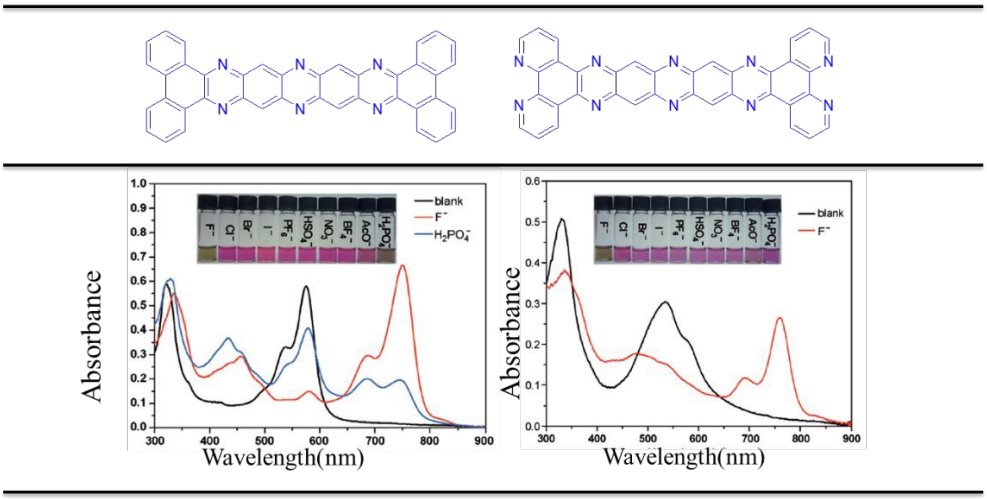

Fig 8. Absorbance spectra of the probe 40 and 41 for detecting F^- and $H_2PO_4^-$. Reproduced with permission from reference 110 (Copyright© 2013 Wiley-VCH Verlag GmbH &Co. KGaA, Weinheim).

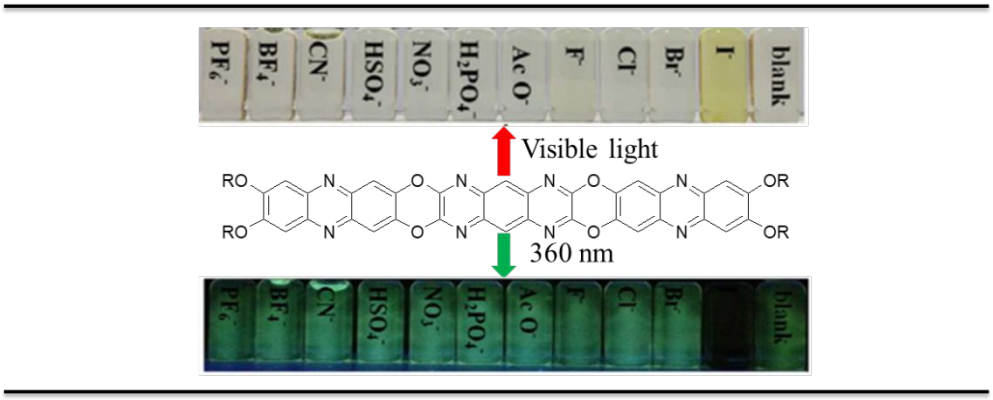

Fig 9. Absorbance spectra of the probe 42 for detecting I^-. Reproduced with permission from reference 111 (Copyright© 2015 The Royal Society of Chemistry).

The *N*−substituted azaacenes were very attractive owning to the important properties and technological applications. An aroyleneimidazo phenazine moiety was successfully introduced into the phenazine system to develop the excellent probe 43 by the Zhang et al.[112]. The probe could

selectively detect CN^- and F^- over another ten anions with the ''turn−off'' fluorescence response and near−infrared absorption signals. The UV−vis absorption spectrum of the probe displayed a broad absorption section, which can be ascribed to ''n–π* and π–π* transitions. Fascinatingly, the fluorescence emission was almost quenched completely after adding the CN^-, but partially quenched by F^- exciting at 365 nm, which illustrated that probe 43 was much more sensitive for CN^- recognition than F^-. The interactions mechanism explored by the UV−vis and fluorescence spectrum was agreed to the anion-π interactions and IET effect between probe 43 and CN^-or F^-. The sensing process is advertised in scheme 30.

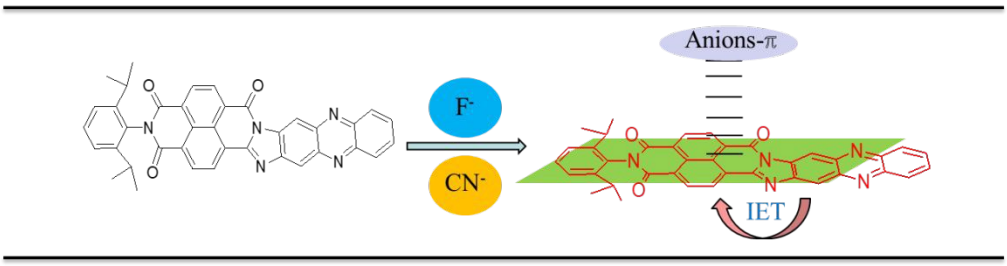

Scheme 30 The sensing mechanism of the probe 43 for detecting $F^-$and CN^-

Generally, the ICT process works on the ''push−pull'' effect directed against the donor (D) and the acceptor (A) moiety rooted in the sensor. Bhattacharya et al.[113] designed and synthesized a series of probes 44−47 based on anthra[1,2-*d*] imidazole-6,11-dione acting as the selective ion sensing acceptors. Each probe exhibited a strong colorimetric response for F^- and CN^- by intramolecular charge transfer (ICT) effect, and appeared a prominent red−shifts upon addition of either F^- or CN^- ion without any interference from the others. However, only the probes 45 exhibited selectively colorimetric recognition for cyanide and fluoride at presence of others ions in the organic medium, viewing a different color change with F^- and CN^-(as shown in scheme 31). The authors regarded as the probes 45 as a ratiometric sensing device for detecting cyanide ion in aqueous organic medium.

Donor-receptor-substituted thiophene functional groups were used to design and synthesize the novel probes 48−50 owing to their special optical peculiarity[114]. The selectivity and sensitivity of the probe 48−50 to the F^- ion were investigated by introducing different functional substituent groups at the 5-position of the biphenyl, such as the probe 49 with the electron-donating ethoxy group, but the probe 50 with electron-withdrawing cyano. As the authors expected, the probe 50 showed the strongest interaction with fluoride ions, yet the probe 49 displayed a weak interaction.

Besides, the probe 48−50 could also provide chelating site for metal ions and resulted in the deprotonation of the imidazole ring and the quinone group. Therefore, the sensing properties of probe 48−50 to the Zn (II), Cu (II), and Hg (II) cations was also explored that the strongest interaction was the probe 48 owning to the strong coordination ability of the metal. While the sensing mechanism of the probes to anions were attributed to the properties of forming the intramolecular hydrogen bond (locating at imidazole ring and quinone carbonyl group), deprotonation process, and proton transfer interactions (PET effect). The detailed mechanism is depicted in scheme 32.

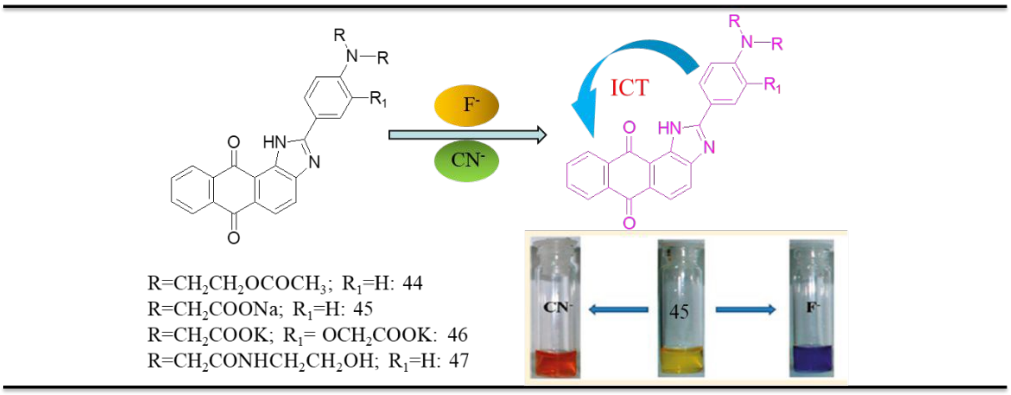

Scheme 31 The sensing mechanism of the probe 44-47 for detecting $F^-$and CN^-. Reproduced with permission from reference 113 (Copyright© 2011 American Chemical Society).

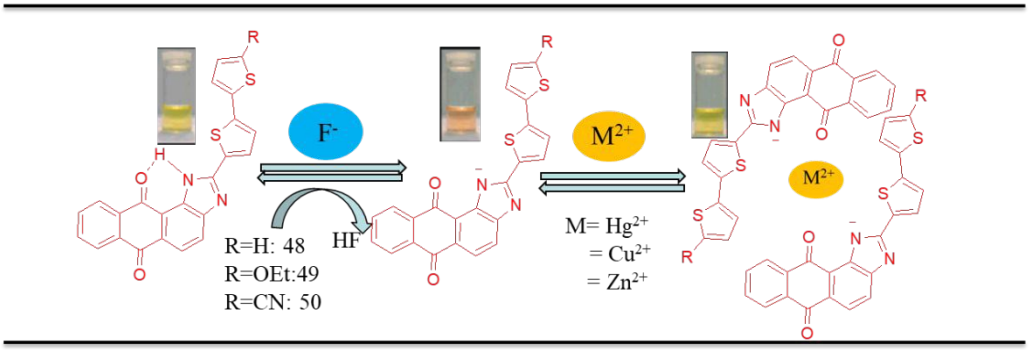

Scheme 32 The sensing mechanism of the probe 48−50 for detecting F^- and metal ion. Reproduced with permission from reference 114 (Copyright© 2007 American Chemical Society).

Cyanide have evolved into a very important toxic anions in wild life and in minimal group. Therefore, detection and identification of CN^- in the surroundings have received much more attention. For example, a "turn−on" fluorescence probe 51 was successfully developed by our research group[115,116] in 2016 based on dihydroxy phenazine for sensing CN^- anions. The probe 51 displayed preferable sensitivity and excellent selectivity for cyanide in pure water over a series of

other anions, and exhibited a good recyclable ability for CN^- response upon the addition of HCl, which could recycle 10 times with a litter fluorescent efficiency loss. The probe 51 for CN^- sensing mechanism may involve a hydrogen bonding interaction and deprotonation leading to the fluorescence enhancement (as shown in scheme 33). The lowest limitation of the probe to CN^- was measured to be 5.65×10^{-7} M, which was inferior to 0.2 ppm standard values.

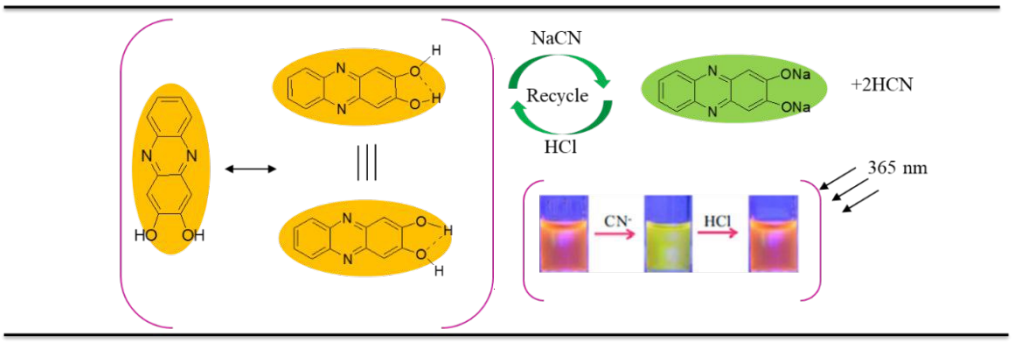

Scheme 33 The sensing mechanism of the probe 51 for detecting CN^-. Reproduced with permission from reference 116 (Copyright© 2016 Elsevier Ltd. All rights reserved).

Benzothiazole derivatives containing anthracenyl, pyrenyl and *N*, *N*-dimethylaminophenyl was triumphantly explored as an excellent probe 52 for detecting the cyanide in the aqueous solution[117]. The fluorescence response showed a rapid color change from greenish yellow to light yellow, and viewed by the naked eyes under the UV−vis light emission. After gradual addition of CN^- ions, the maximum absorption band of probe 52 was monitored at 269 nm, 313 nm and 446 nm, respectively, and the wavelength at 446 nm progressively disappeared, appearing a new absorption band in 357 nm. Meanwhile, the probe 52 displayed a sharp fluorescence response to cyanide ions and the lowest detection limit was determined to be 5.52×10^{-8} mol L^{-1}. The authors explained the sensing mechanism for CN^- should be nucleophilic addition of CN^- to the vinylic linkage. Furthermore, the cytotoxicity of the probe 52 to HeLa cells was estimated by standard MTT tests and the living cells imaging by monitoring color changes of the cyanide ions in intracellular. The fluorescence images are collected in scheme 34.

View Article Online
DOI: 10.1039/D0TC01401J

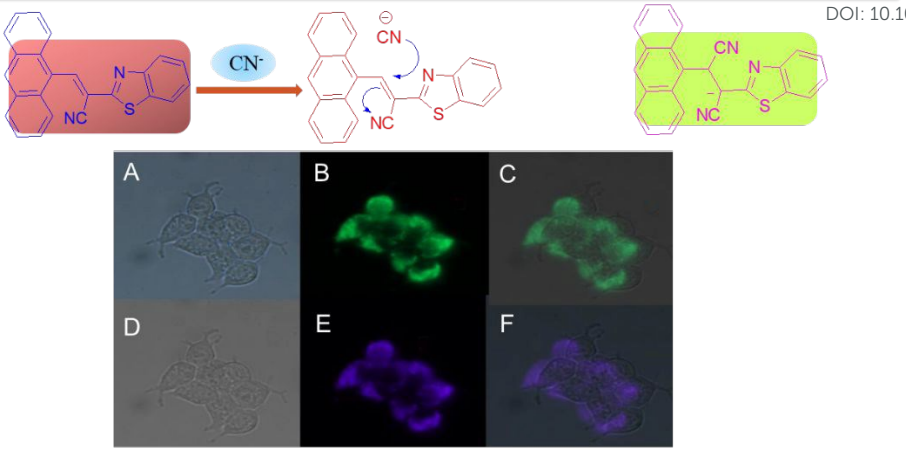

Scheme 34 The sensing mechanism of the probe 52 for detecting CN^- and Live cell imaging application of probe 52 for cyanide imaging; A, D− bright field images of Hela cells incubated with probe alone and probe +KCN respectively; B, E Fluorescence images of Hela cells incubated with probe alone and KCN respectively; C, F overlaid images of A, B and D, E respectively. Reproduced with permission from reference 117 (Copyright© 2016 Elsevier Ltd. All rights reserved).

In 2017, our group reported an amusing Zn (II)-salen probe 53 with colorimetric and fluorescent response for the CN^-[118].The probe 53 displayed high selectivity and sensitivity for cyanide ion via the dual−channel methods, including the fluorescence response and the naked−eye recognition. With gradual addition of CN^-, the Zn^{2+} can be removed by the replacement reaction and produced a distinct color change from red to buff, which could serve as a "turn-on" fluorescent sensor for detecting CN^- (as shown in scheme 35). The low detection limit was determined to be 0.28 μM and 0.98 μM though the colorimetric and fluorometric methods, which indicated that the probe 53 can be used to identify the cyanide at the lower concentration. The interaction mechanism of the probe with CN^- ion was considered that the Zn^{2+} was displaced by cyanide ions under the help of ^1H NMR, fourier transform infrared spectroscopy (FT-IR), and electrospray ionization mass spectrometry (ESI-MS). The detailed detection route is pictured in scheme 35.

View Article Online
DOI: 10.1039/D0TC01401J

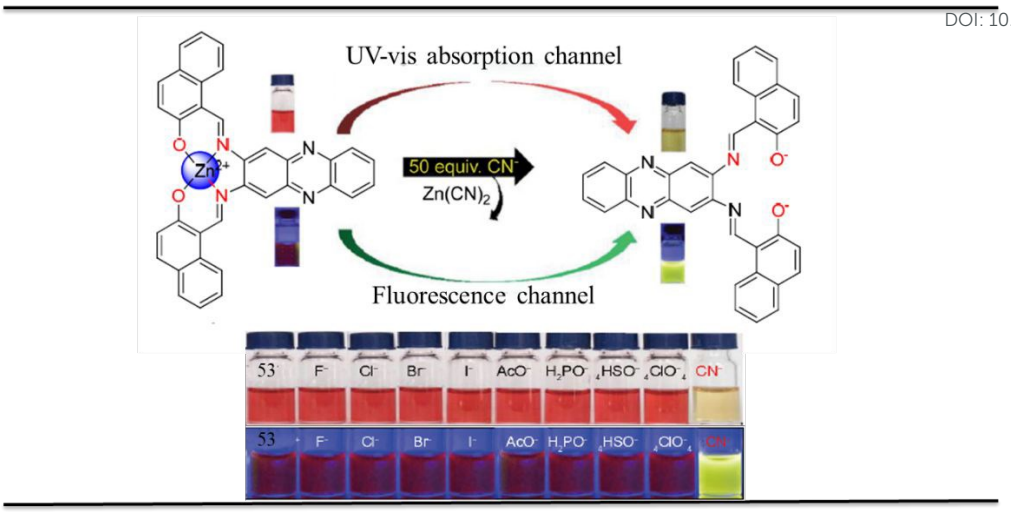

Scheme 35 The sensing mechanism of the probe 53 for detecting CN^-. Reproduced with permission from reference 118. (Copyright© 2017 Science China Press and Springer-Verlag Berlin Heidelberg).

Detection of cyanide has gained considerable attention because of its enormous toxicity to animals and human being. Hua et al.[119] reported a series of probes 54−57 for sensing CN^- based on phenazine backbone modified with a dicyano vinyl group, which made a great progress in design and synthesis of the probe molecules for sensing CN^- [120]. Firstly, the optical properties of the probe 54 and 55 were investigated by observing the variation in absorption spectra and fluorescence spectra. After adding the CN^-, two absorption peaks of probe 54 were found at 670 nm and 416 nm, respectively, and the color of solution system still kept a dark green. And then, a distinct shoulder absorption peak was noticed at 470 nm. The probe 55 could also display similar performance of absorption peaks at 426 nm and 716 nm, respectively, but the fluorescence emission response was not viewed. Although, probe 54 and 55 both exhibited good selectivity and sensitively, probe 54 showed a much lower detection limit approaching 200 nM according to the linear fitting calculation. The interaction mechanism of probe 54 and 55 was believed to the intramolecular charge transfer (ICT) effect[121] resulting from phenazine group leading to no fluorescence emission of the probes at the original state. Upon the addition of CN^-, the ICT effect disappeared and gained a rapid fluorescence enhancement. The sensing mechanism is described in scheme 36. Interestingly, the probe 54 could be used for sensing cyanide in the intracellular of Hela cells showing "off–on" response signals by confocal laser scanning microscopic imaging (as shown in Fig 10). The optical investigation suggested that the absorption spectra of probe 56 exhibited different absorption peaks at 570 nm, 452 nm, 360 nm and 293 nm, respectively. After addition of CN^-, the two absorption

peaks at 570 and 452 nm progressively reduced appearing another obvious decrease at the 360 nm. At the same time, a new emission band appeared at 630 nm accompanied with an obvious solution color variation from brown to yellow, which could be distinguished by the naked eyes. Different from the probe56, the color of the probe 57 (10 μM in CH_3CN) was purple in the beginning, and two main absorption peaks appeared in 545 nm and 372 nm after addition of CN^-. When a superfluous cyanide was added into the above solution of probe 56 and 57, an amazing lager shift and variation in emission peaks was captured (as shown in Fig 11). The sensing process is shown in scheme 37.

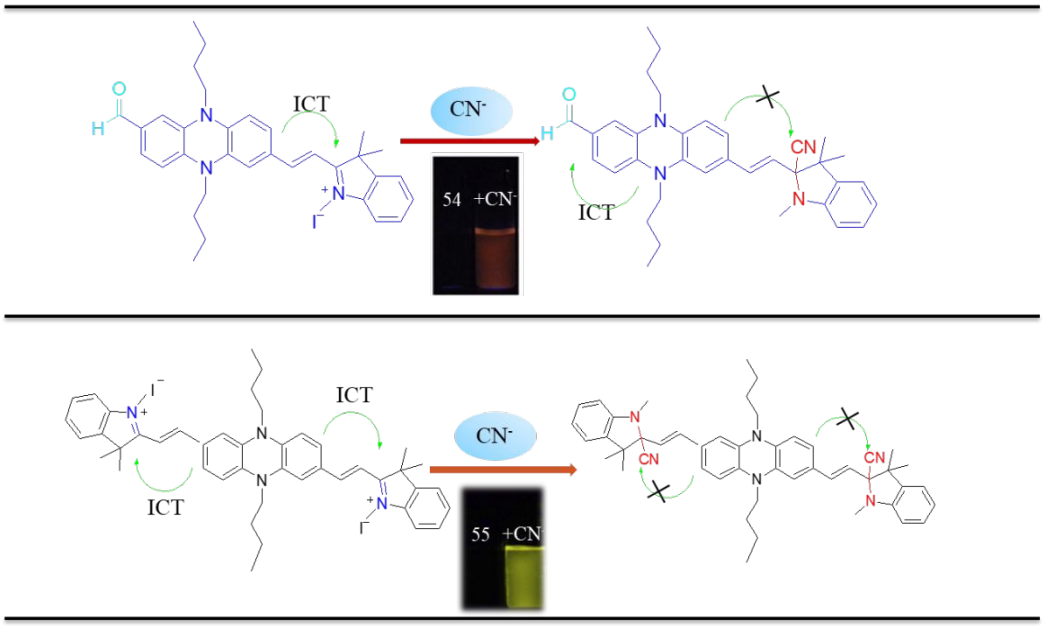

Scheme 36 The sensing mechanism of the probe 54 and 55 for detecting CN^-. Reproduced with permission from reference 119 (Copyright© 2014 Elsevier B.V. All rights reserved).

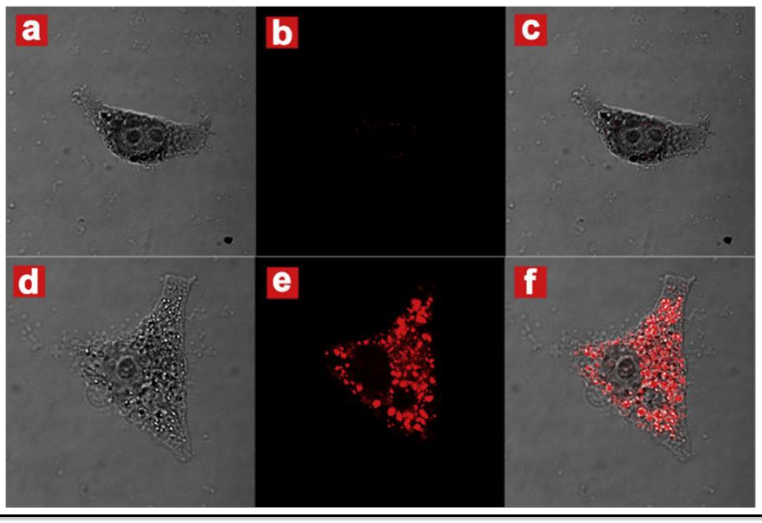

Fig 10. Confocal laser scanning imaging of Hela cells with probe 54 incubated in RPMI−1640, pH

7.4, 37◦C. First row: bright field (a), dark field (b) and merged (c) images of Hela cells incubated with probe 54 for 30 min. Second row: bright field (d), dark field (e) and merged (f) images with following incubated with CN^-(2.0 eq.) for another 30 min. Ex.= 543 nm, Emission was collected by red channel from 650 to 750 nm. Reproduced with permission from reference 119 (Copyright © 2014 Elsevier B.V. All rights reserved).

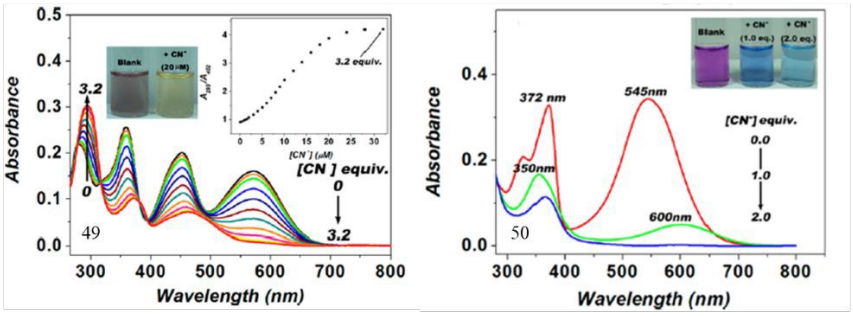

Fig 11. The UV−vis spectra of probe 56 and 57 (10 μM) in CH_3CN upon the addition of CN^- (0−32 μM). Reproduced with permission from reference 121(Copyright © 2013 American Chemical Society).

Velmathi et al.[122] reported probe 58-61containing heterocyclic ring connected with thiourea groups, which can be used to selectively identify the poisonous cyanogen ions in 25% aqueous DMSO medium. In the presence of CN^- ion, a quick colorimetric response was noticed from orange to purple for 58-59 and light yellow to orange for 60-61, respectively. In addition, the interaction mechanism between the probe 58-61 and CN^- ion was further studied by spectrometric tests. The results showed that the heterocycles in 58 and 59 have strong ICT effect (intramolecular charge transfer between anthraquinone carbonyl and adjacent NH) in a slightly longer region of 492 nm. Probe 60 and 61 exhibited a new absorption peak at 495 nm and another band was mildly red shifted from 422 nm to 427 nm after addition of CN^- ion without the inference of others anion. The sensing mechanism for those probes for detecting CN^- was agreed to a nucleophilic reaction between CN^- ion and the carbonyl unit bearing with the thiophene or furan rings. The proposed sensing mechanism is described in scheme 38.

View Article Online
DOI: 10.1039/D0TC01401J

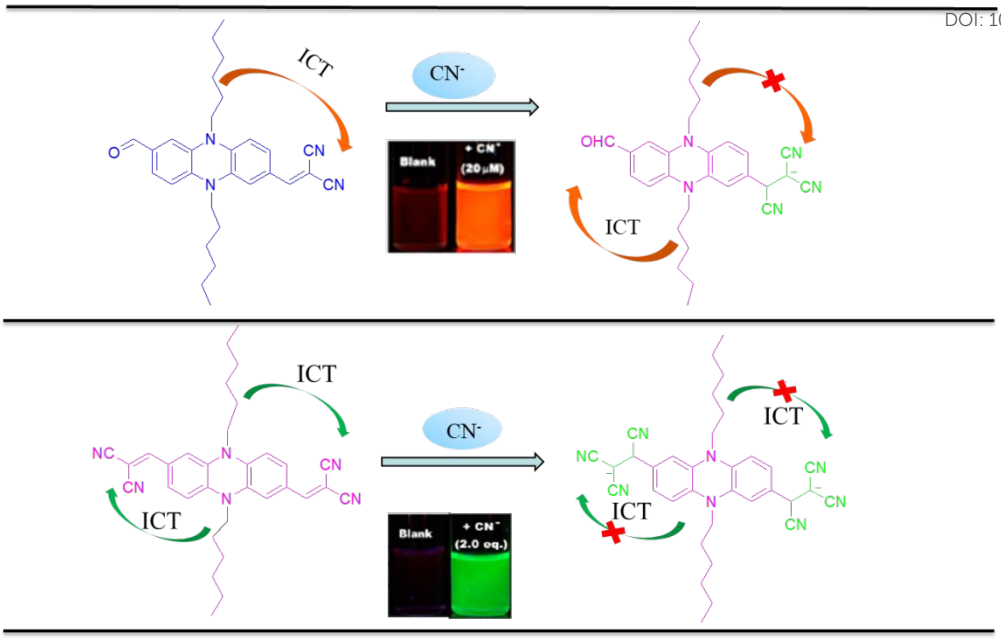

Scheme 37 The sensing mechanism of the probe 56 and 57 for detecting CN^-. Reproduced with permission from reference 120 (Copyright© 2013 American Chemical Society).

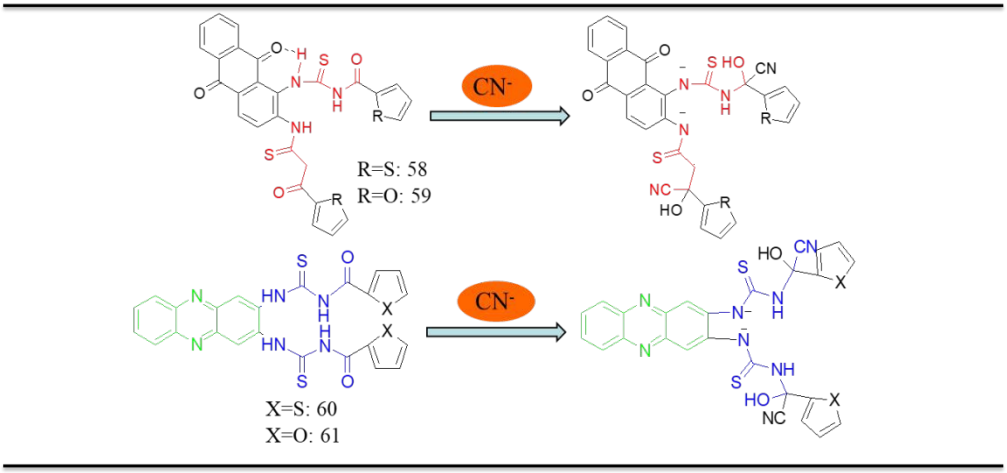

Scheme 38 The sensing mechanism of the probe 58-61 for the detecting CN^-.

Yoon et al.[123] reported a synthesis based on the oxazole phenazine derivatives by introducing cyanide with a special microfluidic platform to obtain the probe 62 for selective detection of CN^-. This probe 62 could display preferable green fluorescence response upon the addition of CN^-, obtaining a high selectivity for cyanide ions over many of anions. The sensing mechanism could be ascribed to the nucleophilicity addition reaction of cyanide ions and aldehyde group in aqueous solution. The reaction process is advertised in the scheme 39. Moreover, the probe displayed a saturation phenomenon after continuous addition of 50 equiv. of cyanide ions and obtained a 200-fold enhancement of emission intensity, exhibiting a 'OFF-ON' type fluorescence response. The

practical application was proved by detecting the cyanide in the living cells, monitoring an obvious green fluorescence in the cell images by laser confocal microscopy. The corresponding images are listed as in scheme 39.

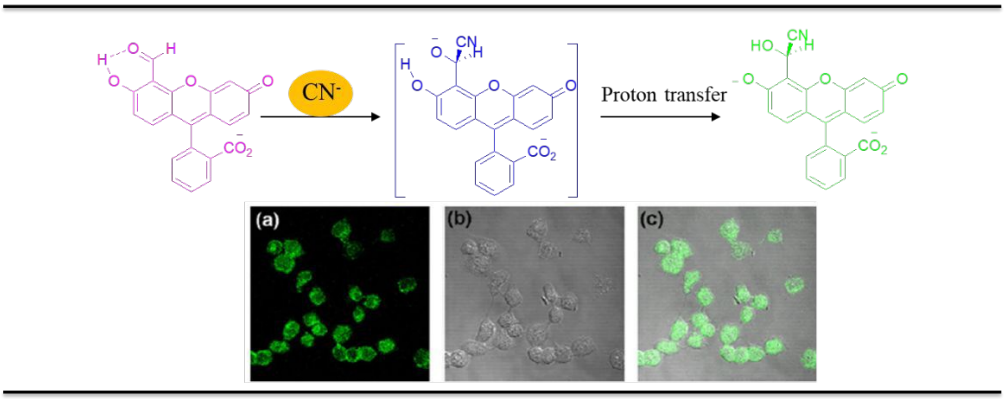

Scheme 39 The sensing mechanism of the probe 62 for CN^- and images of HaCaT cells treated with 20 μM of NaCN after incubated with 20 μM of probe. (a) Fluorescent images, (b) DIC images, (c) merged images. (excitation=488 nm, emission =505–530 nm). Reproduced with permission from reference 123 (Copyright©2008 Elsevier Ltd. All rights reserved).

Due to the long−chain alkyl is easy to crosslink each other, it is advantage to form the soft materials supramolecular gel. Thus, our group attempted to prepare the special probe 63 for CN^- identification based on the supramolecular gel[124]. The fluorescence response showed that the probe 63 can selectively recognize the CN^- leading to complete fluorescence quenching. The interaction mechanism of probe 63 was attributed to a nucleophilic addition reaction and destruction of π–π stacking occurring in imidazole group (as shown in scheme 40). And others anions have barely influence on the sensing process (as shown in Fig 12), obtaining the lowest detection limits of probe 63 for CN^- (4.18×10^{-10} M), which was much lower than other fluorescent sensors for detection of CN^-.

In 2019, our group successfully synthesized and developed another novel probe 64 by introducing the functional group with 2-(methylthio) oxazolo into the phenazine skeleton[125]. The probe 64 could exhibit high sensitivity and excellent selectivity for hypochlorite identification based on the oxidation reaction. Upon the addition of ClO^-, the absorption peaks of the probe 64 disappeared at 390 nm and a new shoulder peak appeared at 430 nm, observing a distinct color change from green to yellow (as shown in Fig 12). The sensing mechanism was agreed that the hypochlorite oxidized sulfur atoms to sulfoxide and destroyed the π–π stacking interaction of free probe molecule. The sensing mechanism is described in scheme 40.

View Article Online
DOI: 10.1039/D0TC01401J

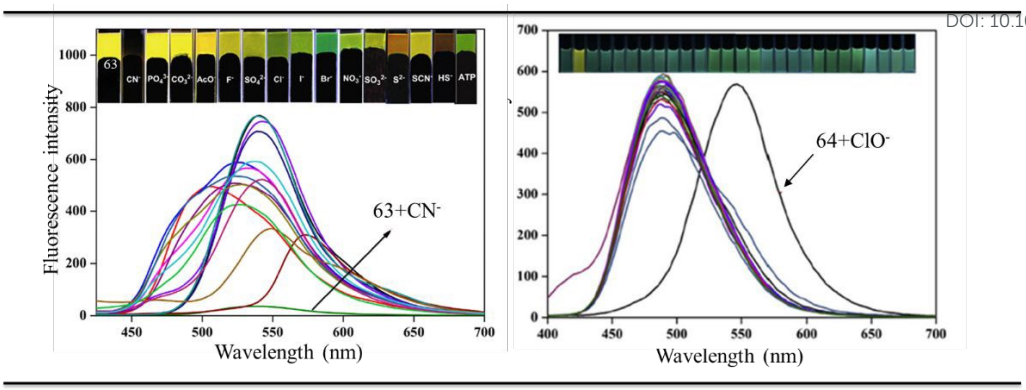

Fig 12. Fluorescence spectra of probe 63 and 64 for detecting CN^- and ClO^-. Reproduced with permission from reference 124,125 (Copyright © 2020 Elsevier B.V. All rights reserved Copyright © 2019 Elsevier B.V. All rights reserved).

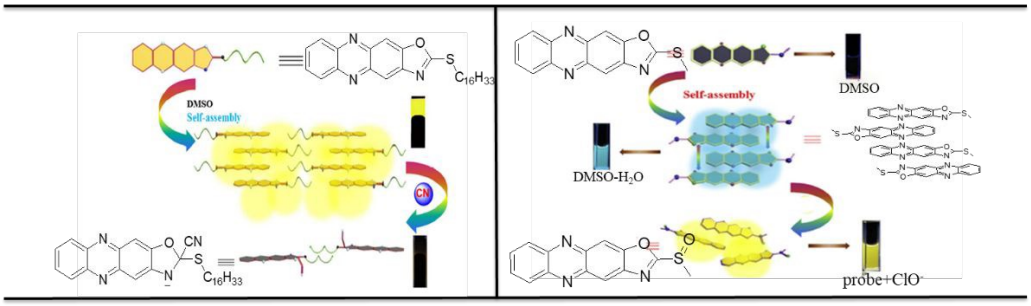

Scheme 40 The sensing mechanism of the probe 63 and 64 for detecting CN^- and ClO^-. Reproduced with permission from reference 124,125 (Copyright © 2020 Elsevier B.V. All rights reserved Copyright © 2019 Elsevier B.V. All rights reserved).

In 2015, the Yoon et al.[126] designed a probe 65 containing the imidazoline-2-thione unit to detect the oxidizing ClO^- anions via the specific reactions, gaining a corresponding fluorescent imidazolium ion. The probe 65 was powerfully confirmed to sever as an excellent biomarker to detect the ClO^- in t RAW 264.7 cells and HeLa cell (as shown in Fig 13), which indicated that probe 65 has potential and wide applications in bioimaging. The sensing mechanism is shown in scheme 41.

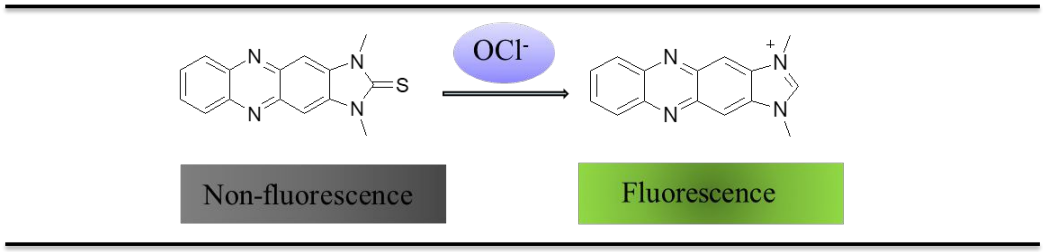

Scheme 41 The sensing mechanism of the probe 65 for detecting OCl^-

View Article Online
DOI: 10.1039/D0TC01401J

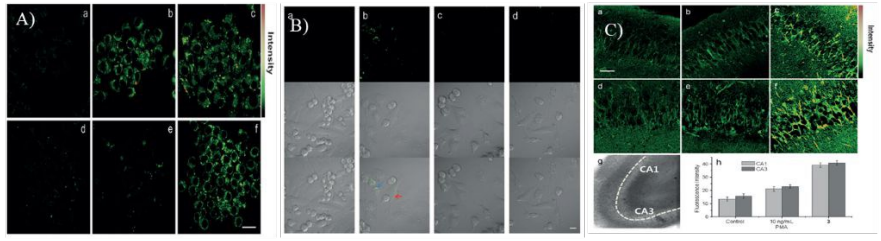

Fig 13. A) TPM images of RAW 264.7 cells labeled with a–e) probe 65 and f) controlled probe (10 mm, 1DMF=0.5%). a) Control image. b) Cells pretreated with NaOCl (200 mm) for 30 min and then incubated with probe. c) Cells pretreated with LPS (100 ng) for 16 h, IFN-g (400 UmL^{-1}) for 4 h, PMA (10 nm) for 30 min, and then probe. d) Cells pretreated with LPS, IFN-g, and 4-ABAH (50 mm) for 4 h, and then incubated with probe. e) Cells pretreated with LPS, IFN-g, and FAA (50 mm) for 4 h and then probe. g) Average TPEF intensities in (a–f), n=5. Scale bar: 20 mm. B) Fluorescence (upper) and bright−field (middle) and merge (lower) images of RAW 264.7 macrophages and HeLa cells treated with various stimulants and then incubated with probe 65. C) Images of a rat hippocampal slice stained with probe. Reproduced with permission from reference 126 (Copyright©2013 John Wiley & Sons, Inc. All rights reserve).

In earlier times, Jang et al.[127] synthesized a mixed receptor binding different anions based on the phenazine derivatives, named as probe 66, which could bind the F^-, Cl^-, Br^-, CH_3COO^- and $H_2PO_4^-$ and achieved corresponding bind constants. Moreover, the probe 66 endowed strong binding ability due to the hydrogen bond interaction related to the binding procedure, and was able to act as a binding site for designing all kinds of sensors based on the 2-aminobenzimidazole group. The interactions mode is pictured in scheme 42.

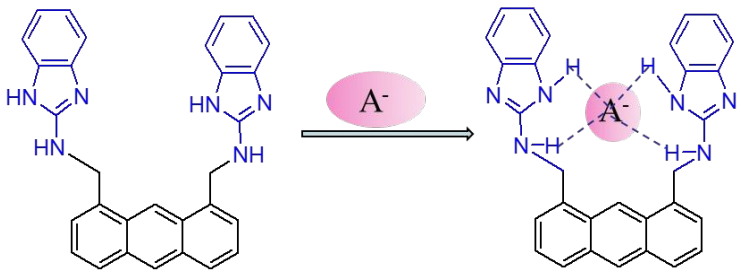

Scheme 42 The sensing mechanism of the probe 66 for anions

As discussed before, many probes employed to sense various anions were summarized based on their structural characteristics, optical properties and bioimaging. After carefully comparing the sensing performance (as shown in Table 3) of probe 27-66 for F^-, CN^-, Cl^-, Br^-, ClO^-, CH_3COO^-, $H_2PO_4^-$, a close relationship was fully illustrated between functional groups or ligands tuning of

phenazine derivatives and sensing properties. In addition, the sensing mechanism of those probes were concluded as the hydrogen-bond interaction, anions-π interaction, intermolecular charge transfer (ICT), deprotonation process, and proton transfer interactions (PET). It is expected those design and application of obtained probe could provide empirical guidance for exploring novel probes. Table 3 Comparison of different the probes for sensing various ions

View Article Online
DOI: 10.1039/D0TC01401J

Table 3 Comparison of different the probes for sensing various metal ions

Number	Ions	limitation(M)	Solvent	Sensing mode	Ref
27	F^-	8.62×10^{-5}	DMSO	FL/Col	102
28	F^-	1.79×10^{-6}	DMSO/H_2O	UV-vis/FL	103
29	F^-	6.2×10^{-6}	DMSO	UV-vis	104
30	F^-	n.d	Mixed	FL, Ele, Opt	105
31-33	F^-	n.d.	CH_3CN	FL/UV-vis	106
34	F^-/OAc^-/CN^-	5.1×10^{-11} 5.1×10^{-11} 5.8×10^{-11}	DMF	FL/UV-vis	107
35	F^-/OAc^-/CN^-	1×10^{-9} 1×10^{-9} 4.8×10^{-9}	DMF	FL/UV-vis	107
36	F^-/OAc^-/CN^-	5×10^{-10} 8×10^{-10} 1.2×10^{-9}	DMF	FL/UV-vis	107
37	F^-/OAc^-/CN^-	5×10^{-10} 7.3×10^{-9} 6×10^{-10}	DMF	FL/UV-vis	107

View Article Online
DOI: 10.1039/D0TC01401J

38/39	$F^-/H_2PO_4^-/CN^-$	n.d.	DMSO	UV-vis	109
40/41	$F^-/H_2PO_4^-$	n.d.	DMF	UV-vis	110
42	I^-	n.d.	NMP	FL/UV-vis	111
43	F^-/CN^-	n.d.	THF	UV-vis/FL	112
45-47	F^-/CN^-	n.d	$DMSO/CH_3CN$	UV-vis	113
48-50	F^-	n.d	CH_3CN	FL/UV-vis	114
51	CN^-	5.65×10^{-7}	H_2O	FL/UV-vis	116
52	CN^-	5.52×10^{-8}	CH_3CN	FL/UV-vis	117
53	CN^-	2.8×10^{-7} 9.86×10^{-7}	$DMSO/H_2O$	FL/UV-vis	118
54/55	CN^-	1.4×10^{-6} 2×10^{-7}	$DMSO/H_2O$	FL/UV-vis	119
56/57	CN^-	n.d.	CH_3CN	NIR/UV-vis	119
58-61	CN^-	n.d.	$DMSO/H_2O$	FL/UVvis/Col	122
62	CN^-	n.d.	CH_3CN/H_2O	FL/UV-vis	123
63	CN^-	4.18×10^{-10}	gel	FL	124

View Article Online
DOI: 10.1039/D0TC01401J

64	ClO^-	7.0×10^{-5}	DMSO/H_2O	FL	125
65	ClO^-	n.d.	H_2O	FL	126

4.0 Sensing pH and biological molecule

A novel arylamine-substituted benzo[*a*] phenazines was successfully synthesized by Thomas et al.[128] by taking advantage of a simple sequential Michael-addition reaction to obtain probe 67. The absorption performance of probe 67 derived from the charge transfer transition based on the amine and pyrazine segments. Although, the nature of the solvents could not change the absorption spectra of the probe 67, an obvious red-shift accompanied with the solution color change from the yellow to blue was observed due to the protonation in absorption spectra after continuously adding the trifluoroacetic acid (TFA). Therefore, protonated products can improve the receptivity of electrons. The authors explained that addition of TFA can cause an excellent protonation of the quinoxaline group and generate a meaningful halochromism, which can be applied as the H^+/OH^- probe (as shown in Fig 14). In view of this, the electronic structure of probe 67 was optimized by using DFT computations and redshifted absorption peaks were identified to a π-π* transition from the charge transfer between the donor and acceptor fragments.

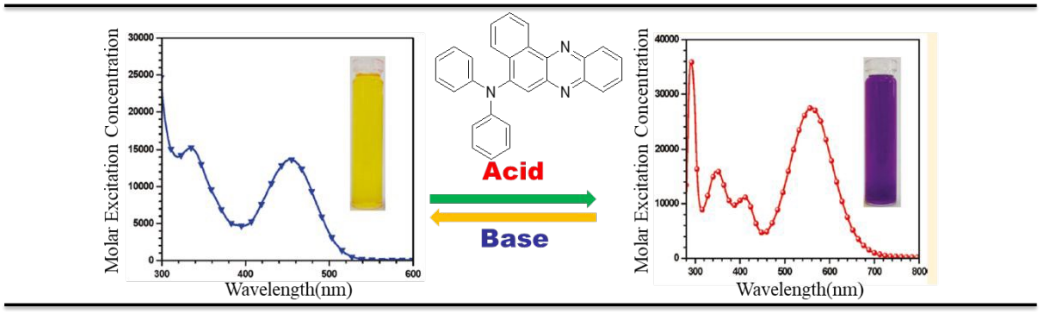

Fig 14. Absorption spectra of the probe 67 for detecting H^+/OH^-. Reproduced with permission from reference 128 (Copyright© 2011 American Chemical Society).

Several benzos[*a*]phenoxazine derivatives connected with *N*-aromatic groups were explored owning to their pH-dependent response based on the absorption and emission properties. Recently, many studies manifested that benzo[*a*]phenoxazine was a stable, nontoxic compound with excellent bioactivity, which could be applied as the probes 68-72 for sensing H^+ ions in the solution and the living cell[129]. Because protonation can cause red shifted up to 121nm of the maximum absorption band based on the π–π conjugated benzo[*a*]phenoxazine derivatives, the intensity of the emission

maximum of probe 68 was slightly quenched in the lower pH conditions. The observations indicated that probe 68 could act as a colorimetric pH indicator in the acid conditions, displaying excellent sensing performance. Nevertheless, when the methoxy group with electron-donating properties presented in probe 68 was replaced by an electron withdrawing nitro group to obtain the probe 69, which could not only cause the colorimetric sensing for pH, but also obtain the fluorescence response. And, the intensity of the maximum emission was enhanced by 32-fold from a very weak band at 641 nm to a more intensive one (locating at 720 nm) with the gradual increase of hydrion concentration. Those observations illustrated that the *N*-substituent groups afforded an equilibrium between benzo[*a*]-phenoxazine and benzo[*a*]phenoxazinium, regulating a near neutral or acid pH conditions. Therefore, the authors expected to introduce the electron-withdrawing group into the benzo[*a*]phenoxazine to construct novel fluorescent pH probes. Afterwards, the probe 70-72 was reported with the *N*-pyridiniumylbenzo-[*a*]phenoxazines by applying the alkylation reaction based on their pyridinyl derivatives. The emission properties of the probe 70-72 was investigated by the similar methods. After adding the alkali, the absorption maximum band of the probe 70 emerged at 650 nm in buffer solution, yet the absorption band of probe 71 presented at 694 nm with weak emission, and shifted to 697 nm along with remarkable emission in the acidic conditions (pH =3.6). The probe 72 exhibited less emission at 723 and 729 nm, obtaining an obvious blue-shifted under acidic conditions. Eventually, the fluorescent response of the probe 70-72 in the living cells was estimated by fluorescence imaging in HeLa cells (as shown in Fig 15).

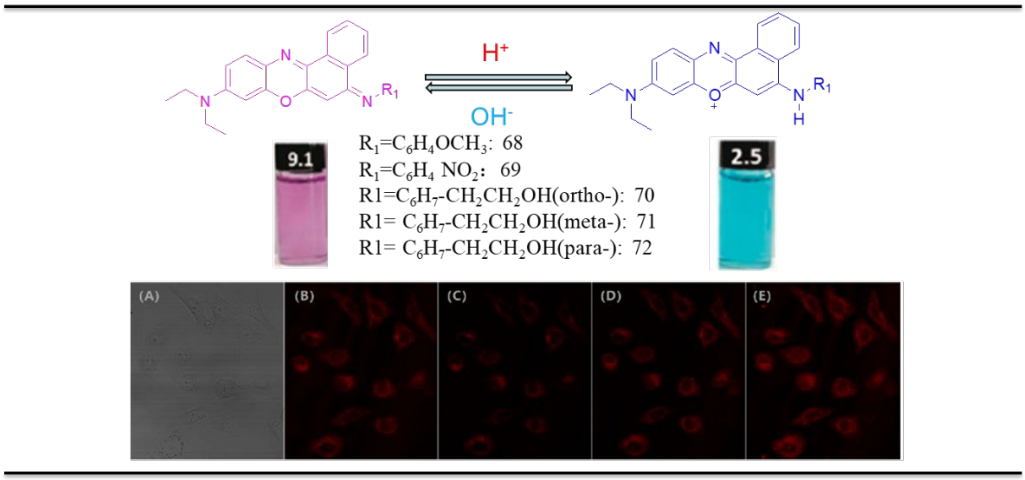

Fig 15. The sensing process of the probe 68-72 for the detecting H^+/OH^- and the fluorescence images of HeLa cells with composite probe of 68-72 (mole ratio of 3a/3b/3c = 2:1:2): (A) bright-field image; (B)fluorescence image of HeLa cells incubated with the composite probe (0.8 μM) in PBS buffer

(pH = 7.4) for 20 min; (C) fluorescence image of HeLa cells incubated with high K^+ buffer (pH = 8.0) with nigericin (2 μg·mL^{-1}) for 10 min; (D) fluorescence image of HeLa cells incubated with high K^+ buffer (pH = 6.0) with nigericin (2 μg·mL^{-1}) for 10 min; (E) fluorescence image of HeLa cells incubated with high K^+ buffer (pH = 4.0) with nigericin (2 μg·mL^{-1}) for 10 min. Reproduced with permission from reference 129 (Copyright © 2013 American Chemical Society.)

Organic π-conjugated compounds based on the phenazine derivatives featured the donor-π-bridge-acceptor backbone structure. In 2016, the Sekar et al.[130] exploited this feature to design and synthesize a special acceptor for sensing the TFA and Et_3N as a new probe 73. Interestingly, the probe 73 can not only detect the TFA or Et_3N by the naked-eyes, but also can be recycled by neutralization reaction between the acid and alkali. According to this phenomenon, the author believed that the probe 73 could exhibit commendably acid-alkali equilibria in the THF solutions. The sensing mechanism was ascribed to a strong ICT effect[131]. The detailed sensing diagram is shown in scheme 43.

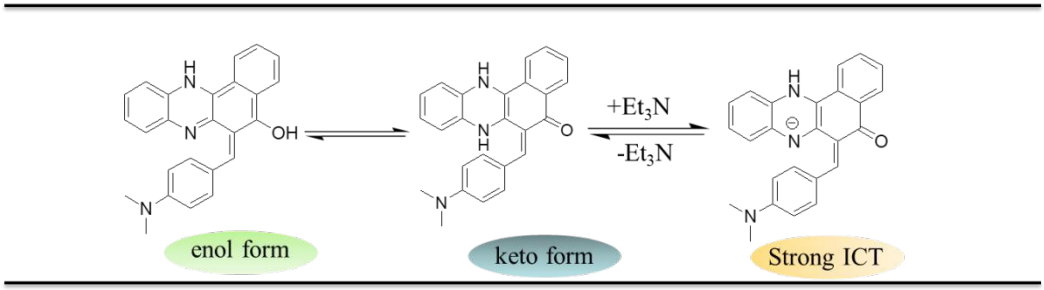

Scheme 43 The sensing mechanism of the probe 73 for sensing the acid and base

Another compound named probe 74, was synthesized by the Chen et al.[132] as a dual channel sensor for detecting H^+ in the solution. Generally, the sensing mechanism is attributed to protonation and deprotonation process due to a heterocycle backbone bearing with nitrogen atoms containing electron donating group. This probe could exhibit fluorescent and colorimetric sensing performance for H^+, appearing a corresponding color change from the light yellow to light green after addition alkali. Meanwhile, the maximal emission band of the probe 74 shifted to 511 nm accompanied with the pH changing from 2 to 7. Different observation is that the absorption band could achieve a saturation state at weak acid conditions (pH=6). The authors considered that this probe can be used to act as fluorescent pH probe without any interference. The sensing process is described in scheme 44

View Article Online
DOI: 10.1039/D0TC01401J

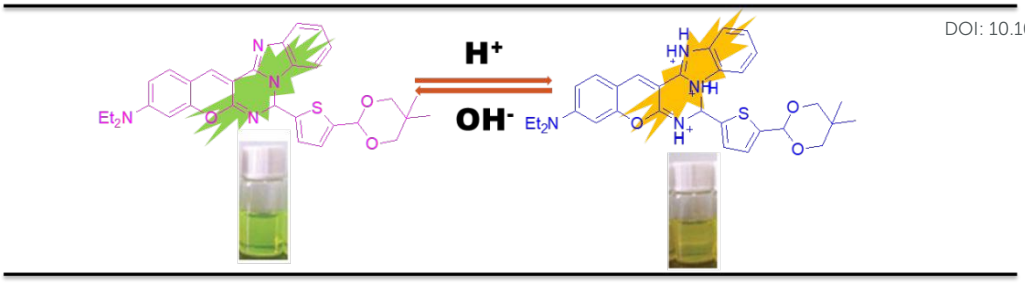

Scheme 44 The sensing mechanism of the probe 74 for detecting H^+/OH^-. Reproduced with permission from reference 132 (Copyright © 2012 Wiley Periodicals, Inc).

In 2016, Zhang et al.[133] reported another a new type of probe named probe 75 (2-(perfluorophenyl)-1*H*-imidazo[4,5-*b*]phenazine, PFIPZ), which exhibited an excellent optical performance to picric acid (PA) over a series of electron−deficient compounds and acid compounds (e.g. CH_3CCOH, TFA, CSA, m-cresol, BN, NB,, 1,2-DBN, 1,4-DBN). Although, the structure of probe 75 was similar to the probe 27, the sensing mechanism of probe 75 can be addressed by the photoinduced electron transfer (PET), which fully explained that the optical responses of the phenazine derivatives extremely depended on the active functional group modified in the phenazine backbone.

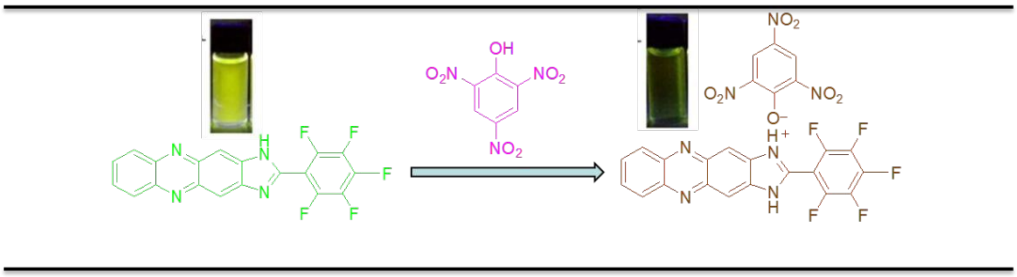

Scheme 45 The sensing mechanism of the probe 75 for detecting PA. Reproduced with permission from reference 133 (Copyright © 2016 The Royal Society of Chemistry).

In 2017, song et al.[134] synthesized a novel red-emitting fluorescent probe 76 based on the phenothiazine coumarin dyes by introducing phenothiazine backbone as fluorophore. The probe 76 can be used for detecting thiophenol with a high selectivity, excellent sensitivity, and large Stokes shift. The free probe 76 could display a maximum absorption band at 506 nm together with the solution no fluorescence emission. Nevertheless, a 24 nm blue-shift was observed in the absorption spectrum, appearing a strong red-emitting band at 623 nm with the gradual increase of thiophenol. And the probe exhibited a remarkable stokes shift (around 141 nm), which can effectively decrease the self−absorption interference and extremely improve the fluorescence sensitivity. This phenomenon is explained by the author as the cyclization and hydrolysis reaction caused by partial

cracking of 2,4-dinitrophenol in aqueous solution initiated by thiophenol (as shown in scheme 46). Inspired by the excellent sensing performance of the probe 76, the authors further estimated the availability of probe 76 to selectively sense thiophenol in living HeLa cells. The confocal microscopic images are collected in Fig 16.

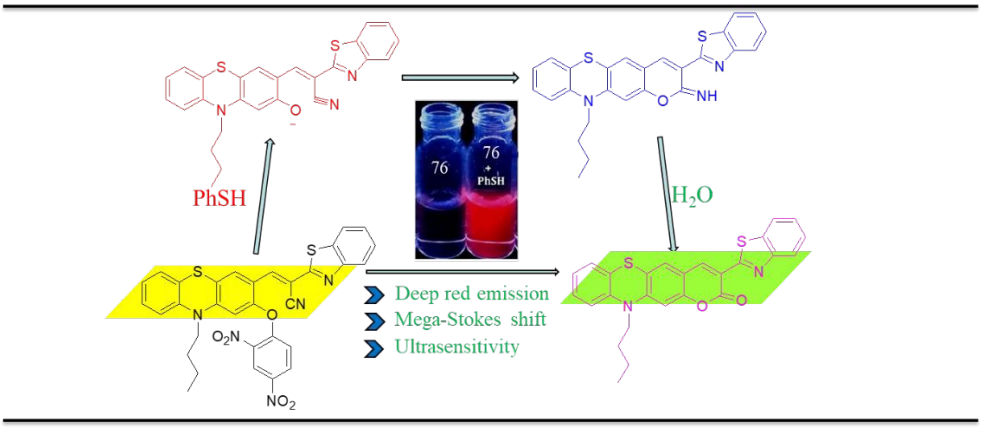

Scheme 46 The sensing mechanism of the probe 76 for detecting thiophenol. Reproduced with permission from reference 134 (Copyright © 2017 Elsevier B.V. or its licensors or contributors).

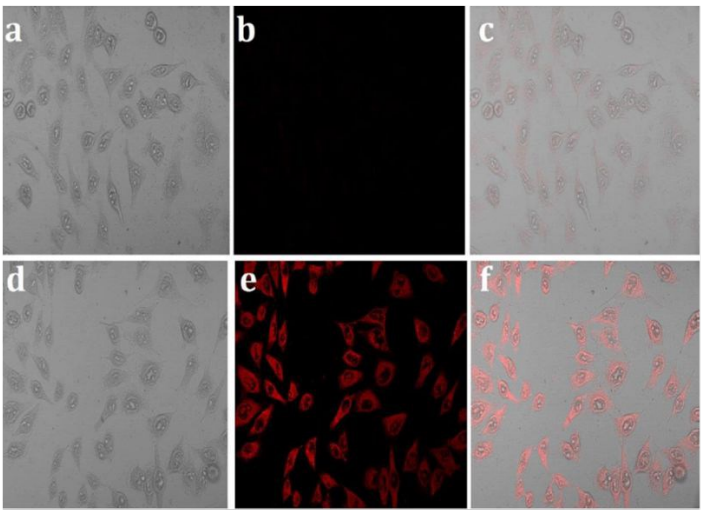

Fig 16. Confocal microscopic images of probe 76 in living HeLa cells. (a-c) HeLa cells incubated with 10 μM probe and 1 mM CTAB for 30 min; (d-f) HeLa cells pre-treated with 20 μM thiophenol for 20 min then incubated with 10 μM probe and 1 mM CTAB for additional 30 min. (a, d) Bright field images; (b, e) fluorescence images; (c, f) overlap of bright-field and fluorescence images. Emission was collected at 600-650 nm window upon excited at 488 nm. Reproduced with permission from reference 134 (Copyright © 2017 Elsevier B.V. or its licensors or contributors).

Hua et al.[135] reported a potential compound named 77, which uses naphthalimide as fluorescence group and phenazine as energy receptor. The probe 77 featured intramolecular fluorescence resonance energy transfer (FRET) on basis of effective spectral overlap between the

emission band of naphthalimide and the absorption band of phenazine. The selectivity and sensitivity of probe for cysteine detection were identified by investigating the absorption and emission spectrum. A couple of weak emission at 540 nm and 670 nm were firstly noticed in the fluorescence spectrum. And the fluorescence intensity at 540 nm sharply increased to 5−fold and even10−fold upon addition of the thiols after 2 hours. The authors considered that a cysteine chain with the specific S–S bond played a key role in discerning moiety, producing a prominent fluorescence enhancement at 540 nm, which can be ascribed to the elimination of the disulfide bond based on FRET effect. The diagram of the sensing mechanism is pictured in scheme 47. Finally, the probe 77 was applied to sense bio thiols in Hela cells by using confocal laser scanning microscopy (as shown in Fig 17).

Similar to the probe 77, in 2017, a novel probe 78 was synthesized by Tian et al.[136] by using phenazine−barbituric acids, which could also be applied to detect the cysteine by the colorimetric and near−infrared fluorescent response. An experiment of probe 78 screening various amino acids by the spectral responsivity demonstrated that it could give rise to an obvious variation to amino acids bearing with sulfhydryl, and the other amino acid without sulfhydryl hardly cause distinct changes both in absorption and fluorescence spectrum. The authors considered that the abilities of the intensive nucleophilic attack based on the sulfhydryl could extremely increase the activity of C=C bond, resulting in a nucleophilic addition reaction. Moreover, probe 78 can be used for bioimaging in living cell, fabricating TiO_2 sensor equipment, and quantitatively detecting concentration of the cysteine in serum. The sensing process of probe 78 for biological thiol and bioimaging in living cell (HeLa cell) are shown in Fig 18.

View Article Online
DOI: 10.1039/D0TC01401J

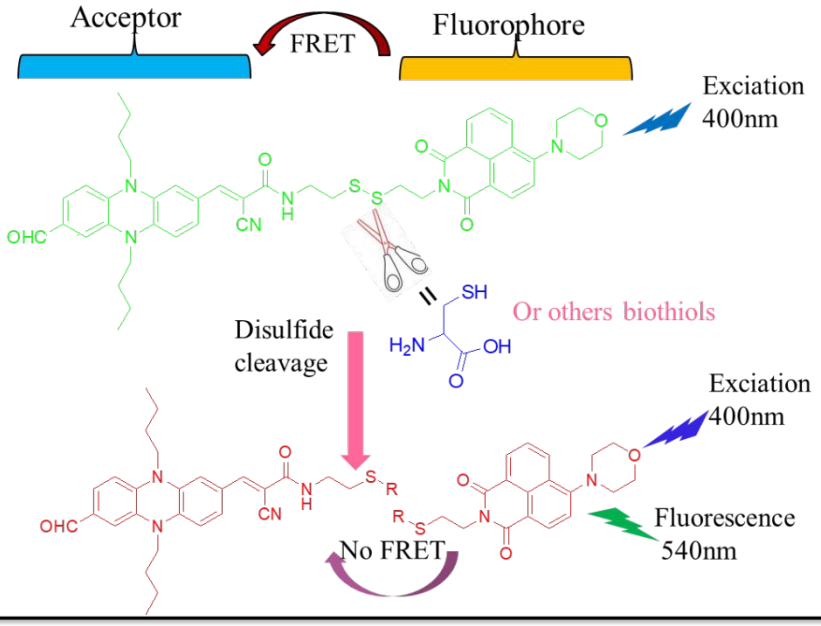

Scheme 47 The sensing mechanism of the probe 77 for detecting cysteine.

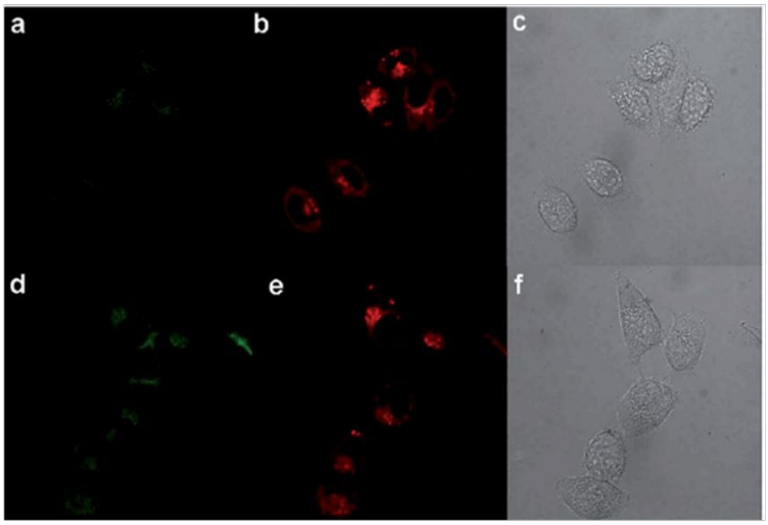

Fig 17. Confocal laser scan images of Hela cells incubated with probe 77 (10 mM) in PBS buffer pH 7.4 (a)–(c) Show the green channel (Ex: 488 nm, Em:525–575 nm), red channel (Ex:561 nm, Em:600–700 nm) and bright field images of the Hela cells incubated with probe 77 (10 mM) for 40 min. (d)–(f) Show the green channel, red channel and bright field images when incubated with probe (10 mM) for 40 min, then added and incubated with cysteine (10 mM) for another 60 min. Reproduced with permission from reference 135 (Copyright © 2015 The Royal Society of Chemistry).

View Article Online
DOI: 10.1039/D0TC01401J

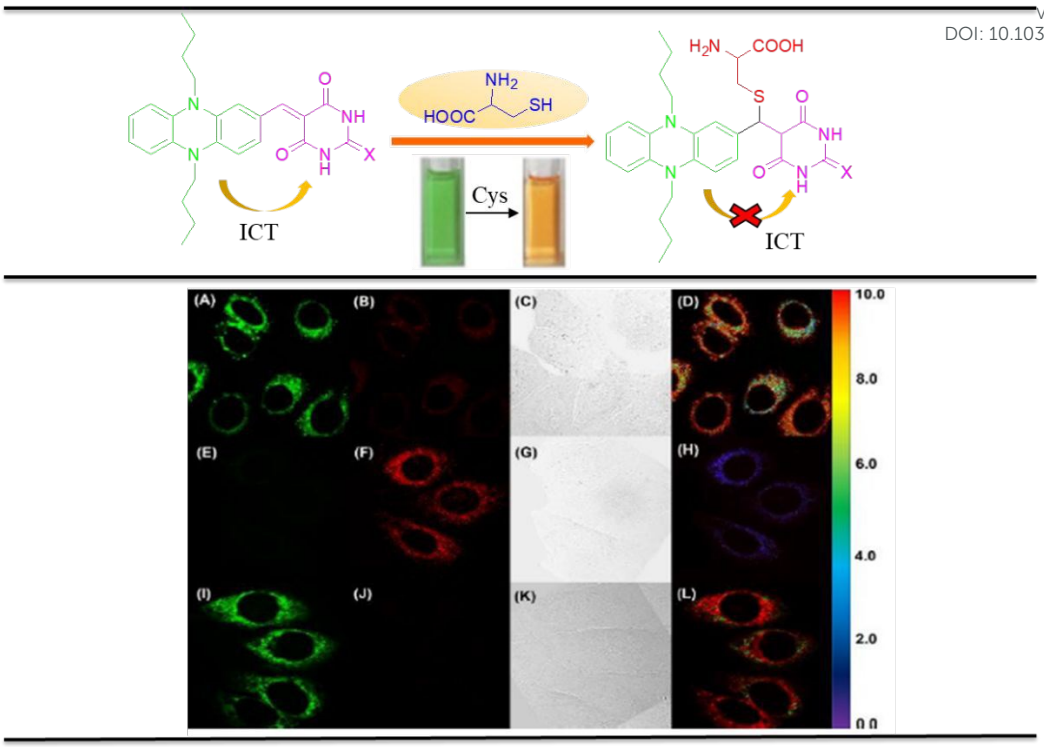

Fig 18. The sensing mechanism of the probe 78 for detecting Cys and a Confocal fluorescence imaging of living Hela cells. (A− D) Images of Hela cells incubated with PBA (10 μM) for 20 min at 37 ℃. (E−H) Images of Hela pretreated with NEM (200 μM) for 60 min, and then incubated with PBA (10 μM) for 20 min at 37 °C. (IL) Images of the preprocessed Hela cells with NEM firstly treated with Cys (50 μM), then strained with PBA (10 μM) for 20 min. (A, E and I) The green channels represented the fluorescence signals at 550−650 nm, λex = 488 nm. (B, F and J) The red channels represented the fluorescence signals at 690−730 nm, λex = 633 nm. (C, G and K) Bright field image. (D, H and L) Ratiometric images generated from generated from green/red channels with the image analysis software, Image J. Reproduced with permission from reference 136. (Copyright © 2017 Royal Society of Chemistry.)

The semiconductor QDs have attracted more and more attention as fluorescent probes, biosensors, and biomarkers widely used in bio sensing fields. A new type phenazine derivatives named 3,7-diamino-2,8-dimethyl-5-phenyl-phenol chloride hydrochloride, severed as molecular adhesives for fixing protein molecule, building the analytical membrane and detecting the DNA molecules. In 2016, He et al.[137] reported a phenazine derivative as probe 79 modified with GSH−CdTe QDs. The probe 79 was the firstly applied to selectively detect hsDNA of bio molecule via the “turn on” fluorescence response with a perfect sensitivity, proper selectivity, and the lowest limitation (10.8 ng/mL). The interaction diagram of the probe 79 is shown in Fig 19.

View Article Online
DOI: 10.1039/D0TC01401J

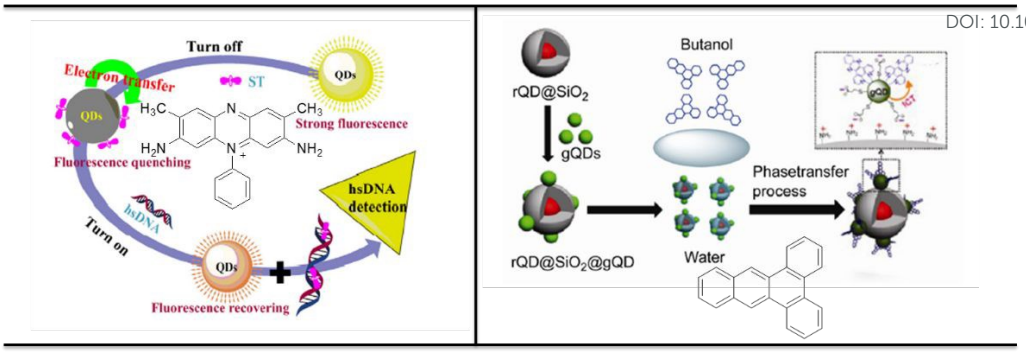

Fig 19. The Schematic diagram of the probe 79 (Left)and probe 80(right) as sensing for hsDNA. Reproduced with permission from reference 137,138 (Copyright © 2017 American Chemical Society. 2016 Elsevier B.V. All rights reserved).

Sun et al.[138] synthesized a novel quantum dot ligand probe as the probe 80. In this probe, the hydrophobic bipyridine phenazine system was used as the signal receiving unit, which is attached to the quantum dot carrier, and applied to ratiometric fluorescence sensing and selective detection of DNA molecules. The probe 80 was superior to QD in sensitivity and selectivity due to the electric neutrality of dipyridyl phenazine. Moreover, probe 80 can detect single nucleotide molecules, showing a specific fluorescence response. Interestingly, the author believes that probe 80 featured the advantages of low cost, not easy to modify, easy to label and simple purification process. Therefore, it is hoped the probe can be severed as an extremely simple and conventional technology for sensing nucleic acids, and it was further applied in DNA targeted drug designs or enhancement of nano delivery techniques. The sensing properties is described in Fig 20.

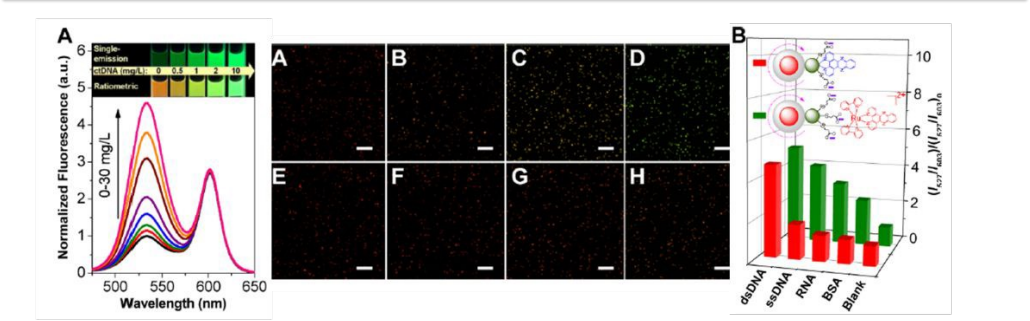

Fig 20. (Left) A: Fluorescence spectra of the probe 80 in the presence of 0, 0.2, 0.5, 1, 2, 5, 10, and 30 mg/L ct DNA.(middle): Fluorescent images of the in the presence of 0, 0.5, 1, and 5 mg/L of ct DNA (A−D) and ssDNA (E−H). Scale bar:1 μm (Right) B: Relative emission intensity of the probe 80 modified different QD. in the presence of different biomolecules. Reproduced with permission from reference 137 (Copyright © 2017 American Chemical Society.).

In conclusion, probes for detecting biomolecules and pH values in different systems are summarized. It can be seen that there have been a lot of research results, and great achievements

have been made in sensing molecules or pH, but the design and development of more living biomolecular sensors (such as amniotic acid and hsDNA) still need to continue to break through.

5.0 Conclusion

In this review, we comprehensively summarized the probes application in optical sensing and living cells bioimaging field based on the phenazine derivatives with fused benzene rings. The phenazine with electron deficient π system and lone pair electrons on N atoms have already been proved to exhibit enormous successes for designing and developing probes, which was applied in ions or molecule identification as well as bioimaging by the supramolecular interactions. Those obtained probes for improving the selectivity and sensitivity have gained great achievements and breakthroughs in vitro detection and recognition. Nevertheless, there is still a desired goal to enlarge the species of detectable ions, explore novel sensing mechanisms, tune excitation wavelength towards the near infrared region, expand the application in the living detection and bioimaging. More importantly, it is high urgent to introduce the water-soluble functional group into the phenazine backbone to increase solubility in aqueous solution and to reduce the toxicity for living tissue. It's encouraging that those probes have opportunity to become the potential fluorescent sensors for detecting targeted ion or molecules and bioimaging in living body. It is expected that this effort will provide some useful and comprehensive guidance for researchers intending to devote themselves to this important area.

Acknowledgment

This work was supported by the National Natural Science Foundation of China (NSFC) (Nos. 21574104; 21662031; 21661028), the Natural Science Foundation of Gansu Province(1506RJZA273) and the Program for Changjiang Scholars and Innovative Research Team in University of Ministry of Education of China (IRT15R56).

Reference:

1. J. Fordos, *Rec. Trav. Soc. Emul. Sci. Pharm.,* 1859, **3**, 30.
2. J. B. Laursen and J. Nielsen, *Chem. Rev.,* 2004, **104**, 1663–1686.
3. M. E. Makgatho, R. Anderson, J. F. O'Sullivan, T. J. Egan, J. A. Freese, N. Cornelius, and C. E. J. Van Rensburg, *Drug Dev. Res.,* 2000, **50**, 195–202.

View Article Online
DOI: 10.1039/D0TC01401J

4. J. R. Dis. Kerr, *Infect. Dis. Rev.,* 2000, **2**, 184–195.

5. J. M. Turner and A. J. Messenger, *Adv. Microb. Physiol.,* 1986, **27**, 211–275.

6. L. C. Vining and *Annu. Rev. Microbiol.,* 1990, **44**, 395–427.

7. R. D. Firn and C. D. Jones, *Nat. Prod. Rep.,* 2003, **20**, 382–391.

8. E. B. Goh, G. Yim W. Tsui and J. A. McClure, *Proc. Natl. Acad. Sci.,* 2002, **99**, 17025–17030.

9. M. E. Hernandez, A. Kappler and D. K. Newman, *Appl. Environ. Microbiol.,* 2004, **70**, 921–928.

10. M. Watanabe, Y. J. Chang, S. W. Liu, T. H. Chao, K. Goto, M. M. Islam, C. H. Yuan, Y. T. Tao, T. Shinmyozu and T. J. Chow, *Nat. Chem.,* 2012, **4**, 574–578.

11. P. Y. Gu, Z. L. Wang and Q. C. Zhang, *J. Mater. Chem. B.,* 2016, **4**, 7060–7074.

12. U. H. Bunz, *Chem. Res.,* 2015, **48**, 1676–1686.

13. C. Wang, J. Wang, P. Z. Li, J. Gao, S. Y. Tan, W. W. Xiong, B. Hu, P. S. Lee, Y. Zhao and Q. C. Zhang, *Chem. Asian J.,* 2014, **9**, 779–783.

14. J. B. Li, S. Chen, Z. L. Wang and Q. C. Zhang, *Chem. Rec.,* 2016, **16**, 1518–1530.

15. Z. wang, P. Gu, G. Liu, H. Yao, Y. Wu, Y. Li, R. Ganguly, J. Zhu, H. Fu and Q. C. Zhang, *Chem. Commun.,* 2017, **53**, 7772–7775.

16. Q. C. Zhang, J. C. Xiao, Z. Y. Yin, H. M. Duong, F. Qiao, F. Boey, X. A. Hu, H. Zhang and F. Wudl, *Chem. Asian. J.,* 2011, **6**, 856–861.

17. Z. He, D. Liu, R. Mao, Q. Tang, and Q. Miao, *Org. Lett.,* 2012, **14**, 1050–1053.

18. S. Miao, S. M. Brombosz, P. V. R. Schleyer, J. I. Wu, S. Barlow, S. R. Marder, K. I. Hardcastle and U. H. F. Bunz, *J. Am. Chem. Soc.,* 2008, **130**, 7339–7344.

19. Z. B. Zhang and Q. C. Zhang, *Mater. Chem. Front.,* 2020, DOI: 10.1039/C9QM00656G.

20. Z. Liang, Q. Tang, J. Xu and Q. Miao, *Adv. Mater.,* 2011, **23**, 1535–1539.

21. S. Chen, F. S. Raad, M. Ahmida, B. R. Kaafarani and S. H. Eichhorn, *Org. Lett.,* 2013, **15**, 558–5611.

22. O. Hinsberg and J. L. Ann, *Chemistry.,* 1901, **319**, 257–286.

23. O. Fischer and E. Hepp, *Chem. Ber.,* 1890, **23**, 2789–2793.

24. C. Neves-Pinto, V. R. S. Malta, M. D. C. F. R. Pinto, R. H. A. Santos, S. L. deCastro and A. V. Pinto, *J. Med. Chem.,* 2002, **45**, 2112–2115.

25. P. W. Iseminger, M. Gregory, T. J. R. Weakley, G. Caple and A. G. Sykes, *J. Org. Chem.*, 1997, **62**, 2643–2645.

26. D. B. Gladilovich, Z. Obshch and J. G. Chem, USSR (Engl. Transl.), 1882, **58**, 1988.

27. G. W. Rewcastle, W. A. Denny and B. C. Baguley, *J. Med. Chem.,* 1987, **30**, 843–851.

28. A. A. El Bahnasawy and M. F. El Ahwany, *Phosphorus*, *Sulfur, and Silicon and the Related Elements.,* 2007, **182**, 1937–1944.

29. A. Chaudhary and J. M. Khurana, *Res Chem Intermed.,* 2018, **44**, 1045–1083.

30. M. M. Barsan, E. M. Pinto and C. M. A. Brett, *Electro Chim. Acta.,* 2008, **53**, 3973–3982.

31. J. Li and Y. Lu, *Am. Chem. Soc.,* 2000, **122**, 10466–10467.

32. X. F. Guo, X. H Qian and L. H. Jia, *J. Am. Chem. Soc.,* 2004, **126**, 2272–2273.

33. L. E. P. Dietrich, A. P. Whelan, A. Petersen, M. Whiteley and D. K. Newman, *Molecular microbiology.,*2006, **61**, 1308–1321.

34. P. Chen and C. He, *J. Am. Chem. Soc.,* 2004, **126**, 728–729.

35. P. Y. Gu, Y. Zhao, J. H. He, J. Zhang, C. Y. Wang, Q. F. Xu, J. M. Lu, X. W. Sun and Q. C. Zhang, *J. Org. Chem.,* 2015, **80**, 3030–3035.

36. G. Jiang, S. Wang, W. Yuan, L. Jiang and Y. Song, *Chem. Mater.,* 2006, **18**, 235–237.

37. H. Xue, X. J. Tang, L. Z. Wu, L. P. Zhang and C. H. Tung, *J. Org. Chem.,* 2005, **70**, 9727–9734.

38. R. Badugu, J. R. Lakowicz and C. D. Geddes, *J. Am. Chem. Soc.,* 2005, **127**, 3635–3641.

39. S. H. Kim, H. S. Choi, J. Kim, S. J. Lee, D. T. Quang and J. S. Kim, *Org. Lett.,* 2010, **12**, 560–563.

40. L. S. Pierson and E. A. Pierson, *Appl Microbiol Biotechnol.,* 2010, **86**, 1659–1670.

41. N. S. Hari Narayana Moorthy and C. Karthikeyan, P. Trivedi, *Medicinal Chemistry.,* 2009, **5**, 549–557.

42. S. Fotso, D. A. Santosa, R. Saraswati, J. Yang, T. Mahmud, T. M. Zabriskie and P. J. Proteau, *J. Nat. Prod.,* 2010, **73**, 472–475.

43. M. L. Lavaggi, M. Cabrera, M. González and H. Cerecetto, *Chem. Res. Toxicol.,* 2008, **21**, 1900–1906.

44. A. Cimmino, A. Evidente, V. Mathieu, A. Andolfi, F. Lefranc, A. Kornienkod and R. Kiss, *Nat.*

View Article Online
DOI: 10.1039/D0TC01401J

Prod. Rep., 2012, **29**, 487–501.

45. L. A. Estrada and D. C. Neckers, *Org. Lett.,* 2011, **13**, 3304–3307.
46. H. J. Song, E. J. Lee, D. H. Kim, S. M. Lee, J. Y. Lee and D. K. Moon, *Synthetic Metals.,*2013, **181**, 98–103.
47. P. Y. Gu, Z. L. Wang, F. X. Xiao, Z. Q. Lin, R. B. Song, Q. F. Xu, J. M. Lu, B. Liu and Q. C. Zhang, *Mater. Chem. Front.,* 2016, **11**, 482–485.
48. B. Kohl, F. Rominger and M. Mastalerz, *Angew. Chem. Int. Ed.,* 2015, **54**, 6051–6056.
49. S. Choudhary, C. Gozalvez, A. Higelin, I. Krossing, M. M. Franco and A. M. Alonso, *Chem. Eur. J.,* 2014, **20**, 1525–1528.
50. S. Yang, B. Shan, X. Xu and Q. Miao, *Chem. Eur. J.,* 2016, **22**, 6637–6642.
51. Q. Miao, T. Q. Nguyen, T. Someya, G. B. Blanchet and C. Nuckolls, *J. Am. Chem. Soc.,* 2003, **125**, 10284–0287.
52. P. Anzenbacher, D. S. Tyson, K. Jursíková and F. N. Castellano, *J. Am. Chem. Soc.,* 2002, **124**, 6232–6233.
53. Q. Miao, *Adv. Mater.,* 2014, **26**, 5541–5549.
54. K. Imato, K. Ohira, M, Yamaguchi, T. Enokia and Y. Ooyama, *Mater. Chem. Front.,* 2020, **4**, 589–596.
55. X. M. Wu, X. R. Sun, Z. Q. Guo, J. B. Tang, Y. Q. Shen, T. D. James, H. Tian and W. H. Zhu, *J. Am. Chem. Soc.,* 2014, **136**, 3579–3588.
56. G. Qian, X. Z. Li and Z. Y. Wang, *J. Mater. Chem.,* 2009, **19**, 522–530.
57. X. Chen, S. W. Nam, G. H. Kim, N. Song, Y. Jeong, I. Shin, S. K. Kim, J. Kim, S. Park and J. Yoon, *Chem Commun.,* 2010, **46**, 8953–8955.
58. X. H. Cheng, R. L. Tang, H. Z. Jia, J. Feng, J. G. Qin and Z. Li, *ACS Appl. Mater. Interfaces.,* 2012, **4**, 4387–4392.
59. S. Kothavale and N. Sekar, *Dyes pigments.,* 2017, **136**, 31–45.
60. X. Zhou, F. Su, H. Lu, P. Senechal-Willis, Y. Tian, R. H. Johnson and D. R. Meldrum, *Biomaterials.,* 2012, **33**, 171–180.
61. M. Maniyazagan, R. Mariadasse, M. Nachiappan, J. Jeyakanthan, N. Lokanath, S. Naveen, G. Sivaraman, P. Muthuraja, P. Manisankar and T. Stalin, *Sens. Actuators, B.,* 2018, **254**, 795–

View Article Online
DOI: 10.1039/D0TC01401J

804.

62. X. Zhang, Y. Xiao and X. Qian, *Angew. Chem. Int. Ed.,* 2008, **47**, 8025–8029.
63. X. Qu, Q. Liu, X. Ji, H. Chen, Z. Zhou and Z. Shen, *Chem. Commun.,* 2012, **48**, 4600–4602.
64. J. Fan, M. Hu, P. Zhan and X. Peng, *Chem. Soc. Rev.,* 2013, **42**, 29–43.
65. L. Yuan, F. Jin, Z. Zeng, C. Liu, S. Luo and J. Wu, *Chem. Sci.,* 2015, **6**, 2360–2365.
66. P. C. A. Swamy, S. Mukherjee and P. Thilagar, *Anal. Chem.,* 2014, **86**, 3616–3624.
67. Q. Zou, X. Li, J. J. Zhang, J. Zhou, B. B. Sun, H. Tian, *Chem. Commun.,* 2012, **48**, 2095–2097.
68. N. Kumari, S. Jha, S. Bhattacharya, *J. Org. Chem.,* 2011, **76**, 8215–8222.
69. J. Li and Q. C. Zhang, *ACS Appl. Mater. Interfaces.,* 2015, **7**, 28049–28062.
70. Y. R. Li, L.J. Shi, Y. Y. Zhang, G. C. Sun, L. Sun and J. H. Su, *Dye pigments.,* 2019, **160**, 794–798.
71. G. Y. Gao, W. J. Qu, B. B. Shi, P. Zhang, Q. Lin, H. Yao, W. L. Yang, Y. M. Zhang, and T. B. Wei, *Spec. Act. Part A: Mol. Bio. Spectro.,* 2014, **121**, 514–519.
72. T. B. Wei, G. Y. Wu, B. B. Shi, Q. Lin, H. Yao and Y. M. Zhang, *Chin. J. Chem.,* 2014, **32**, 1238–1244.
73. G. Y. Gao, W. Y. Qu, B. B Shi, Q. Lin, H. Yao, Y. M. Zhang, J. Chang, Y. Cai and T. B. Wei, *Sensors Actuators, B Chem.,* 2015, **213**, 501–507.
74. Q. Lin, F. Zheng, T. T. Lua, J. Liu, H. Lia, T. B. Wei, H. Yao and Y. M. Zhang, *Sensors Actuators, B Chem.,* 2017, **251**, 250–255.
75. B. K. Rani and S. A John, *J. Hazard. Mater.,* 2018, **343**, 98–106.
76. B. B. Shi, P. Zhang, T. B. Wei, H. Yao, Q. Lin, J. Liu and Y. M. Zhang, *Tetrahedron.,* 2014, **69**, 7981–7987.
77. H. L. Zhang, W. T. Li, W. J. Qu, T. B. Wei, Q. Lin, Y. M. Zhang and H. Yao, *Sensors Actuators, B Chem.,* 2017, **239**, 671–678.
78. B. R. Yong, W. J. Qu, L. R. Dang, Q. Lin, H. Yao, Y. M. Zhang and T. B. Wei, *Chemistry select.,* 2019, **4**, 10060–10064.
79. H. T. Zhou, J. Mei, A. Y. Chen, C. L. Chen, W. Chen, Z. Y. Zhang, J. H. Su, P. T. Chou and H. Tian, *Small.,* 2016, **12**, 6542–6546.

View Article Online
DOI: 10.1039/D0TC01401J

80. M. Alfonso, A. T. Arraga and P. Molina, *J. Org. Chem.,* 2011, **76**, 939–947.

81. F. Zapata, A. Caballero, A. Espinosa, A. Tarraga and P. Molina, *J. Org. Chem.,* 2009, **74**, 4787–4796.

82. S. G. R. Avuthu, J.T. Wabeke, B. B. Narakathu, D. Maddipatla, J. S. Arachchilage, S. O Obare and M. Z. Atashbar, *IEEE Sensors Journal.,* 2016, **16**, 8678–8684.

83. K. Aggarwal and J. M. Khurana, *Luminescence.,* 2015, **167**, 146–155.

84. T. B. Wei, B. R. Yong, L. R. Dang, Y. M. Zhang, H. Yao and Qi Lin, *Dyes Pigments.,* 2019, **171**, 107707.

85. D. E. Kang, C. S. Lim, J. Y. Kim, E. S. Kim, H. J. Chun and B. R. Cho, *Anal. Chem.,* 2014, **86**, 5353–5359.

86. J. J. Bryant, Y. X. Zhang, E. A. Davey, A. L. Appleton, B. D. Lindner, X. H. Qian and U. H. F. Bunz, *J. Org. Chem.,* 2012, **77**, 7479–7486.

87. H. X. Shi, W. T. Li, Q. Li, H. L. Zhang, Y. M. Zhang, T. B. Wei, Q. L and H. Yao, *RSC Adv.,* 2017, **7**, 53439–53444.

88. W. T. Li, G. Y. Wu, W. J. Qu, Q. Li, J. C. Lou, Q. Lin, H. Yao, Y. M. Zhang and T. B. Wei, *Sensor Actuators, B Chem.,* 2017, **239**, 671–678.

89. T. B. Wei, H. L. Zhang, W. T. Li, W. J. Qu, J.X. Su, Q. Lin, Y. M. Zhang and H. Yao, *Chin. J. Chem.,* 2017, **35**, 1311–1316.

90. H. L. Zhang, T. B. Wei, W. T. Li, W. J. Qu, Y. L. Leng, J. H. Zhang, Q. Lin, Y. M. Zhang and H. Yao, *Spec. Act. Part A: Mol. Bio. Spectro.,* 2017, **175**, 117–124.

91. G. A. M. Jardim, H. D. R. Calado, L. A. Cury and E. N. S. Júnior, *Eur. J. Org. Chem.,* 2015, **4**, 703–709.

92. P. Ravichandirana, A. B. Czubarab, M. Masłykc, A. P. Bellad, P. M. Johnsond, S. A. Subramaniyane, K. S. Shime and D. J. Yoo, *Dyes Pigments.,* 2020, **172**, 107828.

93. P. Ravichandiran, S. A. Subramaniyan, A. P. Bella, P. M. Johnson, A. R. Kim, K. S. Shim and D. J. Yoo, *Anal. Chem.,* 2019, **91**, 10095–10101.

94. B. B. Shi, Y. M. Zhang, T. B. Wei, Q. Lin, H. Yao, P. Zhang and Y. M. Zhang, *Sensor Actuators, B Chem.,* 2013, **190**, 555–561.

95. H. Woo, Y. M. You, T. Kim, G. J. Jhonb and W. Nam, *J. Mater. Chem.,* 2012, **22**, 17100–

View Article Online
DOI: 10.1039/D0TC01401J

17112.

96. Z. Xu, J. Yoon, D. R. Spring, Chem. *Soc. Rev.,* 2010, **39**, 1996–2006.
97. G. Balamurugana, S. Velmathia, N. Thirumalaivasanb and S. P. Wu, *Analyst.,* 2017, **142**, 4721–4726.
98. N. A. Fakhre and B. M. Ibrahim, *J. Hazard. Mater.,* 2018, **343**, 324–331.
99. B. Wang, B. Luo, M. H. Liang, A. L. Wang, J. Wang, Y. Fang, Y. H. Chang and L. J. Zhi, *Nanoscale.,* 2011, **3**, 5059–5066.
100. G. Punithakumari and S. Velmathi, *Spec. Act. Part A: Mol. Bio. Spectro.,* 2020, **229**, 117887.
101. Erdemir and O. Kocyigit, *Dyes Pigments.,* 2017, **145**, 72–79.
102. C. Y. Wang, G. Li and Q. C. Zhang, *Tetra. Lett.,* 2013, **54**, 2633–2636.
103. S. Naha and S. Velmathi, *Chemistry Select.,* 2019, **4**, 2912–2917.
104. J. Y. Hu, R. Liu, X. L. Zhu, X. Cai and H. J. Zhu, *Chin. Chem. Lett.,* 2015, **26**, 339–342.
105. T. Ghosh, B. G. Maiya and M. W. Wong, *J. Phys. Chem. A.,* 2004, **108**, 11249–11259.
106. X. J. Peng, Y. K. Wu, J. L. Fan, M. Z. Tian and K. L. Han, *J. Org. Chem.,* 2005, **70**, 10524–10531.
107. S. Suganya, J. S. Park and S. Velmathi, *J. Fluoresc.,* 2016, **26**, 207–215.
108. V. Tharmaraj, S. Devi and K. Pitchumani, *Analyst.,* 2012, **137**, 5320–5324.
109. M. S. C. Shive, B. Tanuja and G. Bhaskar, *Tetra. Lett.,* 2008, **49**, 6646–6649.
110. G. Li, Y. C. Wu, J. K. Gao, J. B. Li, Y. Zhao and Q. C. Zhang, *Chem. Asian J.,* 2013, **8**, 1574–1578.
111. P. Y. Gu, J. K. Gao, C. Y. Wang and Q. C. Zhang, *RSC Adv.,* 2015, **5**, 80307–80310.
112. J. F. Zhao, G. Li, C. Y. Wang, W. Q. Chen, S. C. J. Loo and Q. C. Zhang, *RSC Adv.,* 2013, **3**, 9653-9657.
113. N. Kumari, S. Jha and S. Bhattachary, *J. Org. Chem.,* 2011, **76**, 8215–8222.
114. R. M. F. Batista, E. Oliveira, S. P. G. Costa, C. Lodeiro and M. M. M. Raposo, *Org. Lett.,* 2007, **9**, 3201–3204.
115. J. Kang, E. J. S. H. Kim, Y. H. Kim, Y. Kim, S. J. Kim and C. Kim, *Tetra. Lett.,* 2013, **54**, 1015–1019;
116. T. B. Wei, W. T. Li, Q. Li, J. X. Su, W. J. Qu, Q. Lin, H. Yao and Y. M. Zhang, *Tetra. Lett.,*

View Article Online
DOI: 10.1039/D0TC01401J

2016, **57**, 2767–2771.

117. B. Vidya, M. Iniya, G. Sivaraman, R.V. Sumesh and D. Chellappa, *Sensor Actuators, B Chem.,* 2017, **242**, 434–442.

118. W. T. Li, W. J. Qu, X. Zhu, Q. Li, H. L. Zhang, H. Yao, Q. Lin, Y. M. Zhang and T. B. Wei, *Sci. China, Chem.,* 2017, **60**, 754–758.

119. L. Yang, X. Li, Y. Qu, W. S. Qu, X. Zhang, Y. D. Hang, H. Ågren and J. L. Hua, *Sensor Actuators, B Chem.,* 2014, **203**, 833–847.

120. F. Wang, L. Wang, X. Q. Chen and J. Y. Yoon, *Chem. Soc. Rev.,* 2014, **43**, 4312–4324.

121. L. Yang, X. Li, J. B. Yang, Y. Qu and J. L. Hua, *ACS Appl. Mater. Interfaces.,* 2013, **5**, 1317–1326.

122. S. Suganya and S. Velmathi, *Sensor Actuators, B Chem.,* 2015, **221**, 1104–1113.

123. S. K. Kwona, S. Kou, H. N. Kim, X. Q. Chen, H. J. Hwang, S. W. Nama, S. H. Kim, K. M. K. Swamy, S. S. Park and J. Y. Yoon, *Tetra. Lett.,* 2008, **49**, 4102–4105.

124. H. Fang, W. J. Qu, H. H. Yang, J. X. He, H. Yao, Q. Lin, T. B. Wei and Y. M. Zhang, *Dyes Pigments.,* 2020, **174**, 108066.

125. Y. M. Zhang, H. Fang, W. Zhu, J. X. He, H. Yao, T. B. Wei, Q. Lin and W. J. Qu, *Dyes Pigments.,* 2020, **172**, 107765.

126. Q. L. Xu, C. H. Heo, G. Kim, H. W. Lee, H. M. Kim and J. Y. Yoon, *Angew. Chem. Int. Ed.,* 2015, **54**, 1–6.

127. J. Kang, H. S. Kim and D. O. Jang, *Tetra. Lett.,* 2005, **46**, 6079–6082.

128. P. Singh, A. Baheti and K. R. J. Thomas, *J. Org. Chem.,* 2011, **76**, 6134–6145.

129. W. Liu, R. Sun, J. F. Ge, Y. J. Xu, Y. Xu, J. M. Lu, I. Itoh and M. Ihara, *Anal. Chem.,* 2013, **85**, 7419–7425.

130. S. R. Patil, A. S. Choudhary and N. Sekar, *Tetrahedron.,* 2016, **72**, 7968–7974.

131. S. Achelle, J. R. Lopez, N. Cabon and R. Guen, *RSC Adv.,* 2015, **5**, 107396–107399.

132. H. Q. Li, J. Guo, X. B. Zhang and Z. Chen, *Heteroatom Chemistry.,* 2012, **23**, 551–559.

133. P. Y. Gu, C. Y. Wang, L. Nie, G. K. Long and Q. C. Zhang, *RSC Adv.,* 2016, **6**, 37929–37932.

134. W. Q. Chen, X. X. Yue, W. X. Li, Y. Q. Hao, L. L. Zhang, L. L. Zhu, J. R. Sheng and X. Z. Song, *Sensor Actuators, B Chem.,* 2017, **245**, 702–710.

View Article Online
DOI: 10.1039/D0TC01401J

135. L. Yang, W. Qu, X. Zhang, Y. Hang and J. Hua, *Analyst.,* 2015, **140**, 182–189.

136. X. Zhang, Y. C.Yan, Y. D. Hang, J. Wang, J. L. Hua and H. Tian, *Chem. Commun.,* 2017, **53**, 5760–5763.

137. L. Wang, S. Liu, C. Hao, X. Zhang, C. Wang and Y. He, *Sensor Actuators, B Chem.,* 2016, **229**, 145–154.

138. Y. Liu, M. Ye, Q. Ge, X. Qu, Q. Guo, X. Hu and Q. Sun, *Anal. Chem.,* 2016, **88**, 1768–1774.

View Article Online
DOI: 10.1039/D0TC01401J

Graphical Abstract